1985

TRANSPORT OF 2-KETO-D-GLUCONATE AND L-MALATE IN PSEUDOMONAS PUTIDA.

FRANCISCA ROSELINE AKUVI. AGBANYO
University of Windsor

CANADIAN THESES ON MICROFICHE

I.S.B.N.

THESES CANADIENNES SUR MICROFICHE

National Library of Canada
Collections Development Branch

Canadian Theses on
Microfiche Service

Ottawa, Canada
K1A 0N4

Bibliothèque nationale du Canada
Direction du développement des collections

Service des thèses canadiennes
sur microfiche

NOTICE

The quality of this microfiche is heavily dependent upon the quality of the original thesis submitted for microfilming. Every effort has been made to ensure the highest quality of reproduction possible.

If pages are missing, contact the university which granted the degree.

Some pages may have indistinct print especially if the original pages were typed with a poor typewriter ribbon or if the university sent us a poor photocopy.

Previously copyrighted materials (journal articles, published tests, etc.) are not filmed.

Reproduction in full or in part of this film is governed by the Canadian Copyright Act, R.S.C. 1970, c. C-30. Please read the authorization forms which accompany this thesis.

AVIS

La qualité de cette microfiche dépend grandement de la qualité de la thèse soumise au microfilmage. Nous avons tout fait pour assurer une qualité supérieure de reproduction.

S'il manque des pages, veuillez communiquer avec l'université qui a conféré le grade.

La qualité d'impression de certaines pages peut laisser à désirer, surtout si les pages originales ont été dactylographiées à l'aide d'un ruban usé ou si l'université nous a fait parvenir une photocopie de mauvaise qualité.

Les documents qui font déjà l'objet d'un droit d'auteur (articles de revue, examens publiés, etc.) ne sont pas microfilmés.

La reproduction, même partielle, de ce microfilm est soumise à la Loi canadienne sur le droit d'auteur, SRC 1970, c. C-30. Veuillez prendre connaissance des formules d'autorisation qui accompagnent cette thèse.

THIS DISSERTATION
HAS BEEN MICROFILMED
EXACTLY AS RECEIVED

LA THÈSE A ÉTÉ
MICROFILMÉE TELLE QUE
NOUS L'AVONS REÇUE

NL-339 (r. 82/08)

Canada

TRANSPORT OF 2-KETO-D-GLUCONATE AND L-MALATE IN *PSEUDOMONAS PUTIDA*

by

Francisca Roseline Akuvi Agbanyo

A Dissertation
Submitted to the Faculty of Graduate Studies through the
Department of Chemistry in Partial Fulfillment
of the Requirements for the Degree of
Doctor of Philosophy at the
University of Windsor

Windsor, Ontario, Canada

1984

816594

ABSTRACT

TRANSPORT OF 2-KETO-D-GLUCONATE AND L-MALATE IN PSEUDOMONAS PUTIDA

by

Francisca Roseline Akuvi Agbanyo

Glucose- and succinate-grown whole cells of P. putida transport 2KGA by a saturable process with apparent Km values of 5.7±0.5 μM and 9.1±0.6 μM, respectively; the Vmax values obtained are 4.6±0.09 nmol.mg protein.$^{-1}$ min.$^{-1}$ and 2.7±0.05 nmol.mg protein.$^{-1}$ min.$^{-1}$, respectively.

The transport of 2KGA by membrane vesicles prepared from glucose-grown P. putida occurs by a facilitated diffusion process, with an apparent Km of 111.0±2.9 μM and a Vmax of 0.55±0.04 nmol.mg protein.$^{-1}$ min.$^{-1}$. The provision of phenazine methosulphate (PMS)/ascorbate or L-malate/FAD results in a stimulation of the initial rate of transport, the accumulation of 2KGA and a significant decrease in Km value to 50.2±2.1 μM and 34.8±2.9 μM, respectively. The Vmax however, remains virtually unchanged. 2KGA transport is inhibited by the respiratory chain inhibitors, antimycin A and rotenone, and the uncoupler 2,4-dinitrophenol (DNP) in the presence of L-malate/FAD. Both 4F2KGA and 5F2KGA inhibit 2KGA transport competitively, with K_i values of 50 μM and 160 μM, respectively. With vesicles prepared from

succinate-grown cells, 2KGA transport occurs by a non-specific diffusion process with a Km of ∞.

Vesicles prepared from glucose- or succinate-grown cells generate a proton-motive force (Δp) of -145 mV and -140 mV, respectively, when provided with PMS/ascorbate. Both the ΔpH and $\Delta\psi$ components of Δp are collapsed in the presence of DNP. In the presence of L-malate/FAD a Δp of -129 mV is generated by vesicles from glucose-grown cells, while no Δp is detected with vesicles from succinate-grown cells. Studies with nigericin, valinomycin and carbonylcyanide-m-chlorophenylhydrazine (CCCP) indicate that the active transport of 2KGA by vesicles from glucose-grown cells is coupled predominantly to the ΔpH component of Δp at pH 6.6.

L-Malate is transported by a non-specific diffusion process with a Km of ∞ in vesicles from glucose-grown P. putida. In vesicles from succinate-grown cells however, L-malate transport and L-malate induced proton uptake display saturation kinetics with Km values of 14.3 mM and 16.0 mM respectively. The Vmax values are 313 nmol.mg protein.$^{-1}$min.$^{-1}$ for L-malate uptake and 667 nmol.mg protein.$^{-1}$min.$^{-1}$ for L-malate induced proton uptake. During L-malate transport, oxaloacetate is produced extra-cellularly, while succinate appears to accumulate intra-cellularly. Based on these observations the transport of L-malate in this organism is considered to be more elaborate than hitherto documented.

DEDICATION

To My Parents

ACKNOWLEDGEMENTS

I would like to express my sincere thanks to Dr. N.F. Taylor, my supervisor, for his support and guidance throughout these studies.

I would also like to thank Dr. K.E. Taylor, Dr. R.J. Thibert and Dr. B. Mutus for their help and advice during the course of this work.

My sincere thanks also go to the Faculty of Graduate Studies (University of Windsor), The Government of Ghana/ Ghana Cocoa Marketing Board and Dr. N.F. Taylor for their financial support during my studies.

Thanks are due to Barbara Zielinski for her help in preparing the electron micrographs and to my friends, colleagues, and all the members of staff and faculty at the Department of Chemistry for their help and co-operation throughout my studies.

Finally, I would like to express my sincere gratitude to my family for their continued support and encouragement.

TABLE OF CONTENTS

LIST OF FIGURES

LIST OF TABLES

LIST OF ABBREVIATIONS

ATP	- Adenosine-5'-triphosphate
ATPase	- Adenosine-5'-triphosphatase
CCCP	- Carbonylcyanide m-chlorophenylhydrazone
CPM	- Counts per minute
DAP	- Meso-diaminopimelic acid
DBP	- Dicarboxylic acid binding protein
DCCD	- Dicyclohexylcarbodiimide
DCIP	- 2,6-Dichlorophenol-indophenol
DDA^+	- Dibenzyldimethyl ammonium
DHA	- Dihydroxyacetone
DN'ase	- Deoxyribonuclease
DNP	- 2,4-Dinitrophenol
2DOG	- 2-Deoxy-D-glucose
DPM	- Disintegrations per min
EC	- Enzyme Commission
ED	- Entner-Doudoroff Pathway
EDTA	- Ethylenediaminetetraacetate
FAD	- Flavin adenine dinucleotide
$FADH_2$	- Flavin adenine dinucleotide (reduced form)
FCCP	- Carbonylcyanide p-(trifluoromethoxy)phenyl-hydrazone
3FG	- 3-Deoxy-3-fluoro-D-glucose
4FG	- 4-Deoxy-4-fluoro-D-glucose
3FGA	- 3-Deoxy-3-fluoro-D-gluconic acid
4FGA	- 4-Deoxy-4-fluoro-D-gluconic acid
3F2KGA	- 3-Deoxy-3-fluoro-2-keto-D-gluconic acid

4F2KGA	- 4-Deoxy-4-fluoro-2-keto-D-gluconic acid
F-PTS	- Fructose-1-phosphate phosphotransferase system
GBP	- Glucose binding protein
h	- Hour
HMP	- Hexose-monophosphate pathway
HPLC	- High pressure liquid chromatography
HPr	- Histidine-containing protein of the PTS
K	- Kelvin
2KGA	- 2-Keto-D-gluconic acid
K_i	- Inhibition constant
Km	- Michaelis-Menton Constant
KJ	- Kilojoules
KPa	- Kilopascals
LPS	- Lipopolysaccharide
M	- Molar
mCi	- Millicurie
mg	- Milligrams
min	- Minute
mL	- Millilitre
mM	- Millimolar
mmol	- Millimoles
mol	- Moles
N	- Normal
NAD^+	- Nicotinamide adenine dinucleotide
NADH	- Nicotinamide adenine dinucleotide (reduced form

$NADP^+$	- Nicotinamide adenine dinucleotide phosphate
NADPH	- Nicotinamide adenine dinucleotide phosphate (reduced form)
NAG	- N-acetylglucosamine
NAM	- N-acetylmuramic acid
nCi	- Nanocurie
nm	- Nanometer
nmol	- Nanomoles
Δp	- Proton motive force
PEP	- Phosphoenolpyruvate
ΔpH	- Proton chemical gradient across the membrane
pH_i	- Internal pH
pH_o	- External pH
PHPr	- Phosphorylated HPr
PMF	- Proton motive force
PMS	- Phenazinemethosulphate
POPOP	- 1,4-Bis-2'(5'-phenyloxazolyl)benzene
PPO	- 2,5-Diphenyloxazole
Prot	- Protein
PTS	- Phosphotransferase system
RN'ase	- Ribonuclease
s	- Seconds
[S]	- Substrate concentration
$[S]_i$	- Internal substrate concentration
$[S]_o$	- External substrate concentration
TCA	- Tricarboxylic acid cycle

TEG	- Toluene ethylene glycol monoethyl ether
TMG	- Thiomethyl-β-D-galactoside
$TPMP^+$	- Triphenylmethylphosphonium
Tris	- Tris(hydroxymethyl)aminomethane
U	- Unit
μ	- Micron
$\Delta\Psi$	- Electrical potential difference across the membrane
[U-^{14}C]	- Uniformly labelled carbon-14 compound
μCi	- Microcurie
μg	- Microgram
$\Delta\mu H^+$	- Electrochemical proton gradient
μL	- Microlitre
μmol	- Micromole
Vmax	- Maximum velocity
w/v	- Weight per volume

CHAPTER I

INTRODUCTION

General Properties of the Genus Pseudomonas

The aerobic pseudomonas are gram-negative bacteria commonly found in soil and water, and are known to participate very actively in the process of mineralization of organic matter in nature. Due to their catabolic versatility and their fast rate of growth in simple media, they have been widely used to investigate numerous degradative pathways (1). Furthermore, Pseudomonas aeruginosa, normally an opportunistic pathogen, is the cause of considerable concern in medical practice (1,2).

Generally, the aerobic pseudomonads are straight or curved unicellular rods measuring 0.5 to 1 μm by 1.5 to 4 μm, though some strains of Pseudomonas putida have been found to exceed the maximum length of 4 μm. These cells are motile by means of one or more polar flagella. This is illustrated by the photographs of Pseudomonas viridiflava and Pseudomonas stizolobii in Figure 1 (1).

The energy yielding metabolism in these organisms is respiratory, never fermentative or photosynthetic (1). Molecular oxygen is used as the terminal oxidant, but some members of the group can live anaerobically in media containing nitrate and a carbon source which does not require oxygen for the initial metabolic reactions.

Figure 1

Cells of P. viridiflava and P. stizolobii. [From Palleroni (1).]

Legend:

Left; P. viridiflava, negative staining with uranyl acetate.

Right; P. stizolobii, chromium shadowing

Figure 1

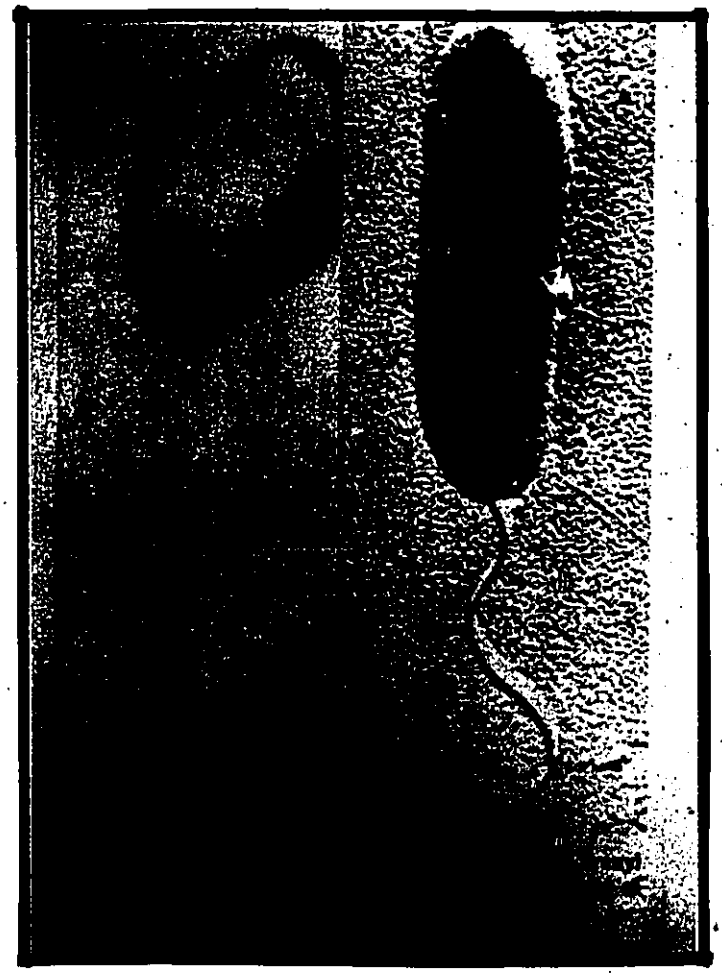

Examples of these are P. aeruginosa, Pseudomonas flourescens (biotypes B, C, and D only) and Pseudomonas stutzeri (3). All members are chemoorganotrophs, but some species such as Pseudomonas facilis and Pseudomonas ruhlandii are facultative chemolithotrophs capable of using hydrogen as an energy source (1,4). P. flourescens, P. aeruginosa and P. putida are members of a group of pseudomonads which produce water-soluble flourescent-type pigments in many different media and are consequently referred to as flourescent pseudomonads (1).

The Cell Envelope of Gram-Negative Bacteria

The cell envelope of gram-negative bacteria is represented schematically in Figure 2 (5). It is comprised of five regions; the outer membrane, the peptidoglycan layer, the inner and outer periplasmic space and the cytoplasmic membrane. The outer membrane consists of glycolipids, phospholipids and lipopolysaccharides (LPS) arranged to form a lipid bilayer and serves as a permeability barrier against various hydrophilic compounds. Most of the phospholipids are found in the inner leaflet of the outer membrane while the glycolipids and LPS are found in the outer leaflet. The general features of LPS are illustrated by the LPS structure of Salmonella typhimurium (Figure 3). It is an unusual molecule consisting of three regions; lipid A, core oligosaccharide and O side chain (6). Lipid A is a phospholipid which contains no glycerol and instead, utilizes D-glucosamine as a skeleton. Five

Figure 2

Schematic Diagram of the Cell Envelope of Gram-Negative Bacteria.

Legend:

BP - Binding Protein

CM - Cytoplasmic Membrane

OM - Outer Membrane

PC - Porin Channel

PG - Peptidoglycan

PS - Periplasmic Space

TP - Transport Protein

Lipopolysaccharide (LPS)

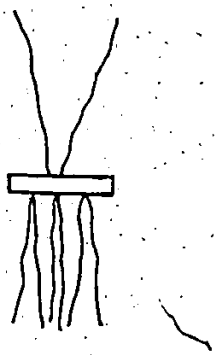

Polysaccharide

Glucosamine

Hydrocarbon Chains

Phospholipid

Polar Head Group

Hydrocarbon Chains

Figure 2

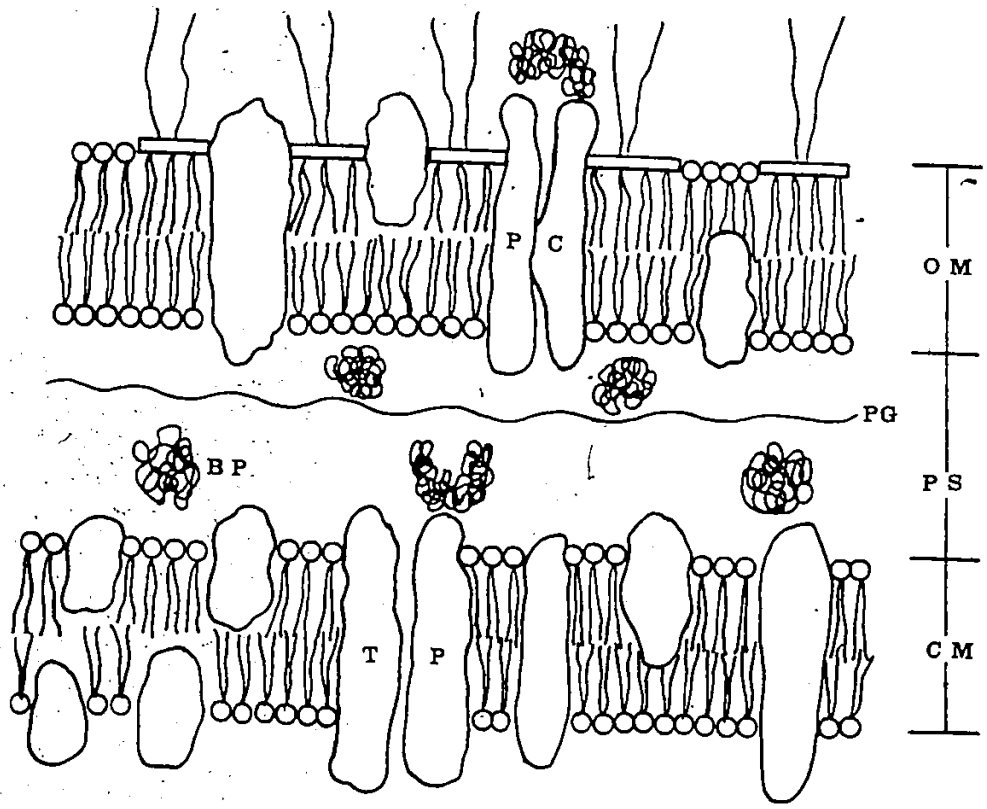

Figure 3

A. Lipopolysaccharide Structure of S. typhimurium [From Nikaido (6)].

Legend:

Abe-OAc - Abequose (O-Acetylated)
CO - Core Oligosaccharide
EtN - Ethanolamine
FA - Fatty Acyl Chain
Gal - Galactose
Glc - Glucose
GlcN - Glucosamine
GlcNAc - N-Acetyl-Glucosamine
Hep - Heptulose
KDO - 2-Keto-3-Deoxyoctonate
LA - Lipid A
Man - Mannose
OSC - O Side Chain
P - Phosphate
PP - Pyrophosphate
Rha - α-L-Rhamnose

—●—(14)— 3-OH-tetradecanoic acid
—(12)— dodecanoic acid
—(14)— tetradecanoic acid
—(16)— hexadecanoic acid

The structure shows a pyrophosphate bridge between the lipid A regions of two basic "monomer" units of LPS. All sugar residues are α-anomers except where β-conformation is specified.

B. Structures of Some Rare Sugars Found in Lipopolysaccharides.

Legend:

Same as that for (A) above.

Figure 3

A.

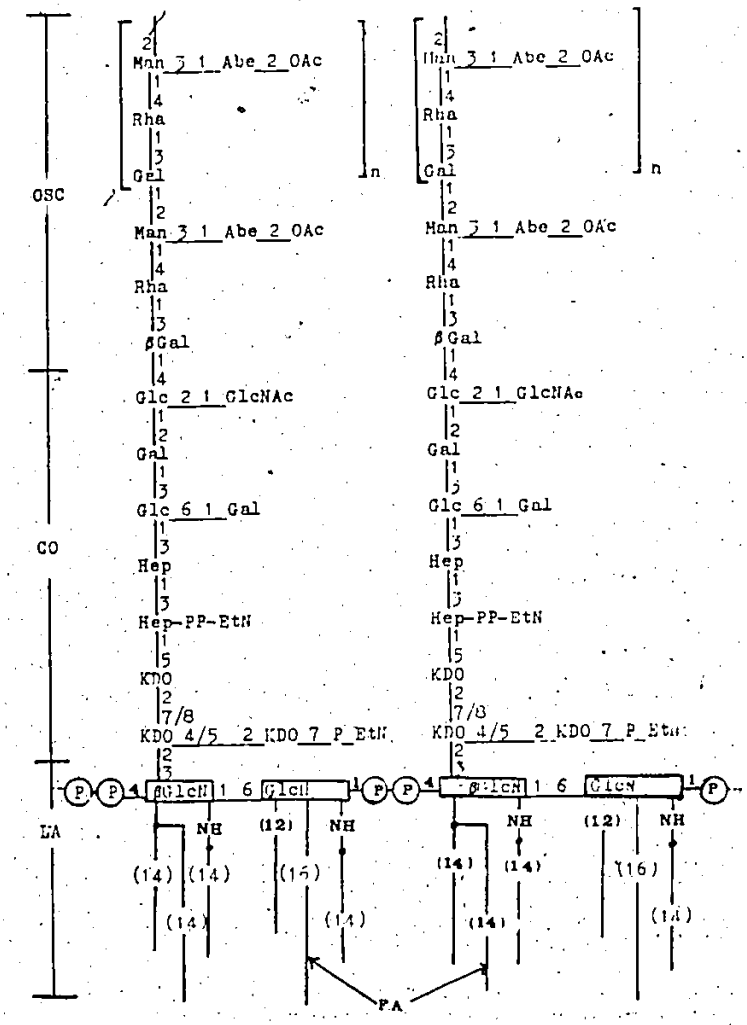
OSC
CO
LA
Man 3 1 Abe 2 OAc
Rha
Gal
n
Man 3 1 Abe 2 OAc
Rha
βGal
Glc 2 1 GlcNAc
Gal
Glc 6 1 Gal
Hep
Hep-PP-EtN
KDO
KDO 4/5 2 KDO 7 P EtN
P
βGlcN 1 6 GlcN
NH
(12)
(14)
(16)
PA

B.

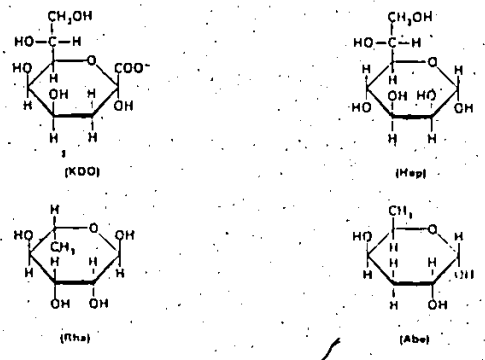
(KDO)
(Hep)
(Rha)
(Abe)

saturated fatty acid chains, including three 3-hydroxy-tetradecanoic acid residues are linked to the free hydroxyl and amino groups of the two glucosamine residues via ester and amide linkages respectively. A sixth saturated fatty acid is ester-linked to the hydroxyl group of a 3-hydroxy-tetradecanoic acid residue. The core oligosaccharide region contains ten sugar units while the O side chain is made up of repeating tetrasaccharide units. LPS is arranged in the outer leaflet such that the antigenic polysaccharide chains extend towards the external hydrophilic environment. This arrangement confers antigenic and serological properties on the outer membrane (7). The cytoplasmic membrane is also a permeability barrier of the bacterium. Unlike the outer membrane, the cytoplasmic membrane consists entirely of a phospholipid bilayer (Figure 2) and acts as the site of oxidative phosphorylation (7). The proteins embedded in both lipid bilayers may or may not span the entire thickness of the membrane. Sandwiched between the two bilayers is the periplasmic space within which the rigid peptidoglycan layer is situated. This layer separates the periplasmic space into its inner and outer regions and is composed of glycan strands that are interconnected through peptide chains [Figure 4a (8)]. The glycan moiety consists of linear strands of alternating β-1,4-linked pyranoside-N-acetyl-glucosamine (NAG) and N-acetylmuramic acid (NAM) residues. These bonds are susceptible to cleavage by egg white lysozyme (5). The carboxyl of the lactyl groups of NAM

Figure 4a

A Portion of the Peptidoglycan Monolayer of Escherichia coli.

Legend:

D-Ala - D-Alanine

L-Ala - L-Alanine

D-Glu - D-Glutamic Acid

G - N-acetyl-glucosamine

M - N-acetyl-muramic acid

$\frac{(L)}{DAP}$ - Meso-diaminopimelic acid

$\frac{}{(D)}$

----→ - Interpeptide linkage

——→ - Intrapeptide linkage

Figure 4b

Basic Structural Unit of the Peptidoglycan Monolayer.

Legend:

NAG - N-acetyl-glucosamine

NAM - N-acetyl-muramic acid

Figure 4a

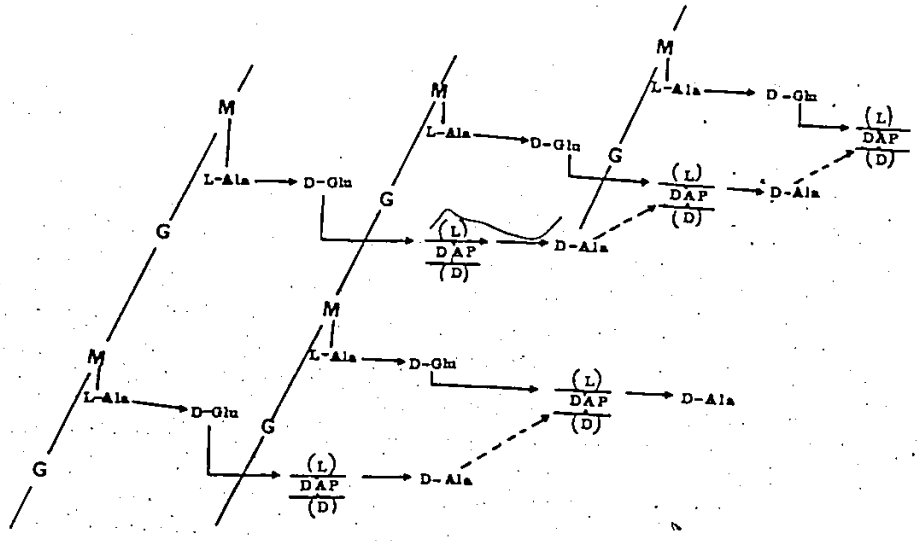

Figure 4b

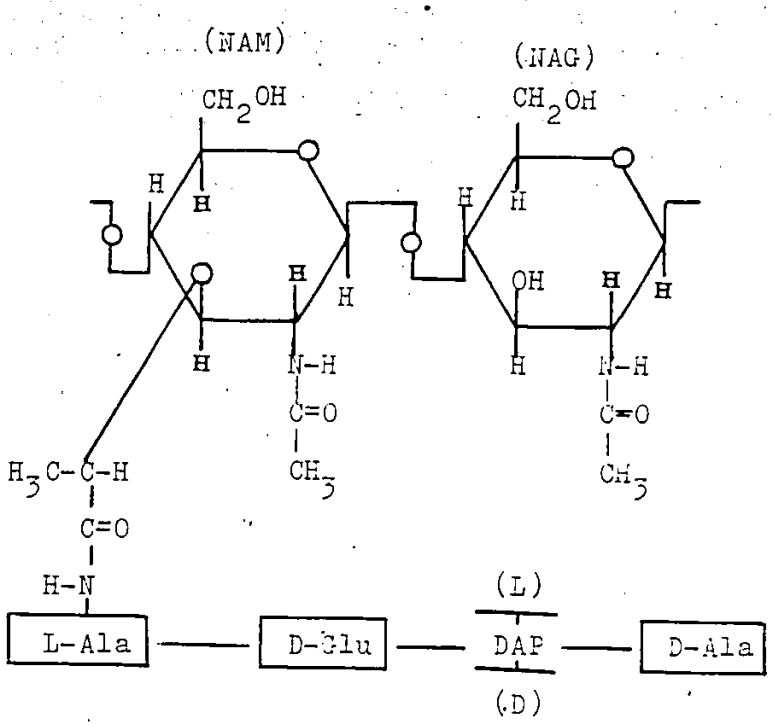

provide the point to which peptides are amide-linked to the glycan strands [Figure 4b (9).] In chemotype I, a group to which Escherichia coli and probably all other gram-negative bacteria belong, the interpeptide bond is a D-alanyl-(D)-meso-diaminopemelic acid linkage and occurs at a C-terminal position (8,9). The peptidoglycan layer confers shape and mechanical strength on the bacterium and its loss causes protoplast formation and osmotic instability. Also located within the inner and outer periplasmic space are the low molecular weight periplasmic binding proteins (below 50,000) which may either be associated with the cell wall components or exist in the free form (5,7,10).

The cell envelope of gram-negative bacteria forms a hydrophobic barrier through which hydrophilic nutrients must be transported from the external environment to the cytoplasm where metabolism occurs. During translocation the solute may interact with the proteins located in more than one of the four regions of the cell envelope. It is now well established that the outer membrane proteins are involved with the uptake of certain solutes that are relatively large in size and are likely to be present in the medium at low concentrations (5,11). An outer membrane receptor for vitamin B_{12} has been identified in E. coli. This protein is a required component of a unique and highly specific transport system; it interacts directly with the substrate with high affinity and may itself take part in

catalyzing substrate transport (11). Lo and Bewick demonstrated that the matrix protein in the outer membrane of E. coli (also referred to as protein I or porin) is the only outer membrane integral protein actively involved in dicarboxylate transport (12). It is however, unable to serve as an efficient and specific transport channel for dicarboxylic acids in the absence of functional cell surface dicarboxylate binding proteins (DBP). Thus the cell surface DBP seems to bind to the porin channels and confer substrate recognition properties on the otherwise nonspecific porin channels (5,12). Evidence has also been presented which suggests that 4-deoxy-4-fluoro-D-glucose binds to an inducible/repressible protein located in the outer membrane of P. putida, with subsequent flouride release (13). The proteins in the cytoplasmic membrane (14,15) as well as the periplasmic space (16,17) also play a major role in catalyzing solute translocation. A detailed discussion of these two catalytic systems will be presented in the next section.

In view of the complex nature of the cell envelope, it is virtually impossible to understand the molecular mechanisms involved in solute transport using kinetic data derived from whole cell studies without a knowledge of the individual protein binding steps of the four regions of the cell envelope. In addition, a meaningful kinetic analysis of transport systems is complicated by subsequent metabolism of the transported solutes. To circumvent these problems, bacterial cytoplasmic membrane vesicles are now widely used

as models for studies of active transport. Membrane vesicles, prepared by osmotic shock of spheroplasts, have been shown to be predominantly right-side out and capable of carrying out active transport of several metabolites (18). These vesicles are devoid of cytoplasmic contents and their metabolic activities are restricted to those provided by the enzymes bound to the cytoplasmic membrane. Thus the energy source for the transport of a particular substrate can be determined by studying which substrates stimulate solute accumulation. The use of membrane vesicles for studying transport processes however, has its disadvantages. The vesicles may not behave in the same manner as the intact organism, especially when outer membrane and periplasmic space proteins are involved in solute transport. Moreover, two populations of vesicles, half right-side out and half inside-out and/or one population of vesicles with each vesicle being a mosaic of differently oriented patches of membrane could be produced (19). It may seem that no matter how carefully vesicles are prepared they are still artifacts, and *in vitro* studies with them may be inadequate to determine *in vivo* mechanisms. Their value for biochemical investigations is unquestionable, but data obtained from studies using vesicles need to be complemented with results from whole cell studies before unambiguous conclusions about the physiological form of the membrane can be drawn. This combined approach has been used to investigate different mechanisms of solute transport across the cell envelope of gram-negative bacteria.

Energy Coupling Mechanisms of Active Transport in Gram-Negative Bacteria.

In recent years a great deal of research has been directed towards the elucidation of molecular mechanisms by which hydrophilic compounds are transported through the hydrophobic cell barrier of procaryotic and eucaryotic cells. The universality of nutrient transport mechanisms in bacteria and eucaryotes is becoming apparent. Bacteria have evolved a variety of mechanisms for nutrient acquisition. In one translocation process termed "simple diffusion", the solute moves down a concentration gradient until it equilibrates across the cytoplasmic membrane (18). The solute does not interact specifically with any molecular species in the membrane. This process is probably not very significant in bacteria when solutes are present in the external environment at very low concentrations. Alternatively, the solute may be transported by a process termed "facilitated diffusion". This process catalyzes the rapid equilibration of substrates across the cytoplasmic membrane and differs from simple diffusion in the sense that the solute interacts specifically with membrane components. Neither of the above mechanisms requires metabolic energy, nor do they lead to solute accumulation against concentration gradients. The facilitated diffusion process is exemplified by glycerol transport in E. coli (20,21). Hayashi and Lin showed that the Km of glycerokinase for its substrate (1.3 μm), and the Km of intact cells for the

uptake of glycerol (0.9 μm), were similar in E. coli mutant strains possessing glycerokinase activity but lacking L-α-glycerolphosphate dehydrogenase activity (20). These cells were able to accumulate labelled glycerol as L-α-glycerophosphate whereas mutants of E. coli lacking glycerokinase transported but could not accumulate labelled glycerol. Unfortunately no kinetic studies were carried out with the glycerokinase deficient mutants. These findings suggest that any accumulation of glycerol was due to trapping of glycerol by the action of glycerokinase rather than the transport process itself. This may serve as an energy conserving mechanism since a concentrative uptake of glycerol will be accompanied by a rapid passive efflux due to its fair solubility in the lipid bilayer. The facilitator thus serves to supply saturating amounts of glycerol to glycerokinase (20,22).

Solute translocation processes which are coupled to metabolic energy are referred to as "active transport systems." These systems are capable of accumulating substrates within the cell and may involve a conformational change of the carrier structure while the solute passes from one side of the membrane to the other. Active transport systems are classified according to the source of metabolic energy providing the force for the conformational change of the carrier structure. The three basic active transport mechanisms known to occur in gram-negative bacteria are "group translocation", "osmotic shock-sensitive" and "proton linked" systems.

Various models describing the molecular mechanisms by which carrier-mediated transport processes occur have been reviewed (5,18) and will not be presented here. However, experimental evidence to date, concerning these different transport mechanisms are presented below.

Group Translocation

Group translocation processes, generally known as the phosphoenolpyruvate-dependent phosphotransferase system (PTS), are absent in strict aerobes but are widely distributed in facultative and obligate anaerobes which metabolize sugar via anaerobic glycolysis (i.e. Embden-Meyerhof pathway) to yield phosphoenolpyruvate (PEP) (23). This renders sugar transport via PTS beneficial to these organisms. PTS is unique in that the substrate is chemically altered during transport. It was first discovered by Kundig et al. in E. coli (24), and is now the subject of several published review articles (25-28). In summary, the transport process catalyzes the transfer of phosphate from PEP to certain carbohydrates according to the reaction scheme shown in Figure 5 (28). The phosphoryl group of PEP is transferred to enzyme I and then to HPr (a heat stable low-molecular-weight protein). The phosphorylated HPr then transfers its phosphoryl group to enzyme III, a peripheral membrane protein that interacts with enzyme II, the actual transport channel. Enzyme III finally transfers its phosphoryl group to the sugar that is being transported. The sugar phosphate derivatives cannot

Figure 5

Reaction Scheme for the PEP-dependent Phosphotransferase System.

Legend:

CM - Cytoplasmic Membrane

HPr - Low-Molecular -Weight Heat Stable Protein.

PEP - Phosphoenolpyruvate

II - Enzyme II

III - Enzyme III

Figure 5

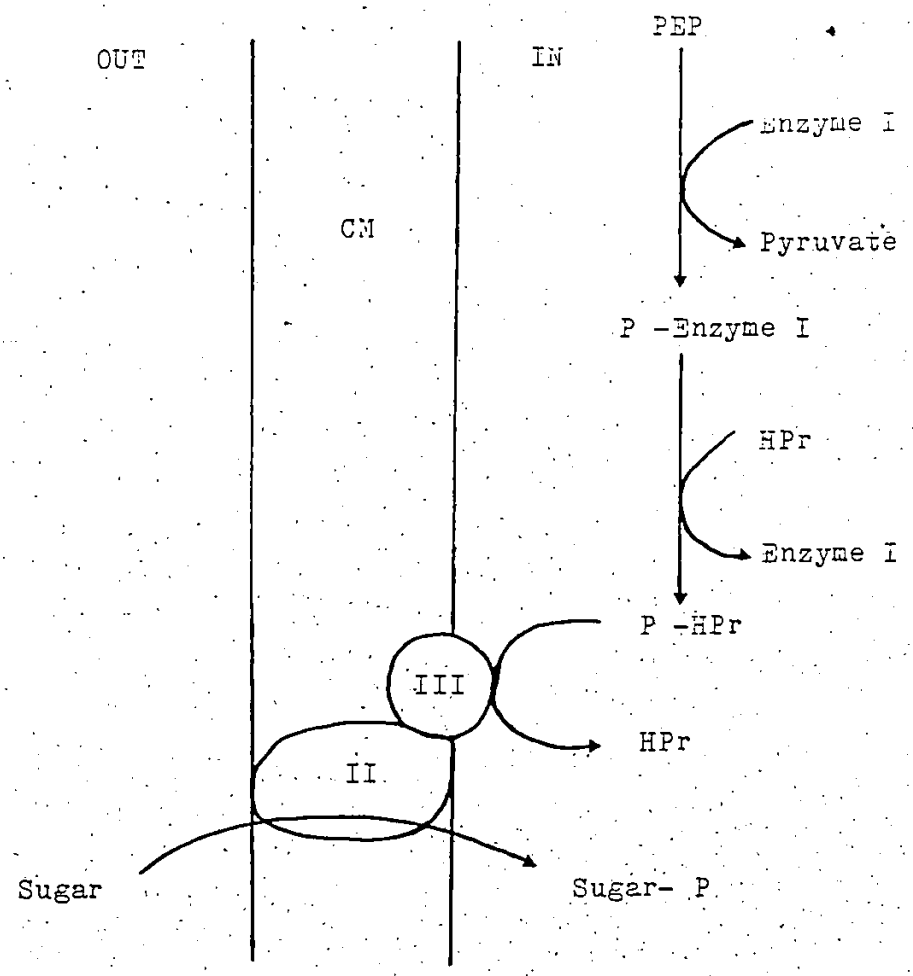

Overall Reaction is:

PEP + Sugar ⟶ Sugar- P + Pyruvate

cross the cytoplasmic membrane and are trapped intracellularly (25). HPr and enzyme I are predominantly soluble proteins which are synthesized constitutively by the bacterial cells. Enzyme II and III are inducible (or derepressible) membrane bound proteins which serve as the sugar recognition components of the system. HPr has been purified to homogeneity from several strains of bacteria (25). Recently Enzyme I was also purified to homogeneity by Weigel et al. from S. typhimurium. (29).

Glucose, fructose, mannose and several other PTS sugars are phosphorylated by the PTS in E. coli (25). Other faculative anaerobes such as Salmonella (25), Photobacterium and Beneckea (30) also possess the PTS. Several seemingly divergent organisms have the characteristic of possessing a single fructose-specific PTS, for example Bacteroides symbiosus (31), an anaerobe and Pseudomonas (32), a strict aerobe were both shown to transport fructose via a fructose-specific PTS. Fructose is however phosphorylated in the C-1 position as opposed to phosphorylation in the C-6 position of other sugars. Recently Durham and Phibbs (33) showed that fructose is catabolized via a phosphoenolpyruvate: fructose-1-phosphate system (F-PTS) in P. aeruginosa. The F-PTS was induced in cells grown on fructose and required a minimum of two components, a soluble enzyme I (molecular weight of 72,000) and a membrane-associated enzyme II complex. Attempts to demonstrate a separate intermediary phosphocarrier protein such as HPr were unsuccesful (33).

Bernsman et al. (34) presented evidence to show the existence of a PEP-dependent inducible gluconate-specific PTS in the gram-positive bacteria, Streptococcus faecalis. Jin and Lin (35) demonstrated that an enzyme II complex of the phosphoenolpyruvate: dihyroxyacetone PTS was induced in E. coli grown on dihydroxyacetone (DHA) as a sole carbon source or in its presence. Thus DHA is accumulated as dihydroxyacetone phosphate. This represents the first example of a triose that can be acted upon by the PTS to provide a central intermediate in glycolysis.

From in vitro studies with purified proteins from E. coli, Misset and Robillard presented evidence which was consistent with phosphoenzyme I acting as an intermediate in the reaction which catalyzes phosphoryl-group transfer from PEP to HPr (36). The active enzyme I molecule is a dimer which at low concentrations dissociate into inactive monomers. The kinetic data presented indicates that HPr and its phosphorylated form (PHPr) occupy binding sites on enzyme I that do not overlap with the binding sites for PEP and pyruvate. Furthermore, interactions can occur between HPr and enzyme I irrespective of their phosphorylated states. Since phosphorylation and transport of PTS sugars are coupled processes, the correct definition of the physical mechanism of enzyme II-catalyzed transport will depend on the correct definition of the phosphorylated state of this enzyme. Misset et al. (37) showed that both the phosphoryl-group transfer from PHPr to glucose or α-methyl-glucose and from glucose-6-phosphate to these same sugars

proceed according to a ping pong mechanism in which a phosphorylated membrane bound enzyme II acts as an obligatory intermediate. Their *in vitro* results, together with data published by other investigators, lead to the proposal of a model describing sugar phosphorylation and transport *in vivo*. (Figure 6). According to this model, unphosphorylated enzyme II(a) has affinity primarily for phosphate donor and does not allow penetration of sugar through the membrane under normal circumstances. A phosphate donor binds enzyme II from the cytoplasmic side (b), becomes phosphorylated (c), and releases the donor (d). The phosphorylated enzyme II undergoes a conformational change which creates a sugar binding site(s), available from the outside probably via a channel. After sugar binding (e), the phosphoryl group is transferred from the enzyme to the sugar (f) and the carrier reverts to its original unphosphorylated conformation which prevents sugar phosphates from leaking out.

In addition to solute translocation, bacterial PTS also serves several important and diverse roles in bacterial cell physiology (25). These include its involvement in chemotaxis towards its substrates and its regulation of adenylate cyclase as well as certain non-PTS permeases (25, 38).

Osmotic Shock-Sensitive Active Transport Systems

Osmotic shock-sensitive active transport systems utilize a chemical form of energy such as ATP or some

Figure 6

Proposed Model Describing Sugar Phosphorylation and Transport. [From Misset et al. (37).]

Legend:

II - Enzyme II

CM - Cytoplasmic Membrane

CYT - Cytoplasm

D - Unphosphorylated Donor

Glc - Glucose

G-6-P - Glucose-6-phosphate

P-D - Phosphorylated Donor

Figure 6

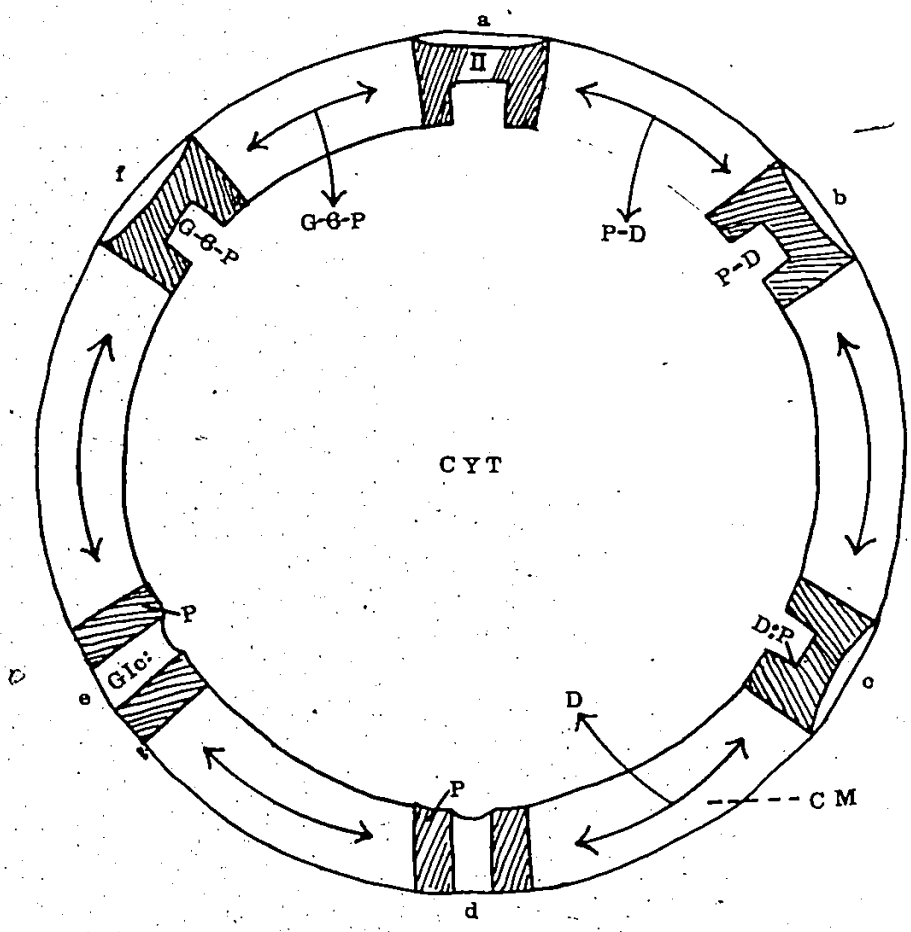

closely related covalent compound to accumulate substrates against a concentration gradient without chemical modification. These shock-sensitive systems involve the participation of substrate binding proteins normally retained within the periplasmic space of gram-negative bacteria (22). Many such transport systems have been reported for the uptake of carbohydrate (39,40,41), amino acids (17,39) and dicarboxylic acids (41) in gram-negative bacteria.

One of the most extensively investigated shock-sensitive systems is the maltose transport system of E. coli (42, 43). Genetic and biochemical evidence presented below suggests that periplasmic binding proteins may play an essential role in whole cell transport (22,42,44). (i) EDTA-osmotic shock treatment of E. coli causes the release of periplasmic maltose binding proteins with a concomitant loss of maltose uptake activity. (ii) A loss of periplasmic binding proteins also occurs during vesicle prepartion, thus the inability of vesicles to accumulate substrates transported exclusively by binding protein systems. (iii) Both the binding protein and the transport system exhibit similar substrate specificity and affinity. (iv) Inhibitors for the binding protein (e.g. N-ethyl-maleimide) usually inactivate the transport system as well. (v) Both maltose binding protein and transport activity are induced more than 10-fold by growth on maltose. (vi) Mutants defective in the binding protein are unable to transport

maltose. (vii) The genetic expression of the binding protein and the transport system are coregulated. Ferenci et al. (43) observed that uncouplers of oxidative phosphorylation (DNP, azide and CCCP) only partially inhibited maltose accumulation. Furthermore, fructose (a glycolytic energy source) stimulated maltose uptake much more than D-lactate in an adenosine triphosphatase (ATPase) negative mutant. This could be explained by the fact that the lowering of ATP pools by the uncouplers is compensated for by ATP pools supplied by substrate level phosphorylation. In mutants lacking ATPase the effect of oxidative phosphorylation uncouplers on primary active transport is greatly reduced compared with the effect on wild-type cells, because most of the ATP pool arises from substrate level phosphorylation and the dependence on oxidative phosphorylation for ATP is eliminated (43). Secondly, the maltose transport system was inactivated by arsenate which acts by reducing ATP pools. Both observations indicate that the shock-sensitive system is a primary active transport system because chemical energy is directly coupled to the uptake process.

Romano et al. (45) showed that the energization of glucose transport in whole cells of P. fluorescens is dependent upon the presence of shock-sensitive glucose binding proteins and phosphate bond energy rather than a proton-motive force-dependent glucose carrier system in the cytoplasmic membrane. Inducible binding proteins for C_4-dicarboxylic acids and glucose were isolated from

P. aeruginosa (41), and the glucose binding glycoprotein purified to homogeneity (46). Contrary to numerous observations implicating ATP as the immediate energy source for shock-sensitive systems (47,48,49), Plate et al. (50) showed that abolishing the proton-motive force in an ATPase negative mutant strain of E. coli with colicin K resulted in inhibition of the shock-sensitive transport systems, even though ATP levels were unaffected. Other investigators also demonstrated energy-coupling defects for both primary and secondary active transport systems in temperature-sensitive mutants strains of E. coli even when ATP pools were elevated, and concluded that binding protein-dependent transport is not directly coupled to chemical energy, but is energized indirectly through an energy-transducing component common to all active transport systems (51). Acetyl-phosphate has also been implicated as the immediate energy source for binding protein-dependent transport systems (52).

It is conceivable from the above discussion that substrate binding proteins in the periplasmic space facilitate solute translocation across this region to the cytoplasmic membrane components and/or maintain a substantial pool of the substrate in the periplasmic space for subsequent transport across the cytoplasmic membrane. However, nothing is known about the mechanisms by which the binding proteins specifically translocate solutes across the outer and inner periplasmic space. It has been demonstrated by genetic means that a specific site(s) is present on the histidine binding protein (His J gene product) for

recognition of the membrane bound His P gene product, and vice versa, and these sites are essential for histidine transport (53,54). This suggests that specific physical interactions between the binding proteins and specific membrane transport component(s) are required for solute translocation. Observations made by various investigators have been discussed by Boos (44). Thus, all mutations that specifically affect maltose transport have been mapped in the mal B region of the E. coli chromosome at 91 min of the linkage map; present in this region are the lamB, malK, malE, malF and malG genes; the product of the malK gene is closely associated with an integral protein of the cytoplasmic membrane (a malG product); the malK gene exhibits homology with the structural gene for the respiratory NADH dehydrogenase; membrane vesicles in the presence of glutamine binding protein can be stimulated to transport glutamine by pyruvate and NADH, suggesting an oxido-reduction mechanism; the maltose binding protein changes its conformation upon binding maltose or maltodextrins; the maltose binding protein interacts with the inner-membrane protein of the maltose system; the molecular mechanism by which energy is channelled into substrate translocation is not mediated via proton symport even though some evidence has been presented which points to the participation of a proton-motive force in maltose transport. Based on these observations a model was presented (Figure 7). Maltose binds to MBP' (unloaded maltose binding protein) resulting in a conformational

Figure 7

A Model for the Unidirectional Energy-Dependent Transport of Maltose by the Mal-B-Dependent Transport System. [From Boos (44)].

Legend:

M : Maltose

MBP' and MBP : Two different conformations of the maltose-binding-protein.

F, G and K : Gene products of malF, malG and MalK respectively.

A, B, C and D: Different conformations of the F-G-K complex. A is the energized complex. B, C and D follow in sequence and are characterized by decreasing conformational energy.

Figure 7

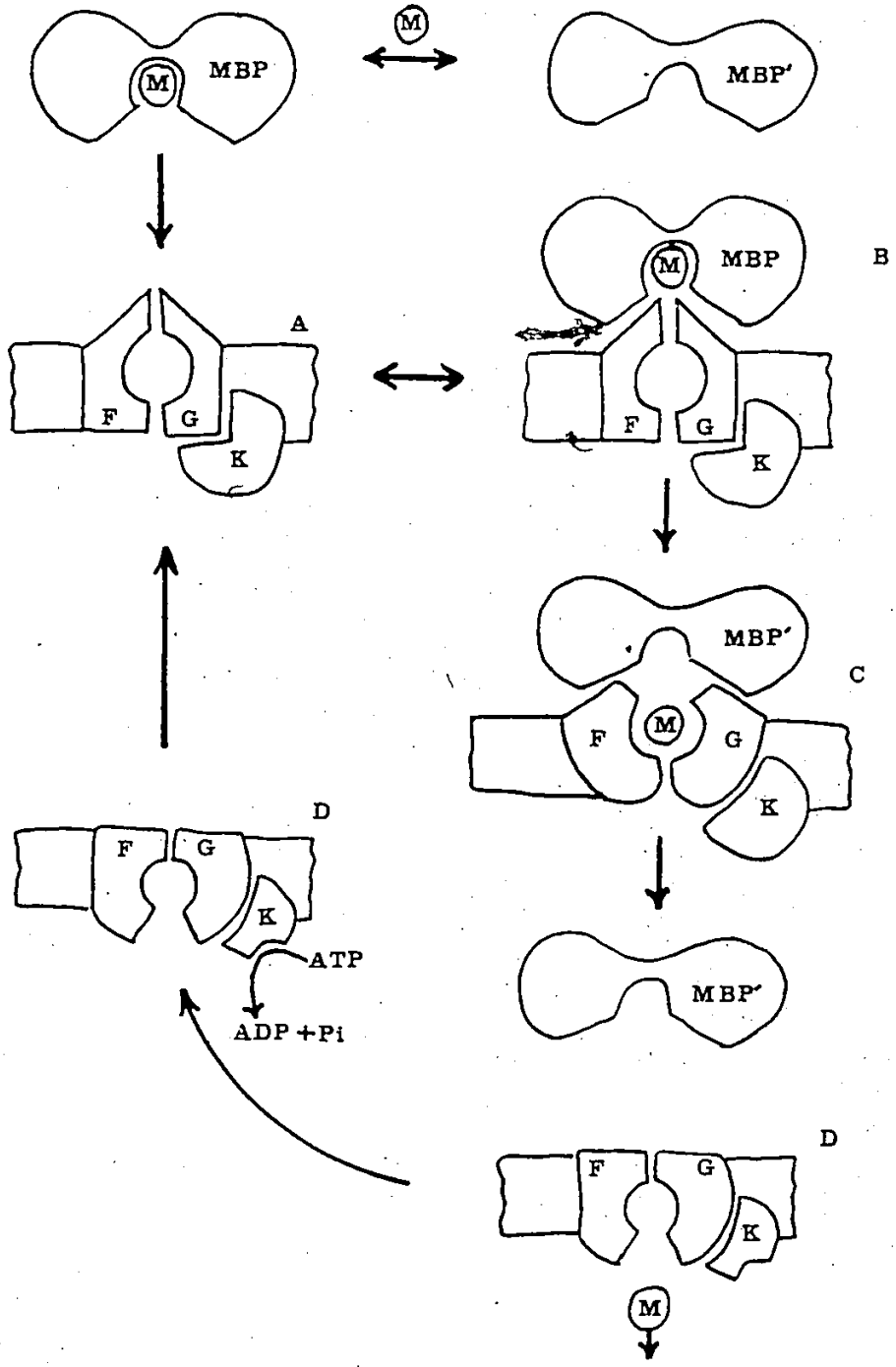

change. MBP (loaded maltose binding protein) then interacts with the energized F-G-K complex (A) of the cytoplasmic membrane (B), creating a pore through which maltose passes (C). After passage of maltose the pore collapses (D), and MBP reverts to the conformation of MBP'. The cycle begins after the F-G-K complex is re-energized by the action of the K-protein functioning as an ATPase or oxido-reductase; the energy expenditure may be stored in the alteration of protein conformation. This is however, only a working model, and requires extensive experimental testing.

Proton-Linked Active Transport

A mechanism for coupling respiration to transport can be envisaged in terms of Mitchell's chemiosmotic hypothesis (55,56,57). Briefly, he postulates that biological oxidations via the electron transport system or ATP hydrolysis via the membrane-bound Ca^{2+}-Mg^{2+}-ATPase result in the translocation of protons outward, thereby generating an electrical potential (interior negative) and, under certain conditions, a pH gradient (interior alkaline) across the membrane. These gradients together constitute an electrochemical potential of protons ($\Delta\bar{\mu}H^+$), which is given by the expression:

$$\Delta\bar{\mu}H^+ = F.\Delta\psi - 2.3RT\Delta pH \quad \ldots\ldots (1)$$

where F is the Faraday constant, $\Delta\psi$ is the electrical potential across the cytoplasmic membrane, R is the gas constant, T is the temperature in degrees Kelvin and ΔpH is

the proton chemical gradient. The expression for the proton-motive force (Δp), which acts as the driving force for several energy-requiring processes in the cytoplasmic membrane can be obtained by rearranging equation (1) in a form similar to the one describing the electron-motive force of an electrochemical cell, i.e.,

$$\Delta p = \Delta\bar{\mu}H^+/F = \Delta\psi - 2.3RT.\Delta pH/F = \Delta\psi - Z\Delta pH \quad .....(2)$$

where Z is the combination of constants (2.3RT/F) and is approximately 60mV/pH unit at 37°C. Thus Δp across a biological membrane is analogous to the electron-motive force of a battery (22, 58).

Proton-linked active transport has been defined as secondary active transport, the primary transport event being the extrusion of protons via biological oxidation or ATP hydrolysis. The coupling of the Δp generated to the influx of solutes or ions occurs such that an endergonic process (solute accumulation) can be coupled to an exergonic process (protons moving down a concentration gradient). It has been suggested that the membrane is impermeable to both protons and hydroxyl ions, and chemiosmotically coupled transport is accomplished by virtue of carriers that translocate simultaneously, both protons and the particular solute. Mitchell proposed the terms "symport" (systems in which two substrates are transported simultaneously in the same direction by the same carrier) and "antiport" (systems in which one carrier transports two substrates simultaneously, but in opposite directions) to define two basic mechanisms by which metabolites are linked to ion

transport (58). In uniport systems, the carrier transports only one substrate (58). These mechanisms are well described by the expression:

$$\log([S]_i/[S]_o) = [(n+m)\Delta\Psi - nZ\Delta pH]/Z \quad .....(3)$$

where i and o refer to the inner and outer aqueous phases respectively, $Z = 2.3RT/F$, m is the charge on S (the solute), and n is the number of protons associated with the transport of a mole of S. Equation (3) is useful for determining the component(s) of Δp required for solute accumulation as well as the concentration ratio $[S]_i : [S]_o$ which a solute can attain for a given value of Δp.

Considerable experimental evidence has been presented in favour of the chemiosmotic concept of sugar transport in bacterial systems (58-62). Generally, metabolic reactions such as glycolysis, respiration and ATP hydrolysis that energize the membrane and stimulate solute accumulation also generate a Δp across the membrane. In addition, reagents and conditions (for example proton-conducting uncouplers, valinomycin plus K^+ and other ionophores) that dissipate Δp also deenergize the membrane and inhibit solute transport. These are exemplified by the following observations (58-62). (i) S. faecalis (an anaerobe lacking a functional respiratory chain) is dependent on ATP hydrolysis via the membrane-bound Mg^{2+}-Ca^{2+}-ATPase for transport of some amino acids and K^+. Active transport is inhibited by the membrane bound ATPase inhibitor, DCCD, in these organisms while transport in mutants with DCCD-resistant ATPase is insensitive to DCCD. (ii) In E. coli β-galactoside

accumulation under anaerobic conditions is sensitive to uncouplers under conditions where ATP levels are unaffected, indicating that a proton gradient generated by hydrolysis of glycolytic ATP was involved in the accumulation of sugars. (iii) Both artificial electron donors, for example ascorbate/PMS, and natural electron donors such as D-lactate and succinate can drive solute transport in vesicles. Uncouplers which function as lipid-soluble proton conductors inhibit active transport by collapsing the proton gradient generated by respiration. Respiratory chain inhibitors also block solute transport, while high concentrations of arsenate (uncoupler of oxidation and substrate level phosphorylation) and DCCD had no effect on solute uptake in vesicles. (iv) Whole cells and membrane vesicles accumulate sugars and amino acids in response to artificially imposed $\Delta\Psi$ and/or ΔpH in the absence of any source of metabolic energy. Again, transport is abolished by proton conductors or ionophores but is unaffected by metabolic inhibitors.

An apparent shortcoming of the mechanism of proton-linked active transport was the observation that no correlation existed between the ability of vesicles to oxidize an electron donor and the ability of that electron donor to drive active transport. E. coli membrane vesicles oxidized succinate and NADH at a faster rate than D-lactate, yet D-lactate was more efficient in energizing the transport of lactose, amino acids (63) and succinate (64) in these vesicles. However, evidence was later presented to show

that the ability of an electron donor to drive transport depends on the ability of that electron donor to generate a $\Delta\Psi$ and/or a ΔpH during its oxidation. Thus D-lactate which generated $\Delta\Psi$ and ΔpH values of -70 mV and -120 mV respectively (65), was very efficient in stimulating transport (63), whereas NADH which does not generate either a $\Delta\Psi$ or ΔpH during its oxidation (65) was less efficient than D-lactate in energizing solute transport (63).

The transport of various solutes have been shown to be dependent on Δp or one of its components in bacterial systems (66,67,68). Evidence presented indicates that the uptake of thiomethyl-β-D-galactopyranoside (TMG) is driven by artificially produced Δp in energy depleted cells of E. coli (69). Active transport of D-lactate, L-lactate and C_4-dicarboxylic acids (succinate, malate and fumarate) in membrane vesicles of E. coli and a fresh water Pseudomonas species are mediated by specific transport systems which are linked to the electron transport chain (64). These substrates are not transported actively by membrane vesicles in the absence of electron donors. Similarly, transport of C_4-dicarboxylic acids in whole cells (70), C_5-dicarboxylate compounds (71), D-glucose and D-gluconate (72), in membrane vesicles of P. putida have been shown to be coupled to respiration. α-aminoisobutyrate transport in vesicles of P. fluorescens (73) and gluconate transport in vesicles of P. aeruginosa (74) are also coupled to respiration. Finally, Lagarde et al have shown in studies involving genetic and kinetic analysis, that 3-deoxy-2-keto-D-

gluconate and other monocarboxylic sugars are taken up against enormous concentration gradients in whole cells or isolated membrane vesicles of E. coli at the expense of respiration. They also presented evidence for a carrier-mediated system which is driven by both components of Δp (75-78).

The initial experimental evidence supporting coupling of substrate accumulation to chemical energy via proton symport was presented by West and Mitchell (67, 79). They demonstrated that the uptake of TMG caused proton influx against an electrochemical gradient in energy depleted cells of E. coli, resulting in alkalinization of the medium. They also showed that the flow of lactose and protons was stoichiometrically coupled by the porter with a ratio of 1:1. Their results were confirmed by later experiments by Collins et al. (80) which clearly illustrated the coupled movements (symport) of TMG and protons. Daruwala et al. have also demonstrated that addition of arabinose or fucose to an anaerobic suspension of energy depleted E. coli cells or membrane vesicles caused an external alkaline pH indicative of sugar-H^+ symport mediated by the membrane bound transport system; the alkaline pH shift was inhibited in the presence of the uncouplers DNP and CCCP (81). The uptake of D-galactose (82), glucose-6-phosphate (83), threonine (84) and proline (85) are all associated with proton movements in E. coli. The uptake of succinate, malate, fumarate and aspartate in lightly buffered medium is

also accompanied by H^+ uptake in cells of E. coli. Based on the observation that two protons entered the cell per molecule of substrate, it was concluded that the C_4-dicarboxylic acids were taken up in an electroneutral form, while aspartate was taken up in a cationic form (86). The pattern of inhibition of succinate by DNP and CCCP was similar to that of succinate-induced proton uptake. Robin and Kepes concluded from extra-cellular pH measurements and kinetic studies that during the early stage of net uptake of gluconate, electroneutrality is maintained by the ions of water (87). This could be achieved by the transport of undissociated gluconic acid; cotransport of the negatively charged gluconate ion with proton or counter transport of gluconate against hydroxyl ions.

Further experimental evidence in favour of the chemiosmotic concept of sugar transport was first provided by Drapeau and MacLeod who demonstrated a marked dependency of α-aminoisobutyric acid accumulation on Na^+ in a marine pseudomonad (88). Since then an increasing number of observations have shown that other bacterial transport systems catalyze a Na^+-substrate symport, with an electrochemical potential of Na^+ rather than a Δp acting as the driving force for solute accumulation. This has been the subject of several excellent reviews (22, 58, 89, 90). Since most bacteria do not possess a primary Na^+ pump, Mitchell proposed that Δp functions to maintain a transmembrane Na^+ gradient (Na^+ in < Na^+ out) through the activity of a Na^+-H^+ antiporter (57). A bacterial

Na^+-H^+ antiport activity was first reported in S. faecilis by Harold (91) and then in whole cells (92, 93) and membrane vesicles (94, 95) of E. coli. Borbolla and Rosen also presented results which are consistent with secondary exchange of Na^+ for H^+ catalyzed by an Na^+-H^+ antiporter (96). They showed that when energy starved cells of E. coli were passively loaded with $^{22}Na^+$, sodium efflux could be initiated by the addition of metabolic energy, the source of energy being a Δp. Thus in the presence of a Δp, the Na^+-H^+ antiporter functions to maintain internal Na^+ at a low level such that solute accumulation (an uphill process) can be coupled to Na^+ moving down a concentration gradient. It has also been shown that PMS/ascorbate stimulation of Na^+ efflux from E. coli membrane vesicles is prevented by the uncoupling agent, FCCP (97).

Na^+-substrate symport is very significant in alkalophilic bacteria (98). These Bacillus species grow at a pH range of 9 to 12, with an optimum pH between 10 and 11. Since their internal pH is maintained at or below 9.5, a large ΔpH, inside acidic, exists at almost all pH values at which growth occurs. Interestingly most of the obligately alkalophilic bacilli show an absolute requirement of Na^+ for growth. In these bacteria, an Na^+-H^+ antiporter presumably functions subsequent to primary proton pumping to establish net acidification of the cell or vesicle interior, while allowing generation of a $\Delta\Psi$, outside positive; i.e., the rate of inward H^+ translocation exceed that of H^+

pumping during respiration, thus acidifying the interior, but the total cations (Na^+ and H^+) extruded is greater than H^+ translocated in, thus producing a $\Delta\Psi$, positive outside in the form of an Na^+ gradient [Figure 8, (96)]. The actual stoichiometries of the processes are not yet known. Further information on the occurrence, properties and proposed roles of Na^+-H^+ antiporters in procaryotes may be obtained from a recent review article (98).

Quantitative estimation of Δp provides the most direct evidence for the existence of the state of "energization" in energy-transducing organelles. Various techniques are available for determining Δp, all of which involve the separate estimation of $\Delta\Psi$ and ΔpH.

The first of these techniques involves the use of optical indicators of $\Delta\Psi$ and ΔpH. The fluorescence of cationic cyanine dyes is quenched when there is a $\Delta\Psi$, negative inside, across the membrane (99). At specific concentrations of dyes and cells, the degree of quenching is proportional to the magnitude of $\Delta\Psi$. Other fluorescent dyes such as quinacrine (100) and 9-aminoacridine (101) are believed to respond to H^+ concentration at the membrane surface (102).

The second technique involves the use of ion-specific electrodes, such as the pH electrode, to detect movement of H^+ into and out of cells and vesicles (103). ΔpH can be calculated from the steady-state values, taking into account the buffering capacity of the external phase and the total

Figure 8

A Model of an Electrogenic Na^+/H^+ Antiporter Together With Primary H^+ Pumping (98).

Legend:

CM - Cytoplasmic Membrane

Figure 8

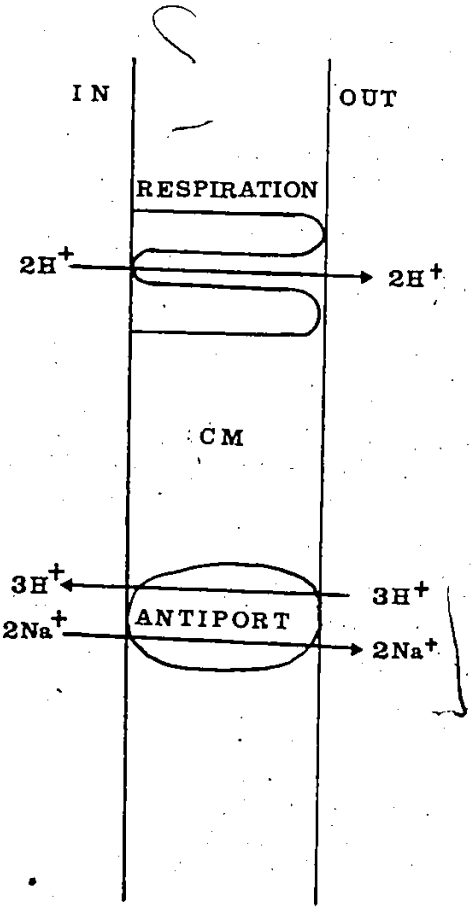

buffering capacity of the preparation (and hence the inner phase). Similarly, K^+-specific electrodes can be used when the membrane has been rendered permeable to K^+ by valinomycin, to determine K^+ ratio in:out (103). In this case the membrane potential can be calculated using the Nernst equation:

$$\Delta\Psi = -2.3RT/mF.\log([\text{cation}]_{in}/[\text{cation}]_{out}) \quad .....(4)$$

Thirdly, $\Delta\Psi$ and ΔpH can be estimated by isotope distribution. $\Delta\Psi$ generated, for example by proton translocation, can be detected by a second ion. This is based on the principle that the second ion will redistribute until electrochemical equilibrium is regained, and the resulting ion distribution will enable $\Delta\Psi$ to be estimated from equation (4). A number of radiolabelled artificial permeant cations such as DDA^+ (104) and $TPMP^+$ (65, 105) have been used as the second ion in bacterial systems. ΔpH can also be measured from the distribution of weak organic acids if the internal compartment of the system is more alkaline than the the external medium, or weak bases if the interior is more acidic than the exterior (63, 65). This measurement is dependent on the fact that weak acids such as acetate and propionate and bases, e.g. methylamine, can permeate the membrane in the uncharged form, while the ionized form remains impermeant. Thus if the internal compartment of the system is more alkaline than the external medium for instance, the equilibrium between the undissociated and dissociated species of the weak acid will be displaced towards the ionic form, which will accumulate

within that compartment. In these measurements, the cells are incubated with labelled substrates and usually separated from the incubation mixture by centrifugation or filtration through membrane filters. However, $\Delta\Psi$ and ΔpH can also be determined using the technique of flow dialysis which was first developed by Colowick and Womack (107) and adapted to bacterial vesicles by Ramos et al. (65). In this method, the concentration of the indicator in the incubation mixture is monitored continously by its rate of diffusion across a semipermeable membrane into a steady flow of medium. Again, $\Delta\Psi$ can be calculated from equation (4), while ΔpH can be calculated directly from a similar equation (106):

$$\Delta pH \text{ (in mV)} = 2.3RT/F.\log([\text{acid}]_{in}/[\text{acid}]_{out}) \ldots (5)$$

As mentioned earlier, various compounds such as ionophores and uncoupling agents which affect Δp also deenergize the membrane and inhibit chemiosmotically coupled solute transport. Ionophores are antibiotics which possess a hydrophobic exterior (rendering it lipid soluble), together with a hydrophilic interior to bind ion (108, 109). They function either as mobile carriers and diffuse across the membrane, or as channel formers. Valinomycin and monactin are mobile carriers which catalyze uniport of K^+, thereby transferring charge but not protons. Nigericin, another mobile carrier, loses a proton when it binds a cation, thus forming a neutral complex which can diffuse across the membrane. The protonated non-complexed form of nigericin is also mobile; this results in an overall electroneutral exchange of K^+ for H^+. "Uncouplers" or

proton translocators have dissociable protons and are permeable across bilayers in the protonated and deprotonated forms (108, 109). They increase the proton conductance of the membrane by shuttling across it. Examples of uncouplers are DNP, CCCP and FCCP.

The measurement of $\Delta\Psi$ and ΔpH in conjunction with the similar effects of uncouplers and ionophores on the magnitude of Δp and on active transport have been used to demonstrate the relationship between Δp and solute accumulation. Ramos et al (65) showed that the composition of Δp in energized E. coli vesicles depended on the external pH (pH_o). They observed a Δp of approximately -180mV at pH_o 5.5, the major component being a ΔpH of -110mV. Since the internal pH (pH_i) remains essentially at pH 7.5, a ΔpH could not be detected at pH_o of 7.5 while $\Delta\Psi$ remained at approximately -75mV at this external pH. They also demonstrated that ΔpH and $\Delta\Psi$ values can be manipulated by titrating with ionophores (valinomycin and nigericin) and the uncoupler CCCP. In experiments performed at pH_o of 5.5, valinomycin collapsed $\Delta\Psi$ and slightly increased ΔpH, while nigericin collapsed ΔpH and increased $\Delta\Psi$ from about -60mV to -90mV. CCCP collapsed both the ΔpH and $\Delta\Psi$ components of Δp. By similar titrations with valinomycin and nigericin, Ramos and Kaback (83) concluded that at pH_o of 5.5, one class of compounds is driven primarily by Δp (lactose, proline, serine, glycine, tyrosine, glutamate, leucine, lysine, cysteine and succinate) while another class is driven primarily by a ΔpH (glucose-6-phosphate,

D-lactate, gluconate and glucuronate). However, at pH_o of 7.5, all the transport systems are driven by $\Delta\psi$ which comprises the only component of Δp at this external pH. In experiments by Hirata et al. (110), an artificial $\Delta\psi$ was created by inducing electrogenic efflux of K^+ from K^+-loaded vesicles with valinomycin or monactin. Under these conditions, a transient accumulation of proline, glycine, lysine, lactose and TMG by the vesicles was observed.

It is apparent from the above discussion that solute accumulation can be coupled to ΔpH and/or $\Delta\psi$. In fact the chemiosmotic hypothesis implies that transport of organic acids or anionic sugars is dependent upon the chemical gradient of protons; the undissociated acid is transported through the membrane, and is presumed to accumulate in the ionized form due to the relative alkalinity of the internal compartment (83). Positively charged compounds are transported in response to $\Delta\psi$ while neutral substrates respond to Δp via proton-symporters (83).

Inspite of the large body of evidence amassed in favour of proton-linked active transport, the actual molecular events that occur during substrate translocation is still a controversial issue. Evidence presented for and against various models have previously been discussed elsewhere (60, 61).

In a recent article, Henderson et al. (111) pointed out that a common feature of all the sugar-H^+ symport systems

is the presence of essential thiol group(s). Furthermore, as reviewed by Konings et al. (112), (i) the redox state of these groups is determined by the redox potential of the environment and Δp; (ii) the proteins have a high affinity for solute in the reduced, dithiol form, and an affinity of at least a 100-fold lower in the oxidized form; (iii) there are two sets of dithiols on a non-movable carrier or channel which can undergo a dithiol-disulphide interchange reaction, with one set of dithiols located near the outer surface of the membrane while the other is located near the inner surface. Based on these observations, a model was proposed for a redox-controlled H^+-solute symport system [Figure 9, (112, 113).] When a $\Delta\Psi$, interior negative, or a ΔpH, interior alkaline, is imposed on the membrane, the equilibrium of the dithiol-disulphide interchange reaction is shifted towards the state in which all the outer sites are reduced high-affinity and the inner sites are oxidized low-affinity. Binding of ligand A to the outer high affinity site (a) is accompanied by binding of H^+ on the base B^-, located in the vicinity of the dithiol (b) causing a decrease both in the apparent pK of the dithiol and the midpoint potential of the redox transition. The result is the oxidation of the dithiol to a disulphide (c). Hydrogens move across the membrane (b) reducing the inner redox center and raising the pK of the inner base, BH. The base deprotonates (c), releasing protons into the inner solution. The change in redox states of the inner and outer sites causes the outer site to become low affinity and the

Figure 9

Proposed Model for a Redox-Controlled H^+-Solute Symport (112, 113).

Legend:

A - Solute

B - Base

Figure 9

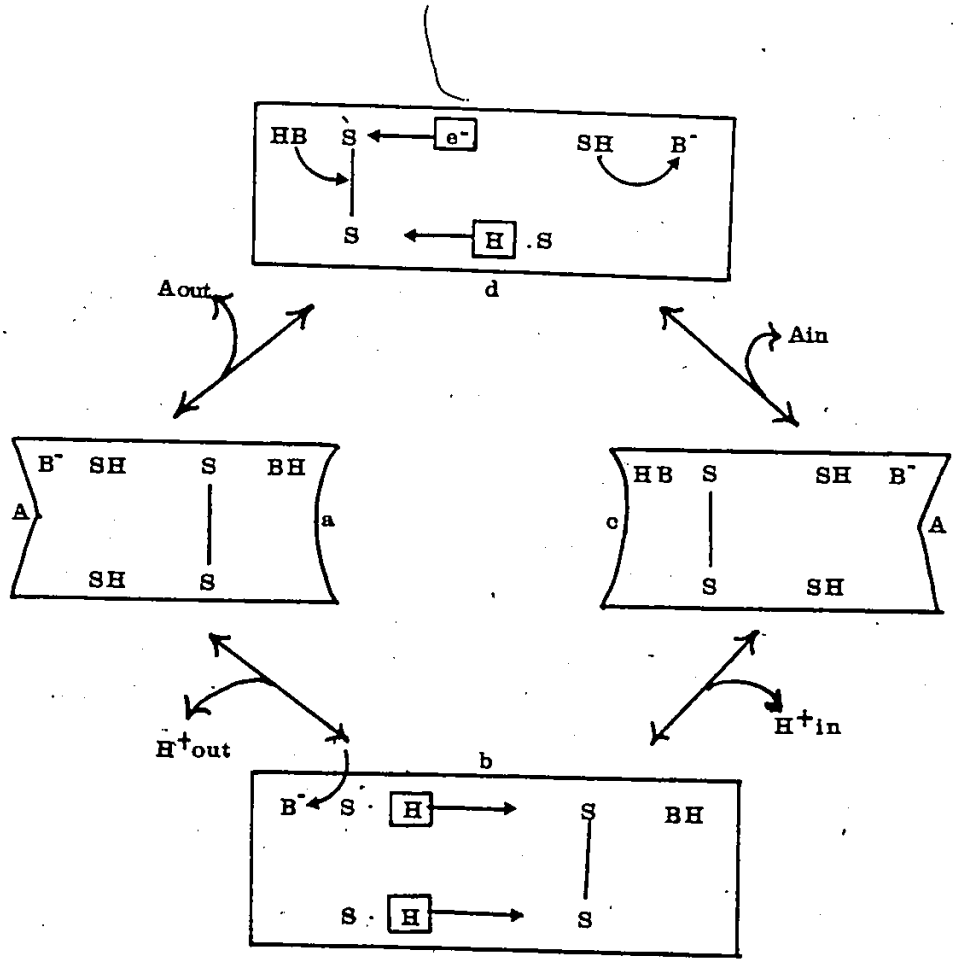
HB
S
e⁻
SH
B⁻
S
H
.S
d
Aout
Ain
B⁻
SH
S
BH
A
a
SH
S
HB
S
SH
B⁻
c
A
S
SH
H⁺out
H⁺in
b
B⁻
S
H
S
BH
S
H
S

inner sites high affinity. Consequently, substrate is drawn through the channel and bound at the inner site. The redox equilibrium of the carrier is re-established by movement of electrons back to the outer redox center (d). The inner site becomes oxidized and releases the substrate, while the outer site becomes reduced to complete the cycle. To avoid proton leakage by this mechanism, H^+ is translocated only if the solute is transported.

Despite the considerable progress made in the past two decades in elucidating the molecular mechanisms involved in solute translocation, our knowledge on the arrangement of the carrier in the membrane is still in its infancy. In addition the structure of the carrier proteins and the conformational changes they undergo during solute translocation still need to be investigated.

Transport and Metabolism of Glucose, Gluconate, 2-Ketogluconate and Dicarboxylic Acids in the Flourescent Pseudomonads.

It has been proposed that aerobic fluorescent pseudomonads have glucose dehydrogenase and gluconate dehydrogenase located on the outer surface of the cytoplasmic membrane (114, 115, 116). These enzymes sequentially convert glucose to gluconate and then to 2-ketogluconate (2KGA) extracellularly. This constitutes the direct oxidative, non-phosphorylated pathway for D-glucose and D-gluconate catabolism in these organism (Figure 10). In the case of P. fluorescens, conversion of

Figure 10

Proposed Scheme for the Transport and Metabolism of D-Glucose, D-Gluconate and 2-Ketogluconate in the Cytoplasmic Membrane and Cytosol of Aerobic Fluorescent Pseudomonads.

Legend:

A	- Glucose Dehydrogenase
B	- δ-Gluconate Lactonase
C	- Gluconate Dehydrogenase
D, E and F	- Carrier Proteins
3-D-2K6PG	- 3-Deoxy-2-Keto-6-Phosphogluconate
ED	- Entner-Doudoroff Pathway
G-3-P	- Glyceraldehyde-3-Phosphate
G-6-P	- Glucose-6-Phosphate
HMP	- Hexose Monophosphate Pathway
2KGA	- 2-Keto-D-Gluconate
2K6PG	- 2-Keto-6-Phosphogluconate
6-PG	- 6-Phosphogluconate
PYR	- Pyruvate
R-5-P	- Ribulose-5-Phosphate
TCA	- Tricarboxylic Acid Cycle.

Figure 10

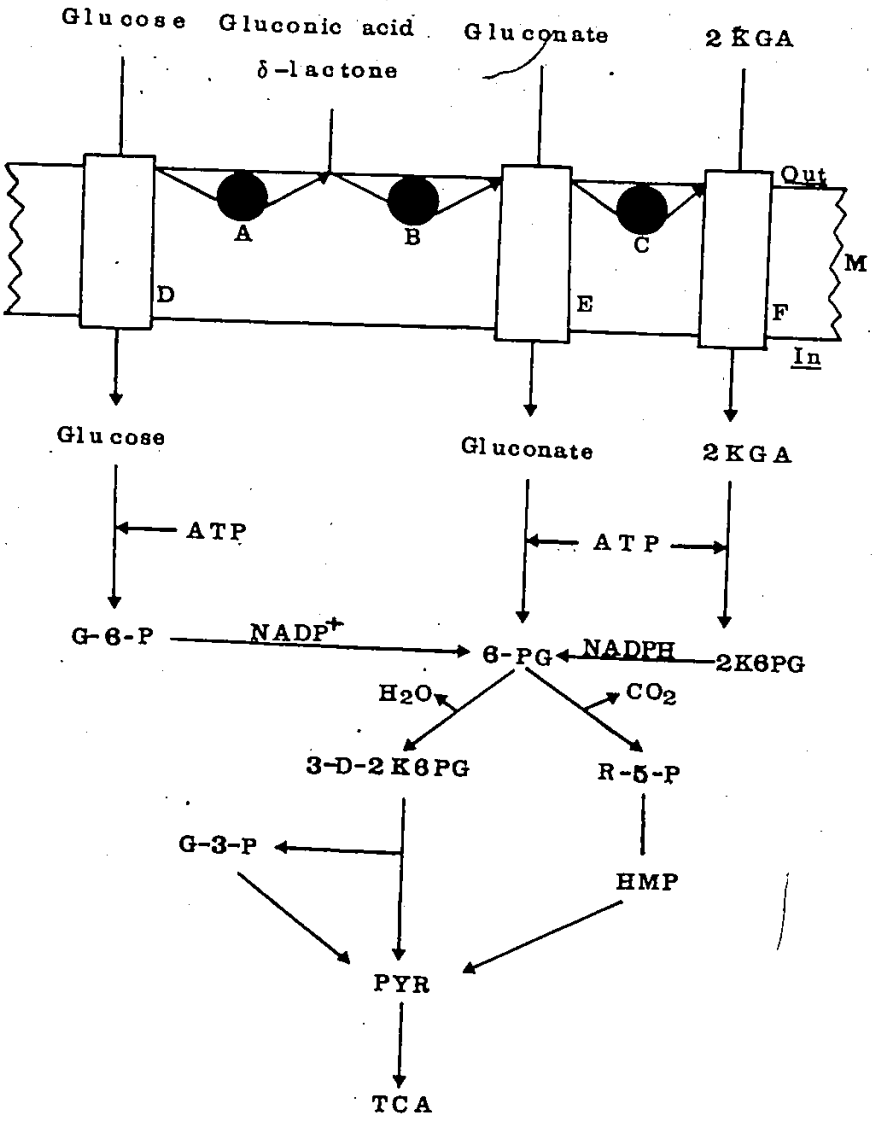
Glucose
Gluconic acid
δ-lactone
Gluconate
2KGA
Out
A
B
C
M
D
E
F
In
Glucose
Gluconate
2KGA
ATP
ATP
G-6-P
NADP+
6-PG
NADPH
2K6PG
H2O
CO2
3-D-2K6PG
R-5-P
G-3-P
HMP
PYR
TCA

glucose to gluconate is believed to occur via the intermediate, D-glucono-δ-lactone which is hydrolysed by the action of a lactonase (117). Whether the formation of this intermediate is a general feature of glucose oxidation in pseudomonads is still uncertain, but the formation of D-gluconate is considered necessary for the induction of the enzymes of the Entner-Doudoroff pathway (also referred to as the 3-deoxy-2-keto-6-phosphogluconate pathway). This is the major pathway for glucose catabolism in these organism (115, 116). Alternatively glucose, gluconate and 2KGA can be transported into the cytoplasm via separate carriers without chemical modification. Evidence has been presented which indicates the presence of specific carriers for glucose and gluconate in P. putida (118); P. fluorescens (119, 120, 121) and P. aeruginosa (116, 122). 2KGA has also been reported to be taken up by an inducible transport system in P. aeruginosa (116). Once inside the cells the sugars are phosphorylated by specific kinases. Glucose-6-phosphate and 2-keto-6-phosphogluconate are both converted to 6-phosphogluconate by glucose-6-phosphate dehydrogenase and 2-keto-D-gluconate-6-phosphate reductase, respectively. 6-Phosphogluconate is subsequently channelled into the Entner-Doudoroff pathway via the key intermediate, 3-deoxy-2-keto-6-phosphogluconate or into the hexose monophosphate pathway via D-ribulose-5-phosphate. Finally the products of both pathways enter the TCA cycle.

The oxidation of glucose and gluconate by the

respective membrane bound dehydrogenases appears to be linked with the electron transport chain in the bacterial membrane (123, 124, 125), and may play a key role in carbohydrate metabolism as well as energy generation in these organisms. Recently, a membrane-bound gluconate dehydrogenase from P. aeruginosa has been purified to homogeneity, and shown to contain an unknown peptide, a cytochrome c and a flavoprotein component (124). In addition, the oxidase activity of the isolated enzyme could be restored by addition of enzyme plus coenzyme Q_2 to the enzyme-depleted membranes.

Studies on the mechanism of energy coupling to carbohydrate transport in pseudomonads have been relatively limited. Furthermore, most of the studies reported were done using whole cells, thus data analysis is complicated by subsequent metabolism. However, results obtained from a few studies using membrane vesicles indicate that carbohydrate transport is coupled to electron-flow via the electron transport chain. Membrane vesicles from P. aeruginosa for example, accumulate gluconate by an active transport mechanism and is coupled to electron-flow via FAD-linked-L-malate dehydrogenase or glucose dehydrogenase (74). Recently Al-Jobore et al. (72) provided evidence for the existence of separate carriers for glucose and gluconate in vesicles prepared from glucose-grown P. putida. They also presented evidence to suggest that transport of these substrates may be coupled to electron-flow from FAD-linked-L-malate dehydrogenase, glucose dehydrogenase or gluconate

dehydrogenase. The transport system for 2KGA still remains to be characterized in detail. Finally, even though the results obtained indicate that glucose and gluconate accumulate in response to a Δp generated by the oxidation of electron donors, no attempt has been made to measure Δp in these organisms.

Dicarboxylic acids are also taken up by pseudomonads and metabolized via the TCA cycle (3). Inspite of the fact that the TCA cycle is of central importance in the catabolism, biosynthesis and terminal respiration in aerobic pseudomonads, very little attention has been devoted to the transport of TCA cycle dicarboxylates in these organisms. To date, it has been demonstrated that C_4-dicarboxylic acids are taken up by an active transport system in whole cells of P. putida (70). The transport system for succinate is induced by succinate, fumarate and malate. Moreover, from a variety of compounds tested, malate and fumarate were the only competitive inhibitors of succinate transport. These observations suggest a common transport system for all three C_4-dicarboxylic acids. Apart from showing that succinate transport was inhibited by KCN, NaN_3 and DNP (which presumably interface with energy production), no further characterization of this system was undertaken.

The objectives of these studies therefore are to:

(i) Synthesize D-[U-^{14}C]2KGA and fluorinated 2KGA analogues. (See APPENDIX X for structures).

(ii) Establish the presence or absence of a 2KGA transport system in membrane vesicles prepared from glucose- or

succinate-grown P. putida.

(iii) Determine the kinetics and specificity of the 2KGA transport system, if present, by investigating the effects of fluorinated 2KGA analogues on 2KGA transport.

(iv) Measure quantitatively, the Δp generated by oxidation of artificial and natural electron donors.

(v) Characterize the L-malate transport system in membrane vesicles from glucose- or succinate-grown P. putida.

A preliminary account of some of these results have been reported elsewhere (126).

CHAPTER II

MATERIALS AND METHODS

Materials

D-[U-^{14}C]glucose (283 mCi/mmol), L-[1-^{14}C]glucose (58 mCi/mmol), L-[U-^{14}C]-malate (sodium salt; 75 mCi/mmol), sodium[1-^{14}C]acetate (54.2 mCi/mmol) and [U-^{14}C]-$TPMP^+$ (iodide salt; 9.0 mCi/mmol) were obtained from Radiochemical Centre (Amersham, Bucks, U.K.). PMS, ascorbic acid, bovine serum albumin, gluconokinase, 6-phosphogluconate dehydrogenase, ribonuclease A, deoxyribonuclease I, lysozyme, o-phenylenediamine, chloramphenicol, valinomycin, nigericin, ATP, NADP, CCCP, DCIP, FCCP and Dowex 1 x 8 resin (chloride form; 200-400 mesh) were obtained from Sigma Chemical Co., (St. Louis Missouri). Yeast extract, agar and nutrient agar were obtained from Difco Laboratories (Detroit, Michigan). Oxaloacetic acid was obtained from Boehringer Mannheim Canada Ltd.(Dorval, Quebec). Crystalline 3FG and 4FG were synthesized in these laboratories. Unless otherwise stated all other carbohydrates, chemicals and reagents were of the highest grade and purchased from Sigma Chemical Co., or Fisher Scientific Co., (Fairlawn, New Jersey). The organism used in this study was *P. putida* (ATCC 12633), formerly classified as *P. fluorescens* A 3.12. This organism, first isolated by Stanier (127), was obtained as freeze-dried samples from American Type Culture Collection (ATCC),

(Rockville, Maryland), and maintained routinely on nutrient agar slopes or glucose- or succinate-mineral salts agar slopes.

Methods

Growth and Characterization of P. putida.

The semi-defined medium of Davis and Mingoli (128) was used for the growth of P. putida throughout these studies. This consists of:

	g/L (final volume)
K_2HPO_4	7.0
KH_2PO_4	3.0
$(NH_4)_2SO_4$	1.0
$MgSO_4.7H_2O$	0.1
Yeast extract	0.2
Trace solution A	1.0 ml
Trace solution B	1.0 ml
Carbon source	2.0

Solutions of trace elements were made up according to Barnett and Ingram (129) and contained the following:

Trace solution A

	mg/100mL (stock solution).
$FeSO_4.4H_2O$	40
$MnSO_4.4H_2O$	40
NaCl	1000

Trace solution B

	mg/100mL (stock Solution).
$ZnSO_4.7H_2O$	20
$CuSO_4.5H_2O$	4
$CoCl_2.6H_2O$	4
$CaCl_2$ (anhydrous)	500
$Na_2MoO_4.2H_2O$	5
KI	30

All the chemicals, with the exception of the carbon source, were dissolved in distilled water (1 litre). The resulting medium, pH 7.1, was sterilized by autoclaving at 120 °C for 15 min in a Pelton and Crane Magna-Clave, Model MC (G.A. Ingram Co. (Canada) Ltd., Windsor, Ontario). A 2% (w/v) solution of glucose or succinate was sterilized separately by membrane filtration in a Nalgene 20 micron filter unit (Nalgene Sybron Corp., Rochester, New York) and the appropriate amount added aseptically to the sterile medium to give a final concentration of 0.2%. Culture volumes of 10, 20 and 250 mL in 50, 125 and 1000-mL Erlenmeyer flasks respectively, were used routinely for batch analysis.

The purity of the organism was tested periodically by a variety of biochemical tests (Table 1).

Preparation of Solid Media.

(a) Mineral Salt/Glucose or Succinate Slopes.

Solutions were prepared and sterilized as outlined

Table 1

Biochemical Tests Used in Determining the Purity of *P. putida*.

Test	*P. putida*
Type of growth in Hugh Leifson's medium (1% glucose)	Acid production only at top of aerobic tube
Methyl Red	-
Voges Proskaver	-
Gelatin liquefaction	-
Indole production	-
Ammonia from arginine	+
Oxidase	+
Catalase	+
Growth in Kroser's citrate medium	+
Growth on milk agar* (130)	+, no hydrolysis no pigmentation

*Used to distiguish between *P. fluorescens* and *P. aeruginosa*.

above except that double strength solutions were used. A 2% (w/v) solution of plain agar was also sterilized by autoclaving. While still hot, the appropriate amount of sterile carbon source was added to the mineral salt media, then equal volumes of the sterile 2% agar solution and mineral salt-carbon source were thoroughly mixed. 10-mL aliquots of the mixture were poured into sterile tests tubes (25 mL) and allowed to cool and solidify in a slanting position. The slopes were stored at 4°C until required.

(b) Nutrient Agar Slopes.

These were prepared by suspending 23g of nutrient agar in 1 litre of distilled water. The suspension was allowed to stand at room temperature for 10 min, dispensed (10-mL aliquots) into 25-mL test tubes, sterilized and allowed to cool and solidify in a slanting position as described in (a).

Culture Techniques.

(a) Preparation of Whole Cell Suspensions.

Inocula for these cultures were prepared from 24-h slopes by washing the slopes with 10 mL sterile distilled water and aseptically transferring an appropriate aliquot (0.05 mL) to a 50-mL Erlenmeyer flask containing 10 mL of the carbon source-mineral salt medium. Glucose- and succinate-grown cells were obtained from cultures trained by at least six subcultures through glucose- or succinate-mineral salt media respectively. The necessary

cell yields for biochemical studies were obtained by growth of P. putida in 1-L flasks, each containing 250 mL of the appropriate medium. The cultures were incubated at 30°C in an orbital rotary shaker, setting at 4 (Lab-Line Instruments Inc., Melrose Park, Illinois). Using this procedure, cell yields in the region of 0.5 to 1.0 mg dry weight cell/mL of medium were obtained after 16-h incubations at which time the cells were in the late exponential phase. The cells were harvested in a Sorvall Superspeed RC2-B centrifuge (Ivan Sorvall Inc., Newtown, Connecticut) at 10,000 x g for 10 min at 30°C, washed twice with magnesium phosphate buffer (0.067 M sodium-potassium phosphate buffer, pH 7.1, containing 0.1% (w/v) $MgSO_4.7H_2O$), and suspended to the desired protein concentration in the same buffer.

(b) Preparation of Cytoplasmic Membrane Vesicles.

For studies with isolated membrane vesicles the cells were harvested as in (a) after 12-h incubations at which time the cells were in the mid-exponential phase. The vesicles were isolated by the same procedure described for P. aeruginosa (74). The pellet was suspended in two-thirds of the original culture volume in a solution containing final concentrations of 2.5% LiCl, 0.75 M sucrose, 10 mM potassium phosphate, pH 7.0, 10 mM $MgSO_4.7H_2O$, and 500 µg/mL lysozyme. The suspension was incubated for 1 h at 30°C on a rotary shaker, and the resulting osmotically

fragile rods were harvested by centrifuging at 10,000 x g for 30 min at 4°C. The pellet was suspended in the smallest possible volume of 2.5% LiCl in 0.75 M sucrose manually, using a loose-fitting teflon rod and glass homogenizer (ACE Glass Inc., Vineland, New Jersey). The suspension was rapidly added to 50 volumes of ice-cold 10 mM potassium phosphate buffer, pH 6.6, containing 1 mM $MgSO_4$ in a Waring blender and blended for 10 sec. Deoxyribonuclease I (DN'ase) and ribonuclease A (RN'ase) were added to a final concentration of 20 µg/mL each, and the mixture was incubated at 25°C with gentle stirring for 30 min. The mixture was centrifuged at 40,000 x g for 30 min at 4°C in an IEC International Preparative Ultracentrifuge, Model B-60 (Needham Heights, Mass.) and the pellet suspended by means of a loose-fitting glass homogenizer in a 1:4 (v/v) ratio in ice-cold 100 mM potassium phosphate, pH 6.6, containing 10 mM $MgSO_4$. Whole cells and large fragments were removed by centrifuging at 800 x g for 30 min at 4°C. The supernatant fluid was centrifuged at 40,000 x g for 30 min at 4°C and the pellets washed twice and suspended in the same buffer to a final concentration of 5-10 mg protein/mL. The vesicles were transferred into vials and stored in liquid nitrogen.

Vesicles were prepared only from organisms kept on slopes for less than six months since organisms kept on slopes for longer periods were found to have lost their transport activity.

Characterization of Vesicles.

(a) Electron Microscopy.

1 drop of vesicle preparation was placed on copper grids (200-mesh, Formvar-coated, carbon-reinforced) and left to stand at room temperature for 1 min. 1 drop of 1% uranyl acetate was then added to the grids containing the sample. The excess solution was removed by blotting with filter paper and the sample allowed to negatively stain for 30 s. The grids were examined using a Phillips EM High Resolution Electron Microscope (Findhoven, The Netherlands). (See Figure 16).

(b) Orientation of Vesicles.

The % accessibility of NADH-cytochrome C reductase, assumed to be located on the inner portion of the cytoplasmic membrane, was used as a measure of vesicle orientation. The activity of the enzyme before and after treatment of the vesicles with a 0.1% solution of Triton X100 (detergent) was determined spectrophotometrically by measuring absorbance change at 550 nm with a Beckman Spectrophotometer, Acta M-Series. (Beckman Instruments Inc., Fullerton, California). The reaction mixture, containing 50 µmol potassium phosphate, pH 6.6, 5 µmol $MgSO_4 \cdot 7H_2O$, 0.5 mg cytochrome c (oxidized), and 100 µL detergent treated or native vesicles (5.0 mg protein.mL^{-1}), was incubated at 30°C for 5 min before initiating the reaction by adding 1.0 mg NADH to a final volume of 1.0 mL (131). The

absorbance was recorded for 10 min against a reagent blank (minus NADH). (See Figure 17).

(c) Intra-Vesicular Volume.

The intra-vesicular volume was determined as described by Rottenberg (132), using a slowly permeable solute, i.e., L-glucose (72). 25 µL of L-[1-^{14}C]glucose (0.086 µmol, 58 mCi/mmol) was added to 1.0 mL of membrane vesicles (1.16 mg protein) and incubated at 30°C for 30 min to achieve full solute equilibration. This was followed by rapid filtration of the incubation mixture through a membrane filter (HRMP 02400, Millipore Corp., Bedford, MA) and washing of all external label from the filter twice with 2 mL of 0.1 M LiCl. The filters were transferred into polyethylene spectravials, dried at 110°C for 10 min and the radioactivity in the vesicles as well as in 0.1 mL of the filtrate were assayed by liquid scintillation after adding 10 mL Beckman Ready-Solv scintillation fluid. The internal volume is given by (^{14}Cfilter/^{14}Cmedium) x volume of medium. An average intra-vesicular volume of 3.6 µL water/mg of vesicle protein was obtained from three determinations.

Preparation of D-[U-^{14}C]2KGA, 3F2KGA and 4F2KGA.

Partially purified enzyme preparations of glucose and gluconate dehydrogenases were obtained by the procedure described by Taylor et al. (133). Glucose grown cells were washed twice with 0.067 M potassium phosphate buffer,

pH 7.0. The final pellet was mixed with an equal volume of 0.67 M potassium phosphate, pH 7.0, and sonicated for 6 x 1 min with a Sonic 300 Dismembrator (ARTEK Systems Corp., Farmingdale, New York). The ruptured cell suspension was centrifuged at 17,000 x g for 10 min. The upper pink layer was poured off with the red supernatant and the two fractions were mixed. This extract was then centrifuged at 150,000 x g for 60 min, and the red particulate fraction was suspended in the same buffer to give a stock particulate suspension of glucose and gluconate dehydrogenases.

D-[U-^{14}C]2KGA was prepared enzymatically from D-[U-^{14}C]glucose. The incubation mixture consisted of 50 µmol potassium phosphate buffer, pH 6.6, 5 µmol $MgSO_4.7H_2O$, 50 µmol glucose, 0.565 µmol D-[U-^{14}C]glucose (283 mCi/mmol) and 2 mg partially purified glucose and gluconate dehydrogenase suspension in a final volume of 3 mL. The reaction mixture was incubated for 12 h at 30°C on a reciprocal shaking incubator (Precision Scientific Co., Chicago, U.S.A.), and the progress of oxidation followed by the decrease in pH. The pH was maintained at 6.6 by periodic additions of small amounts of 1N NaOH. At the end of the incubation period the contents of the flask were centrifuged at 150,000 x g for 60 min, and the supernatant was heated at 60°C for 60 min and recentrifuged. The resulting supernatant was then lyophilized with a Labconco lyophilizer (Labconco Corp., Kansas City, Missouri), and the residue dissolved in 0.1 mL distilled water. 50 µL of this solution was applied to a

Dowex-1-formate anion exchange column (1 x 15 cm); this column was prepared from a Dowex 1 x 8 resin (chloride form; 200-400 mesh) by first treating with 5M ammonium formate until no more chloride was removed, and then washing thoroughly with water (134). The sugars were eluted from the column with a formic acid gradient (0.0 - 1.0M) at a flow rate of 1 mL/min (135). 10-mL fractions were collected and 0.1 mL of each fraction was added to 10 mL of Beckman Ready-Solv scintillation cocktail and counted by liquid scintillation using a Beckman LS-7500 Liquid Scintillation Spectrometer (Beckman Instruments Inc., Irvine, C.A.). The fractions containing radiolabelled 2KGA were pooled and the formate removed by repeated lyophilization. The final residue was dissolved in water to give a stock solution of D-[U-^{14}C]2KGA (2.07 mM, 3.2 mCi/mmol). In a preliminary experiment designed to identify compounds present at the end of the reaction, radiolabelled glucose was omitted from the reaction mixture, so gluconate and 2KGA were determined in the fractions by the methods described below. Stock solutions of 4.7 mM 4F2KGA and 3.6 mM 3F2KGA were prepared in a similar manner from 40 µmol 4FG and 41.2 µmol 3FG respectively. The concentrations of fluoro-α-ketoaldonic acids were determined as described for 2KGA.

Determination of Gluconate

Gluconate was determined as described by Lynch et al. (136). The reaction mixture contained 40 mM Tris (hydroxy-

methyl)aminomethane chloride, pH 7.4, 10 mM $MgCl_2$, 2.5 mM ATP, 1 mM NADP, 0.2 U 6-phosphogluconate dehydrogenase, 0.13 U gluconokinase and 0.1 mL sample containing 0-0.15 µmol gluconate in a total volume of 1 mL. The mixture was incubated at 37°C for 1 h and read at 340 nm.

1 U of 6-phosphogluconate dehydrogenase will oxidize 1 µmol of substrate per min at 37°C and pH 7.4, while 1 U of gluconokinase will oxidize 1 µmol of substrate per min at 30°C and pH 8.0.

Determination of 2KGA

2KGA was determined by reacting it with o-phenylenediamine to form a hydroxyquinoxaline derivative (137). 2 mL of the sample containing 0-100 µg 2KGA was mixed with 1 mL of 2.5% aqueous solution of o-phenylenediamine dihydrochloride. The mixture was heated in a boiling water bath for 30 min and cooled to room temperature. The absorbance was measured at 330 and 360 nm. A 330 nm:360 nm absorbance ratio of 1.51 ± 0.07 is obtained for mixtures containing a 2-ketohexonic acid.

Protein Determination

The biuret method (138) was used for protein determination in whole cells. For membrane vesicles, crude enzyme preparation and glucose binding protein, the method of Lowry *et al.* (139) was used. Bovine serum albumin was used as a standard.

Transport Studies

(a) Transport in Whole Cells

The accumulation of radioactivity by whole cells was determined at 30 °C on a reciprocal shaking water bath. The incubation mixture contained 0.5 mL Mg^{2+}-phosphate buffer (0.067 M sodium-potassium phosphate, pH 7.1, containing 0.1% (w/v) $MgSO_4.7H_2O$), 5 mg chloramphenicol and 1.4 mg protein. The mixture was incubated for 20 min with continuous oxygen gassing and the reaction initiated by adding the appropriate concentration of D-[U-^{14}C]2KGA (5.2 mCi/mmol) in a total volume of 1.0 mL. At time intervals of 30, 60 and 120 s, 0.1-mL aliquots were withdrawn, diluted into 20 volumes of NaCl buffer (Mg^{2+}-phosphate buffer, pH 7.1, supplemented with 1.0% (w/v) NaCl), 25°C, overlaying a Millipore filter HA membrane (HRMP 02400, Millipore Corp., Bedford, MA), filtered under vacuum and immediately washed with another 20 volumes of NaCl buffer. The filters were then transferred into scintillation vials and dried in an oven at 110°C for 10 min. 10 mL of TEG scintillation fluid was added to each vial after cooling and the samples counted by liquid scintillation. TEG consists of 42 mL liquifluor [0.625 g of 1,4-bis-2'(5'-phenyloxazolyl) benzene (POPOP) and 80 g of 2,5-diphenyloxazole (PPO) per 500mL toluene], 1 L toluene and 600 mL ethylene glycol monoethyl ether. Non-specific binding of radiolabel to the filters was determined from similar experiments in which protein was excluded from the incubation mixture. These values were subtracted from the counts obtained for each sample and the

amount of labelled material transported was calculated from the corrected CPM values (See APPENDIX II). The results are expressed as nmol substrate transported.mg protein^{-1}.

(b) Transport in Membrane Vesicles

For transport in membrane vesicles the incubation mixtures consisted of 50 µmol potassium phosphate buffer, pH 6.6, 12 µmol $MgSO_4.7H_2O$, 0.8 to 1.0 mg protein and the appropriate concentrations of electron donors and/or inhibitors when present. The reaction mixtures were preincubated in 10-mL Erlenmeyer flasks with shaking and continuous oxygen gassing at 30°C for 10 min before initiating the reaction by adding known concentrations of radiolabelled substrate to a total volume of 1.0 mL. At time intervals, 0.1-mL samples were withdrawn, diluted into 20 volumes of 0.1 M LiCl, filtered and washed with another 20 volumes of LiCl. The filters were dried and counted as described in (a).

(c) Transport with K^+-Loaded Vesicles

Vesicles were prepared as previously described, resuspended in 0.5 M potassium phosphate, pH 8.0, containing 10 mM $MgSO_4.7H_2O$. The suspension was kept at 48°C for 10 min, then chilled in ice. The vesicles were collected by centrifugation at 40,000 x g for 30 min at 4°C washed once with 0.4 M sucrose containing 5 mM $MgSO_4.7H_2O$, and resuspended in the same solution (110).

0.97 mg of vesicles were resuspended in 100 mM

Tris.maleate, pH 7, 13 mM $MgSO_4.7H_2O$, 280 mM sucrose and either 208 μM [U-^{14}C]-$TPMP^+$ (4.8 mCi/mmol) or 103.5 μM [U-^{14}C]2KGA (3.2 mCi/mmol). The total volume was 1.0 mL. After 10 min incubation at 30°C the reaction was initiated by adding 2 μg valinomycin. At time intervals 0.1-mL aliquots of the suspension were filtered through a membrane at 25°C and immediately washed twice with 2 mL of 0.4 M sucrose containing 5 mM $MgSO_4.7H_2O$ (110). The filters were dried and counted as in (a).

(d) Kinetic Treatment of Data.

The amount of radioactive material transported by vesicles or whole cells in 30, 60 and 120 s was measured as described in sections (a) and (b) at varying substrate concentrations. The amount of substrate transported was then plotted against time to produce a progress curve for each substrate concentration. The initial rates of substrate transport were deduced from the slopes of the progress curves at zero time. The slopes were obtained by drawing tangents to the curves through zero time. Kinetic parameters, Km and Vmax were obtained from double reciprocal or Lineweaver-Burk plots (140) of the initial rates of substrate transport and substrate concentrations. Inhibition constants, Ki, were obtained from Dixon plots (141). See APPENDIX III for derivation of kinetic parameters. Km, Ki and Vmax values were estimated by linear regression analysis of kinetic data (APPENDIX IV), and are the averages

of duplicate trials.

Measurement of Δp

$\Delta\Psi$ and ΔpH were assayed by flow dialysis, using the distribution of [U-^{14}C]-TPMP$^+$ and [1-^{14}C]acetate respectively. Flow dialysis was carried out at 25°C as described by Ramos et al. (106). The upper and lower chambers of the flow dialysis apparatus (Bel-Art Products; Pequannock, N.J.) were separated by Spectrapor dialysis tubing (6,000-8,000 molecular weight cut-off; Spectrum Medical Industries, Los Angeles, C.A.), (APPENDIX V). Membrane vesicles (3 mg protein) suspended in 0.82 mL of 0.05 M potassium phosphate buffer, pH 6.6, containing 0.01 M $MgSO_4.7H_2O$ were added to the upper chamber. Potassium phosphate (0.05 M, pH 6.6) was pumped through the lower chamber at a flow rate of 3.4 mL/min using a 10200 pump (LKB, Sweden). Both chambers were stirred continuously with magnetic stirrers. Aerobic conditions were maintained by passing a stream of oxygen through the aperture in the top well. At appropriate times 20 µL of [U-^{14}C]-TPMP$^+$ (125 µM, 9 mCi/mmol) or 40 µL of [1-^{14}C]acetate (44.3 µM, 54.2 mCi/mmol), 46 µL of electron donor and 20 µL of DNP were added through the aperture in the top well and 1.7 mL fractions were collected. 1-mL aliquots of these fractions were dissolved in 10 mL Beckman Ready-Solv scintillation fluid and assayed for radioactivity by liquid scintillation counting. The amount of radioactivity in each fraction was plotted against fraction number. $\Delta\Psi$ and ΔpH were calculated

as shown in APPENDIX VI. Δp was calculated from

$$\Delta p = \Delta\Psi - 2.303RT/F \times \Delta pH \quad (103).$$

Enzyme Assays

(a) Dehydrogenase Activity.

Dehydrogenase activity was determined by measuring the change in absorbance of DCIP or potassium ferricyanide at 25° C (142). The reaction mixture contained 50 µmol potassium phosphate buffer, pH 6.6, 5 µmol $MgSO_4 \cdot 7H_2O$, the appropriate concentration of substrate and 1.0 µmol ferricyanide or 1.0 µmol DCIP. The reactions were initated by adding 850 µg vesicles in a final volume of 3 mL. Dehydrogenase activity was determined from the decrease in absorbance at 600 nm for DCIP and 420 nm for ferricyanide. The activities were calculated using extinction coefficients of 10 mM^{-1} and 1.0 mM^{-1} for DCIP and ferricyanide respectively.

(b) Oxidase Activity

Oxidase activity was determined polarographically with a clark oxygen electrode (YSI Model 53, Yellow Springs Instruments Co., Yellow Springs, Ohio), connected to a recorder (Fisher Recordall Series 5000; Fisher Scientific Co., Houston TX). The reaction mixture was identical to that for dehydrogenase activity in (a) except that the reaction was initiated by adding the appropriate amount of substrate. All measurements were made in a water-jacketed cell at 30° C. Oxygen uptake was calculated from the

slopes of the recorder traces (See APPENDIX VII).

Glucose Binding Protein (GBP)

(a) Extraction of GBP

Isolation of GBP was based on the method of Stinson et al (41). Glucose grown cells (0.5 g wet weight) were suspended in 30 mL of 0.2 M $MgCl_2$-0.05 M tris (hydroxymethyl) aminomethane-hydrochloride buffer, pH 8.5 (extraction buffer). The suspension was incubated at 25°C for 30 min with constant stirring and then centrifuged at 25°C for 20 min at 16,300 x g. The cells were rapidly suspended in 30 mL distilled water, stirred at 25°C for an additional 30 min and recentrifuged. The supernatant (shock fluid) was removed and combined with magnesium extract and dialyzed against 2 L of 1 mM $MgCl_2$ - 10 mM tris (hydroxymethyl) aminomethane-hydrochloride buffer, pH 7.5 (TM buffer) at 4°C for 24 h. The proteins were precipitated with ammonium sulfate (0 to 95% saturation) and centrifuged at 17,000 x g for 20 min at 4°C. The precipitates were dissolved in a small volume of TM buffer and dialyzed against 2 L of the same buffer overnight.

(b) Assay of GBP

The binding activity of GBP in the crude shock extracts was assayed by equilibrium flow dialysis (107). The upper chamber contained 50 mM potassium phosphate buffer, pH 6.6,

12 mM $MgSO_4.7H_2O$ and 2 mg protein. 50 mM potassium phosphate buffer, pH 6.6, was pumped through the lower chamber at a flow rate of 8 mL/min. At the beginning of a determination, D-[U-^{14}C]glucose (145.5 mCi/mmol) was introduced into the protein solution in the upper chamber to final concentrations of 2.5 μM-10 μM. Total volume in the upper chamber was 1.0 mL. Both chambers were stirred continuously with magnetic stirrers. The labelled glucose equilibrates immediately with GBP, and the rate at which radioisotope enters the lower chamber is proportional to the concentration of unbound glucose in the upper chamber. This rate was measured by collecting 2-mL fractions of the effluent and determining the concentration of the isotope in 0.1-mL aliquots by liquid scintillation counting using Beckman Ready-Solv scintillation cocktail. GBP activity was calculated from the difference in steady state levels of sample and control (GBP omitted), as shown for $\Delta\Psi$ and ΔpH calculations in APPENDIX VI.

Equipment and Method for Measuring pH Changes

The equipment was built as described by Henderson et al (143), and consisted of a water-jacketed 8 mL-capacity glass cell to which two horizontal gas-tight screw-thread joints were connected. A micro-combination pH electrode (90 mm x 6.5 mm; Fisher Scientific Co., Pittsburg, Pa.) was inserted through one horizontal joint and connected to a recorder via a Metrohm Herisau E510 mV/pH meter (Brinkman Instruments Ltd., Rexdale, Ontario). A solid glass rod was inserted

through the second horizontal joint to prevent air and water leakage. Access to the cell was maintained through a vertical glass extension tube, closed by insertion of a tight-fitting polyethylene plug with two narrow holes (0.5 mm diameter). These holes served as gas inlet and outlet as well as a means of adding solutes with a syringe.

Membrane vesicles were prepared as previously described, washed twice with 100 mM-KCl-2 mM-glycylglycine buffer, pH 7.0 (lightly buffered medium) and resuspended in the same medium at 10-15 mg protein (79).

The reaction mixture, consisting of 10 mM $MgSO_4 \cdot 7H_2O$, 50 μM FAD and 7.25 mg protein in lightly buffered medium, was incubated at 30°C in the water-jacketed glass cell. The cell suspensions were stirred by a stream of oxygen or nitrogen for 20 min for aerobic and anaerobic incubations respectively. When present, DMP was added to the preincubation mixture to a final concentration of 100 μM. For anaerobic proton movements, 10 mM KCN was also added to the reaction mixture. After 20 min preincubation, the suspensions were equilibrated at pH 6.69 with small amounts of 0.1 M HCl or KOH and the reaction initiated by adding the appropriate amount of L-malate (also previously equilibrated at pH 6.69). For anaerobic proton movement, L-malate was bubbled with nitrogen for 20 min before used. The total reaction volume was 5.0 mL. The incubation mixture was stirred constantly with a magnetic stirrer. pH changes, obtained from the recorder traces, were converted into nmol of H^+ by using an experimentally determined

conversion factor derived from the addition of known amounts of HCl to the cell suspension (79, 86).

Extraction and Chromatography of Intra-Vesicular Materials.

Vesicles were incubated with 10 mM L-malate under the same conditions described for measurement of pH changes, except KCl-glycylglycine buffer was replaced with 50 mM potassium phosphate buffer, pH 6.6. At time intervals 0.5-mL aliquots were withdrawn, filtered and washed twice with 5 mL of 0.1 M LiCl as previously described for transport studies with membrane vesicles. Substrates were extracted from the filters by adding 2 mL distilled water and heating at 60°C for 60 min (64). The solution was filtered with a Millex-HV millipore filter. (Pore size 0.45 µm; Millipore Corp., Bedford, MA), and the solvent removed on a rotary evaporator. The residue was then dissolved in 30 µL distilled water which had previously been passed through a trace organic removal cartridge (Millipore Corp., Bedford MA), filtered and degassed (i.e. HPLC grade water). TCA cycle intermediates were identified by HPLC.

The HPLC equipment used was a model M-45 Solvent Delivery System (Waters Associates, Milford, MA) equipped with an Aminex HPX-87H cation exchange column (300 x 7.8 mm) for organic acids (no. 125-0140; Bio-Rad Laboratories, Richmond, Calif.). Samples were detected with a model R401 Differential Refractometer connected to a recorder. Ambient temperature was used, and the flow was 0.5 mL/min. A 0.007 N

H_2SO_4 solution (made up with HPLC grade water, filtered and degassed) was used as column eluent (144). Sample volumes injected were in the range of 5-20 uL. A standard mixture containing known concentrations of dicarboxylic acids were separated (see APPENDIX VIII). The detector response value (molar concentration/peak area) was determined for each standard and the molar concentrations of the unknowns were obtained by multiplying their peak areas by the response factor.

*To ensure that the extraction procedure described above did not cause the decomposition of transported solutes, control experiments were done in which after L-malate transport, the intra-vesicular contents were extracted by adding 1 mL of an ice-cold toluene water (5:95, v/v) mixture to the filters and shaking vigorously for 2 min (105). Similar results were obtained with both extraction procedures.

Unless otherwise stated, all the studies described above were carried out in duplicates for each vesicle preparation. The results given are the averages of data obtained from two different vesicle preparations.

CHAPTER III

RESULTS AND DISCUSSION

Due to the fact that labelled 2KGA was unavailable commercially, D-[U-^{14}C]2KGA was prepared enzymatically from uniformly labelled glucose using partially purified glucose and gluconate dehydrogenases obtained from cell free extracts of P. putida. For the purpose of this experiment it was crucial that the 2KGA preparation was free from any traces of glucose or gluconate, since either of these compounds could serve as electron donors for solute transport (72). This required a system which would effect complete separation of 2KGA from glucose and gluconate and also offer maximum 2KGA recovery. Thus, an anion exchange chromatographic procedure previously used by Kay and Grunlund (135) for separating intermediates accumulated during glucose oxidation by P. aeruginosa was employed. In the experiments of Kay and Grunlund (135) glucose, a neutral sugar, bound very lightly to the column and was eluted in approximately 15 min. 2KGA, however, bound fairly strongly to the resin and was eluted in about 200 min. Unfortunately gluconate was not included in these studies. As such, an initial experiment was performed to determine whether a good separation could be obtained for gluconate and 2KGA and secondly, to determine whether a high yield of 2KGA will be obtained from glucose oxidation. Cold glucose was incubated with partially purified glucose dehydrogenase and gluconate

dehydrogenase overnight, and the products separated on a Dowex-1-formate anion exchange column (Figure 11). Gluconate and 2KGA were eluted in 90 and 240 min respectively. In addition a 2KGA yield of approximately 80% was obtained. The elution profile of the products of oxidation of labelled glucose is given in Figure 12. It is apparent from these results that the reaction was virtually complete during an overnight incubation. Furthermore the system used offered an excellent separation of all three carbohydrates. The fractions from the radioactive peak containing 2KGA were pooled and formate was removed by repeated lyophilization. The final residue was dissolved in water to give a stock solution of 2.07 mM D-[U-^{14}C]2KGA (3.2 mCi/mmol). Stock solutions of 4.7 mM 4F2KGA and 3.6 mM 3F2KGA for inhibition studies were prepared in a similar manner. The elution profiles of the two fluorinated 2KGA analogues (from two separate runs) are given in Figure 13. 4F2KGA was eluted in 450 min. 3F2KGA on the other hand, remained on the column after 500 min, and was eluted only after 2 N formic acid was passed through the column for an addtional 170 min. No fluorinated gluconate analogues were detected in any of the fractions containing fluorinated 2KGA analogues. Flourinated glucose analogues were not tested for since these neutral sugars will not bind to the resin to any significant extent and will be eluted before the fluorinated gluconate and 2KGA analogues.

The initial rates of transport of 2KGA in whole cells of P. putida grown on glucose or succinate increased in

Figure 11

Elution Sequence of Gluconate and 2KGA from a Dowex-1-Formate Anion Exchange Column.

Legend:

—o—o— Gluconate

—•—•— 2KGA

The reaction mixture contained 50 µmol potassium phosphate buffer, pH 6.6, 5 µmol $MgSO_4$, 50 µmol glucose and 2mg of partially purified glucose and gluconate dehydrogenase suspension in a final volume of 3.0 mL. The mixture was incubated at 30°C overnight and processed as described in the MATERIALS AND METHODS section. 50 µL of the final solution was applied to a Dowex-1-formate column (1 x 15 cm) and eluted with 0-1.0 N formic acid gradient. The flow rate used was 1.0 mL/min and 10-mL fractions were collected. Gluconate and 2KGA were determined in each fraction using 0.1-mL and 2.0-mL aliquots respectively (See MATERIALS AND METHODS).

Figure 11

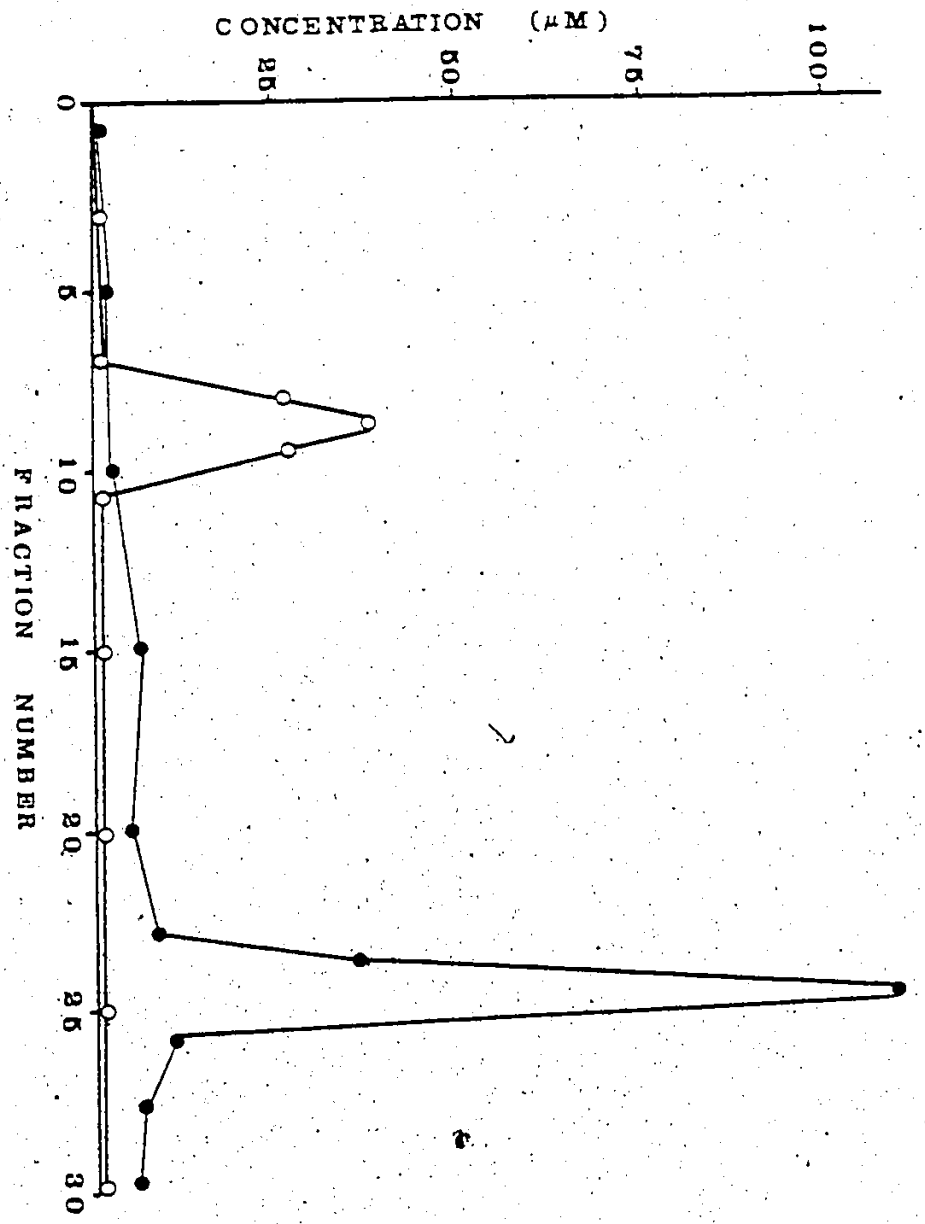
CONCENTRATION (μM)
25
50
75
100
0
5
10
15
20
25
30
FRACTION NUMBER

Figure 12

Elution Sequence of Glucose, Gluconate and 2KGA from Dowex-1-Formate Anion Exchange Column.

Legend:

A - Glucose

B - Gluconate

C - 2KGA

The reaction mixture contained 50 µmol potassium phosphate buffer, pH 6.6, 5 µmol $MgSO_4$, 50 µmol glucose, 0.565 µmol D-[U-^{14}C]glucose (283 mCi/mmol) and 2 mg of partially purified glucose and gluconate dehydrogenase suspension in a final volume of 3.0 mL. The mixture was incubated at 30°C overnight and processed as described in the MATERIALS AND METHODS section. 50 µL of the final solution was applied to a Dowex-1-formate column (1 x 15 cm) and eluted with 0-1.0 N formic acid gradient. The flow rate used was 1.0 mL/min and 10-mL fractions were collected. 0.1-mL aliquots of each fraction were added to 10 mL scintillation cocktail and counted by liquid scintillation.

Figure 12

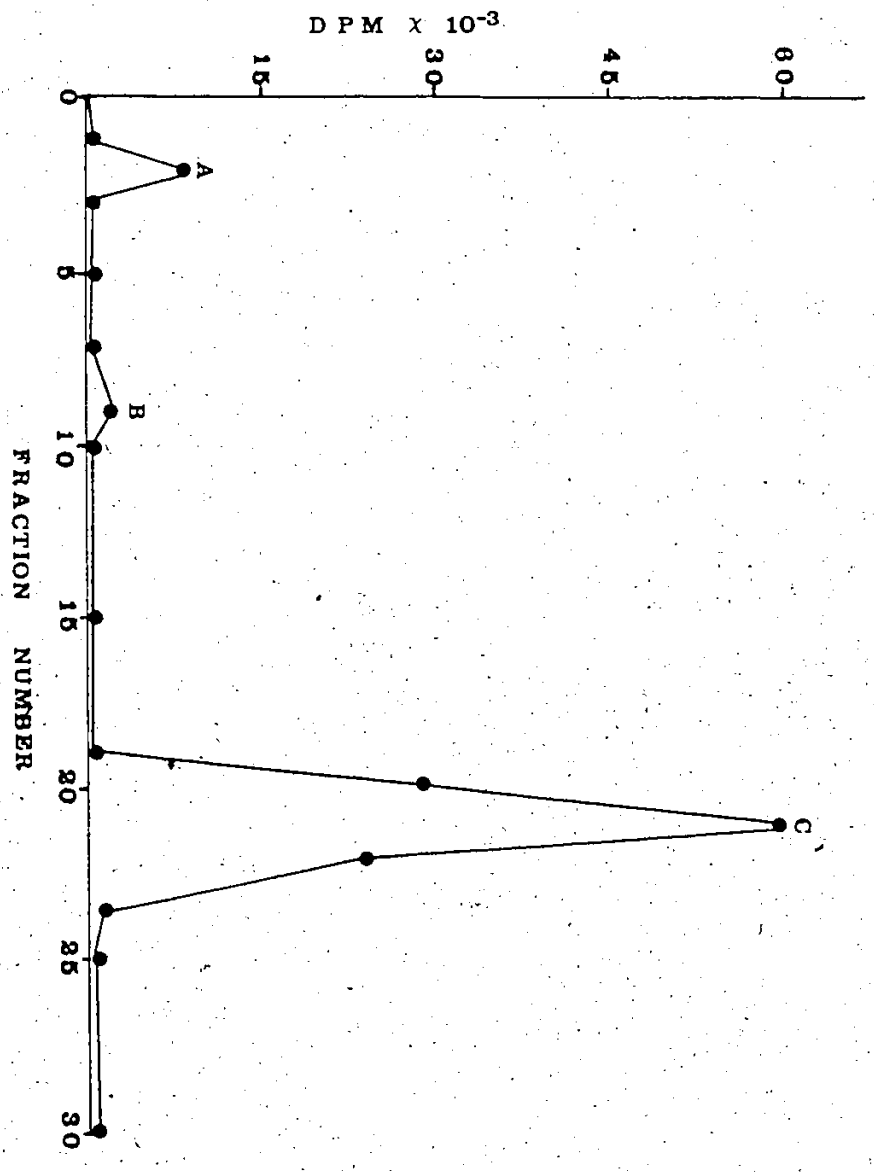

Figure 13

Elution Profile of 4F2KGA and 3F2KGA from a Dowex-1-Formate Anion Exchange Column.

Legend:

—●— 4F2KGA

—○— 3F2KGA

40 µmol 4FG or 41.2 µmol 3FG was incubated with 50 µL potassium phosphate buffer, pH 6.6, 5 µmol $MgSO_4$ and 120 mg partially purified glucose and gluconate dehydrogenase. Incubation, sample preparation, and elution of sample from the column are the same as described for Figure 11 except an additional 200 mL of 2N formic acid was passed through the column at a flow rate of 1.0 mL/min to elute 3F2KGA. 4F2KGA and 3F2KGA were determined by the o-phenylenediamine method used for 2KGA determination. 4FGA and 3FGA were determined by the same method used for gluconate determination (See MATERIALS AND METHODS).

Figure 13

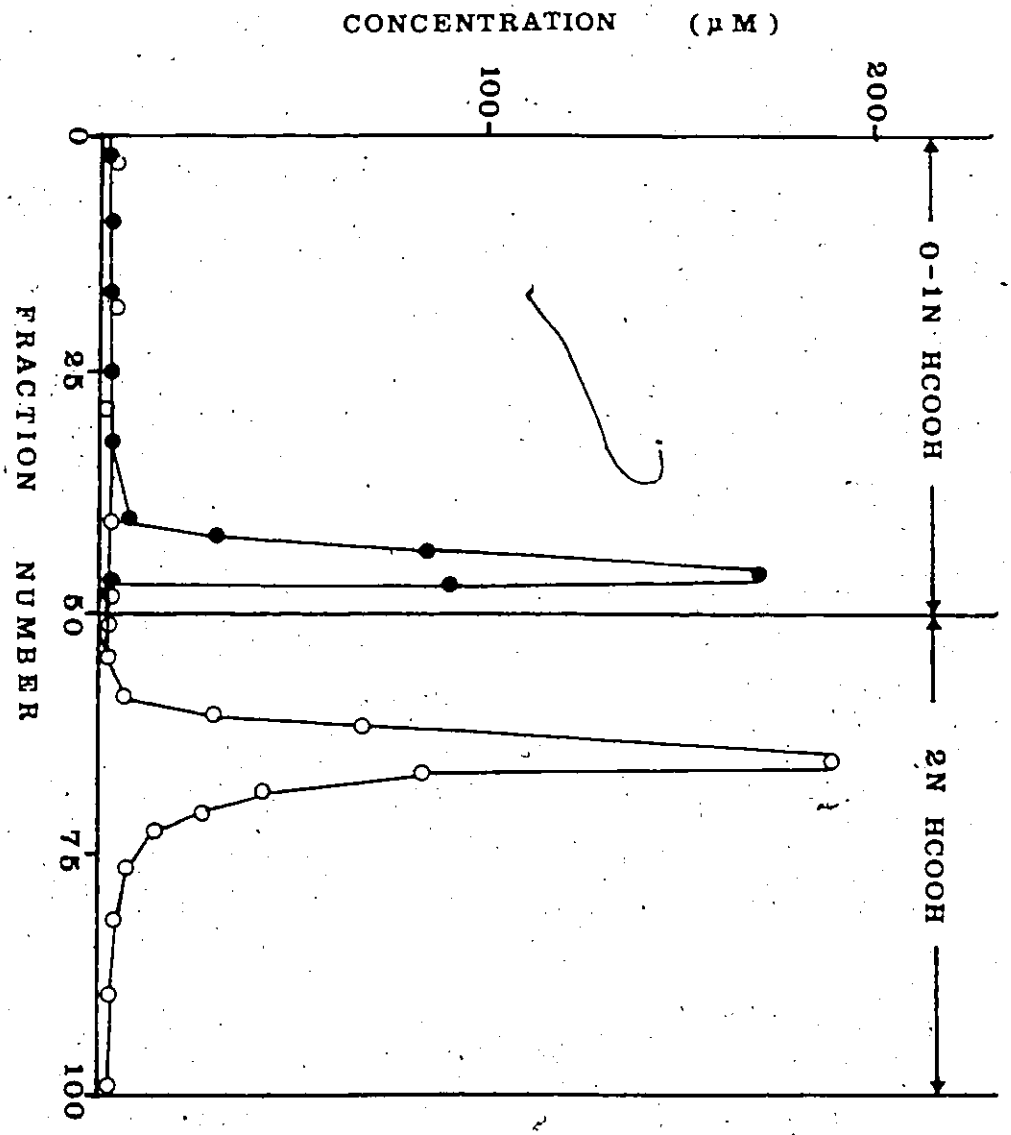
CONCENTRATION (μM)
100
200
0
25
50
75
100
FRACTION NUMBER
0-1N HCOOH
2N HCOOH

response to increased external substrate concentrations (Table 2). Double reciprocal plots of the data in Table 2 gave an apparent Km of 5.7±0.5 μM and an apparent Vmax of 4.6±0.08 nmol.mg protein.$^{-1}$ min.$^{-1}$ for glucose-grown P. putida (Figure 14). Apparent Km and Vmax values obtained for succinate-grown cells were 9.1±0.6 μM and 2.7± 0.05 nmol.mg protein^{-1}.min^{-1}, respectively (Figure 15). The higher Km value of succinate-grown cells indicates a lower affinity of the 2KGA carrier for its substrate in these organisms. Robert et al. (116) have previously shown that the activities of 2KGA catabolizing enzymes and the 2KGA transport system in whole cells of P. aeruginosa were induced when the organisms were grown on glucose, but were absent from organisms grown on succinate. Thus the different Km values obtained for the two sets of cells is due either to repression of the synthesis of the 2KGA carrier during growth on succinate, or its induction or derepression when grown on glucose. Since a Km value of ∞ would be expected if the carrier was completely absent in succinate-grown cells, it would appear that a significant amount of the 2KGA carrier was still present in these cells even after the cells were trained by growth on succinate for six generations. Alternatively, as mentioned earlier, the characterization of the transport system in whole cells could be complicated by substrate metabolism. It is therefore possible that the difference in kinetic parameters of glucose- and succinate-grown cells is a consequence of different rates of 2KGA metabolism in these organisms. A

Table 2

Transport of 2KGA by Glucose- and Succinate-Grown *P. putida*.

2KGA (μM)	Initial Rate of 2KGA Transport ($nmol.mg\ prot^{-1}.min^{-1}$)	
	Glucose-Grown Cells	Succinate-Grown Cells
1.2	0.80	0.32
3.1	1.70	0.64
6.2	2.30	1.10
12.4	3.11	1.60
30.9	3.90	2.40

Whole cell suspensions (1.4 mg protein) of glucose or succinate-grown *P. putida* were incubated at 30°C in Mg^{2+}-phosphate buffer, pH 7.1 containing 5.0 mg chloramphenicol. After 20 min the reaction was initiated by adding the appropriate amount of D-[U-^{14}C]2KGA (3.2 mCi/mmol). Total reaction volume was 1.0 mL. At 30, 60, 90 and 120 s, 0.1-mL aliquots were filtered, washed, and the amount of 2KGA transported determined as described in the MATERIALS AND METHODS section. Results are the averages of duplicate assays.

Figure 14

Double Reciprocal Plots of 2KGA Transport by Glucose-Grown *P. putida*.

Legend:

[S] - 2KGA concentration

v - Initial rate of 2KGA transport

2KGA transport by glucose-grown cells was measured as described in the footnote for Table 2. The line represents the best-fit line derived from linear regression analysis of the kinetic data. Each point is derived from progress curves obtained by plotting the average values of duplicate determinations against time.

Average apparent Km's and Vmax's (3 different cell preparations) are 5.7±0.5 μM and 4.6±0.08 nmol.mg protein.$^{-1}$ min.$^{-1}$, respectively.

Figure 14

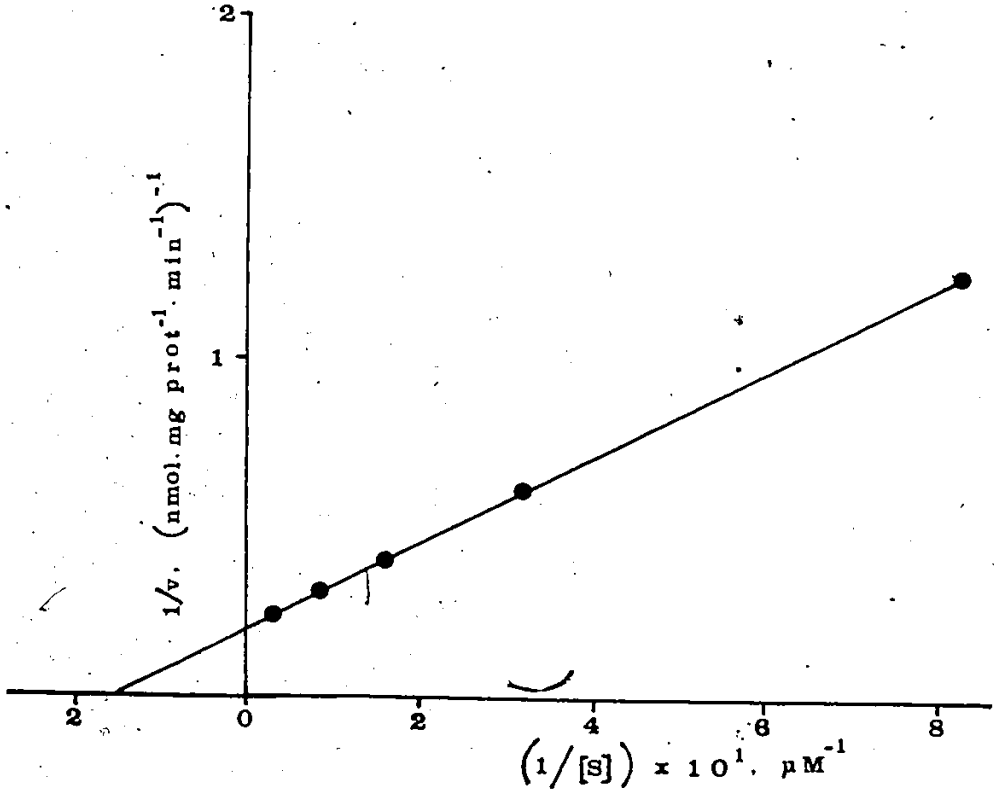

Figure 15

Double Reciprocal Plots of 2KGA Transport by Succinate-Grown *P. putida*.

Legend:

[S] - 2KGA concentration

v - Initial rate of 2KGA transport

2KGA transport by succinate-grown cells was measured as described in the footnote for Table 2. The line represents the best-fit line derived from linear regression analysis of the kinetic data. Each point is derived from progress curves obtained by plotting the average values of duplicate determinations against time.

Average apparent Km's and Vmax's (3 different cell preparations) are 9.1±0.6 μM and 2.7±0.05 nmol.mg protein.$^{-1}$ min.$^{-1}$, respectively.

Figure 15

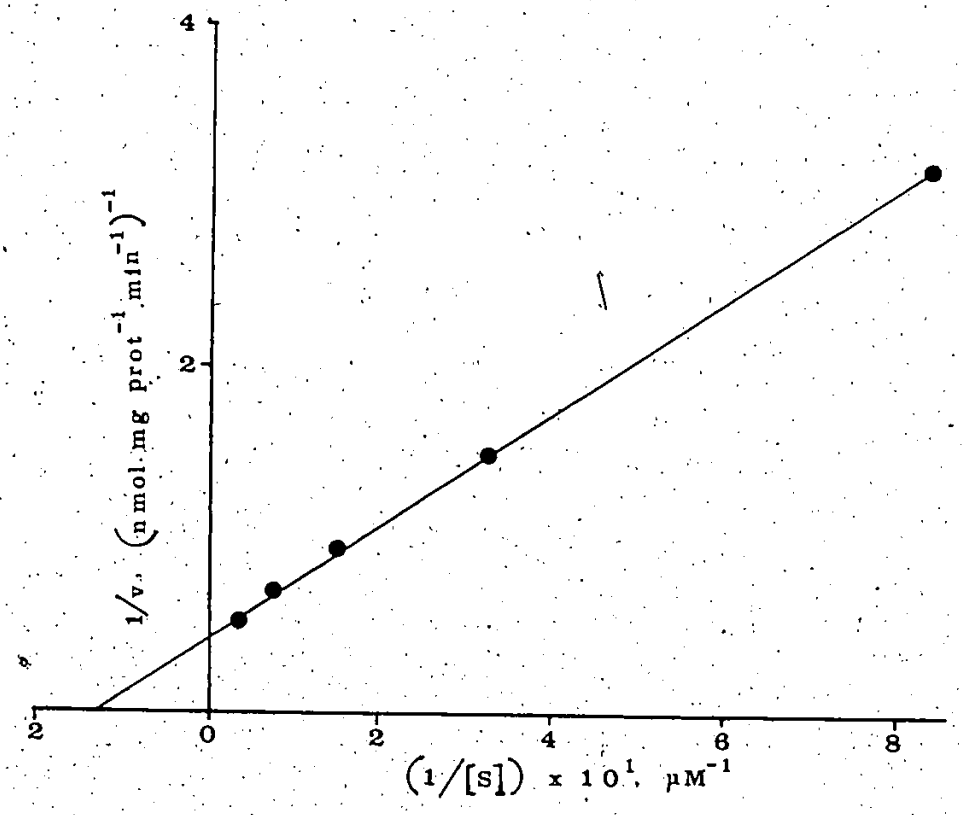

second problem encountered when analysing data derived from whole cells lies in the possibility that the substrate may interact with proteins located in the different regions of the cell envelope. It has previously been demonstrated that the outer membrane of glucose-grown P. putida contains a protein which defluorinates 4FG (145). This defluorination reaction was inhibited by glucose, gluconate or 2KGA, suggesting that all the three carbohydrates interact with the defluorinating protein. In addition the rates of defluorination were drastically reduced when the cells were grown on succinate. This is similar to the lower Vmax obtained for 2KGA transport by succinate-grown P. putida. In view of this, no definite conclusions can be drawn from the above results.

In order to gain further insight into the mechanism of 2KGA transport, isolated bacterial cytoplasmic membrane vesicles were used as a model for studies of active transport. With these vesicles, interactions with outer membrane proteins and periplasmic space binding proteins as well as substrate metabolism by the cytoplasmic enzymes are eliminated.

Membrane vesicles are usually prepared by the Kaback technique which involves the osmotic lysis of spheroplasts obtained from exposing bacterial cells to EDTA, Tris buffer and lysozyme (146). Konings et al. (147) demonstrated that vesicles prepared from P. putida by this technique catalyze the concentrative uptake of proline in the presence of PMS

ascorbate. However, in previous studies carried out in this laboratory (72, 131, 148), membrane vesicles were prepared from P. putida by the method developed by Stinnett et al. (74). Both PMS/ascorbate and L-malate/FAD stimulate the initial rate of transport and accumulation of glucose and gluconate in these vesicles (131, 148). For consistency, the vesicles used in this study were also prepared by the method of Stinnett et al. (74). As can be observed from the electron micrograph (Figure 16), the vesicles are intact structures and not just membrane fragments. They are relatively heterogenous with respect to vesicular size (0.2-0.48 micron in diameter). Similar variations in sizes have been reported for vesicles from P. putida (138, 148).

The orientation of the vesicle preparation was determined by measuring the activity of NADH-cytochrome c oxidoreductase. This enzyme is presumably located on the inner side of the cytoplasmic membrane and is inaccessible to externally added substrate. The enzyme activity was calculated from the slope of absorbance traces at 550 nm (Figure 17), obtained after a 5 min lag period, using a millimolar extinction coefficient of 19 for reduced cytochrome at pH 6.6 (131). NADH-cytochrome c oxidoreductase activity of 4.5 and 1.1 nmol cytochrome c reduced per min was obtained for detergent treated and native vesicles respectively. Thus approximately 76% of the vesicles were in the right-side out orientation. The variation in orientation for six different vesicle

Figure 16

Electron Micrograph of Cytoplasmic Membrane Vesicles from Glucose-Grown P. putida.

Legend:

1 drop of a suspension of membrane vesicles was negatively stained with 1% uranyl acetate solution on formvar grids and examined with a Phillips EM 201C electron microscope.

Figure 16

0.2 μ (x 25,000)

Figure 17

Absorbance against Time for NADH-cytochrome c Oxidoreductase in Membrane Vesicles from Glucose-Grown P. putida.

Legend:

Reaction mixtures containing 50 µmol potassium phosphate buffer, pH 6.6, 5 µmol $MgSO_4.7H_2O$, 0.5 mg cytochrome c (oxidized) and 0.5 mg native or detergent treated vesicles, were incubated for 5 min at 30°C and the absorbance at 550 nm was recorded for 10 min after initiating the reaction by adding 1.0 mg NADH. Absorbance readings were made against a reagent blank minus NADH.

Curve A = NADH - cytochrome c oxidoreductase activity of native vesicles.

Curve B = NADH - cytochrome c oxidoreductase activity of detergent treated vesicles.

Chart speed = 0.5 inch/min

Full scale deflection of recorder = 0.5 absorbance units.

Detergent treated vesicles were obtained by mixing equal volumes of membrane vesicles and 0.1% Triton X100 and incubating the mixture at 30°C for 10 min.

NADH-cytochrome c oxidoreductase activity is expressed as nmol cytochrome c reduced per min, using a millimolar extinction coefficient of 19 for cytochrome c at 550 nm.

Figure 17

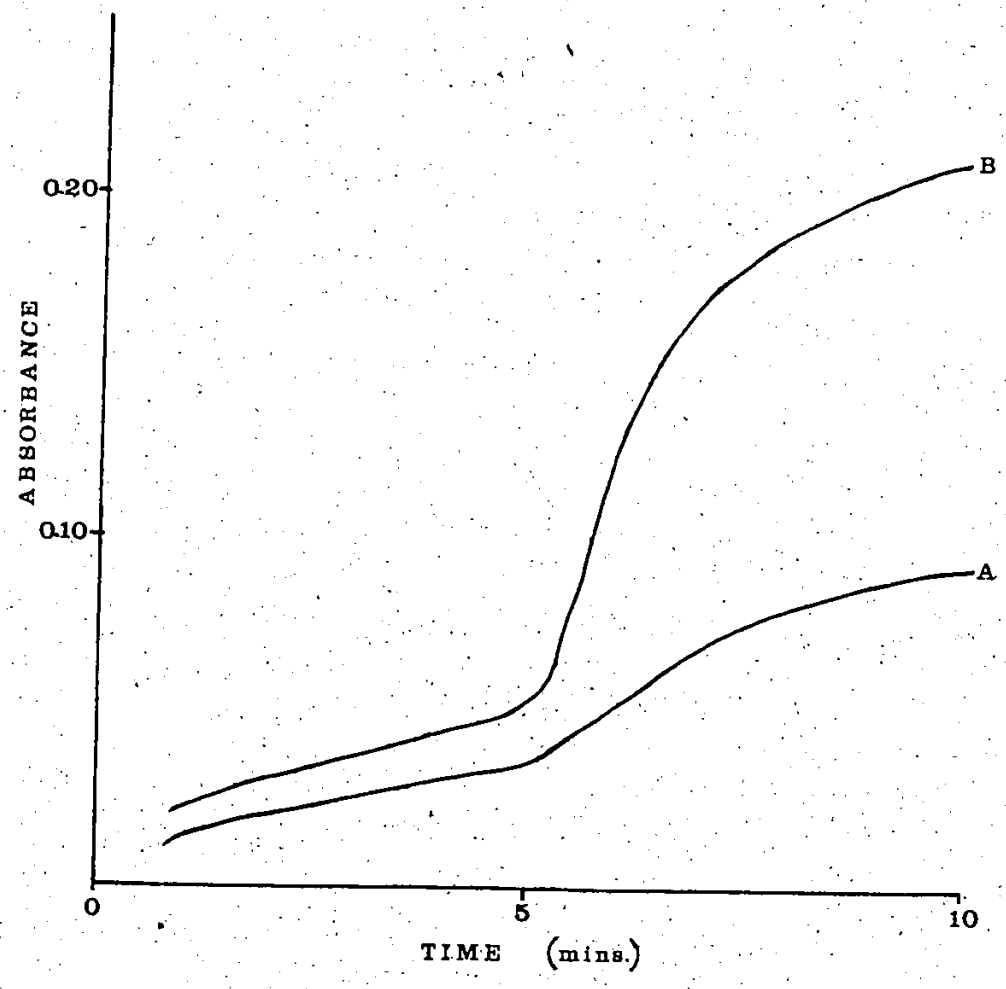

preparations was about 7%, indicating that a fairly consistent vesicle population was obtained for these studies. The fact that changes in the location of certain membrane enzymes occur during preparation of EDTA-lysozyme vesicle must be taken into consideration when estimating the orientation of membrane vesicles by this method (149).

As mentioned previously, aerobic fluorescent pseudomonads possess membrane bound glucose and gluconate dehydrogenases which are located on the external surface of the cytoplasmic membrane (114, 115, 116). A meaningful kinetic analysis of glucose and gluconate transport is therefore complicated by the fact that these sugars can act as electron donors and stimulate their own transport. Al-Jobore has shown that vesicles prepared from glucose-grown P. putida accumulate both glucose and gluconate in the absence of electron donors (148). This indicates that the problem of metabolism was not completely eliminated in these studies. 2KGA however, is the final product of extra-vesicular glucose oxidation and is transported without any metabolism by cytoplasmic membrane bound enzymes.

2KGA transport was measured as a function of time in the presence or absence of artificial and natural electron donors at different external 2KGA concentrations. A comparison of Figures 18 and 19 show that the amount of 2KGA transported by vesicles from glucose-grown P. putida increased with an increased external 2KGA concentration. The addition of L-malate/FAD or PMS/ascorbate increased the

Figure 18

Progress Curve for the Transport of 2KGA in Membrane Vesicles Prepared from Glucose-Grown P. putida in the Presence or Absence of Electron Donors.

Legend:

—●—●— 41.3 μM 2KGA only

—▲—▲— 41.3 μM 2KGA + PMS (0.1 mM)/Ascorbate (20 mM)

—■—■— 41.3 μM 2KGA + L-malate (10 mM)/FAD (50 μM)

The reaction mixture contained 50 μmol potassium phosphate buffer, pH 6.6, 12 μmol $MgSO_4.7H_2O$, 1.0 mg protein and the above final concentrations of Ascorbate/PMS or Malate/FAD. The mixture was incubated at 30°C for 5 min and the reaction initiated by addition of radioactive 2KGA. Total reaction volume was 1.0 mL. At time intervals 0.1-mL aliquots were removed and assayed as described in the MATERIALS AND METHODS section. Each point represents the average of duplicate assays.

The vertical bars indicate the standard deviation of the individual experiments about the mean.

Figure 18

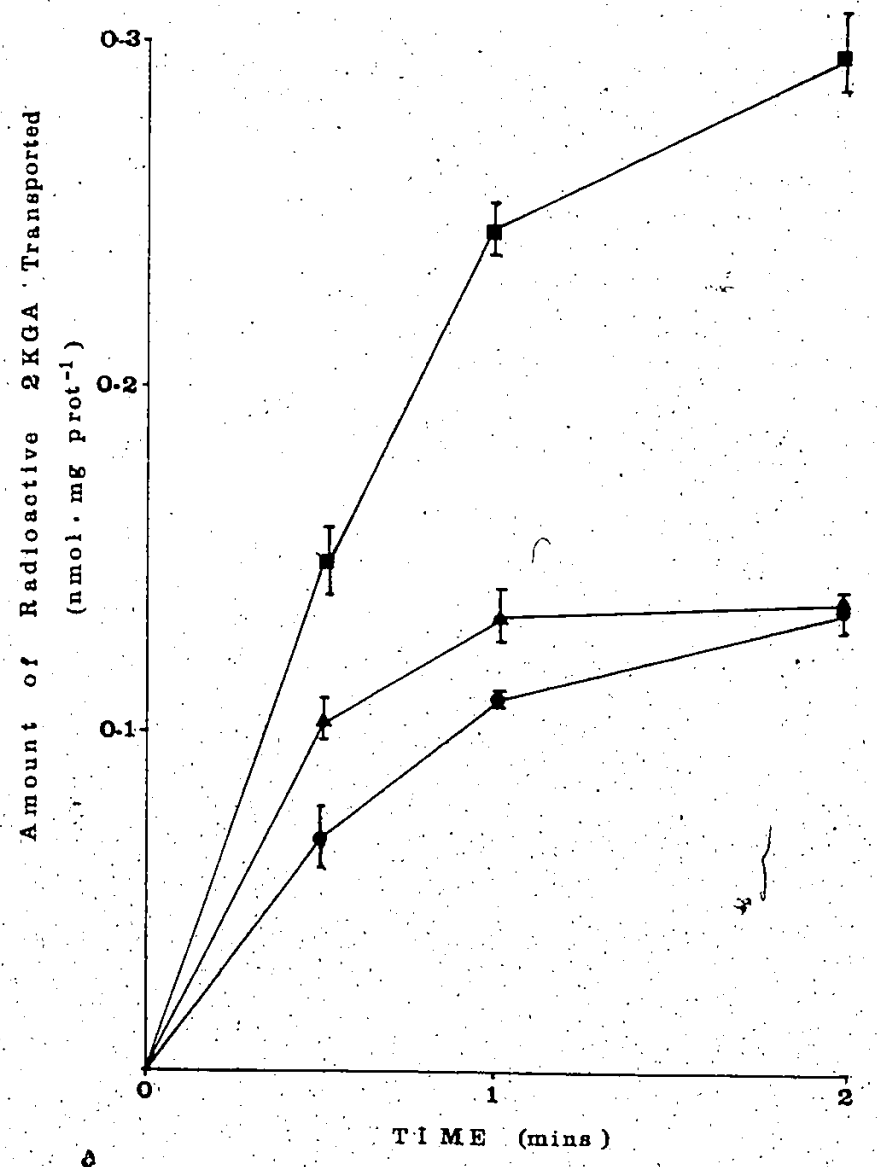
0·3
0·2
0·1
0
1
2
Amount of Radioactive 2KGA Transported
(nmol . mg prot^{-1})
TIME (mins)

Figure 19

Progress Curve for the Transport of 2KGA in Membrane Vesicles Prepared from Glucose-Grown P. putida in the Presence or Absence of Electron Donors.

Legend:

—●—●— 82.8 μM 2KGA only

—▲—▲— 82.8 μM 2KGA + PMS (0.1 mM)/Ascorbate (20 mM)

—■—■— 82.8 μM 2KGA + L-malate (10 mM)/FAD (50 μM)

Experimental conditions are given in the Legend to Figure 18

Figure 19

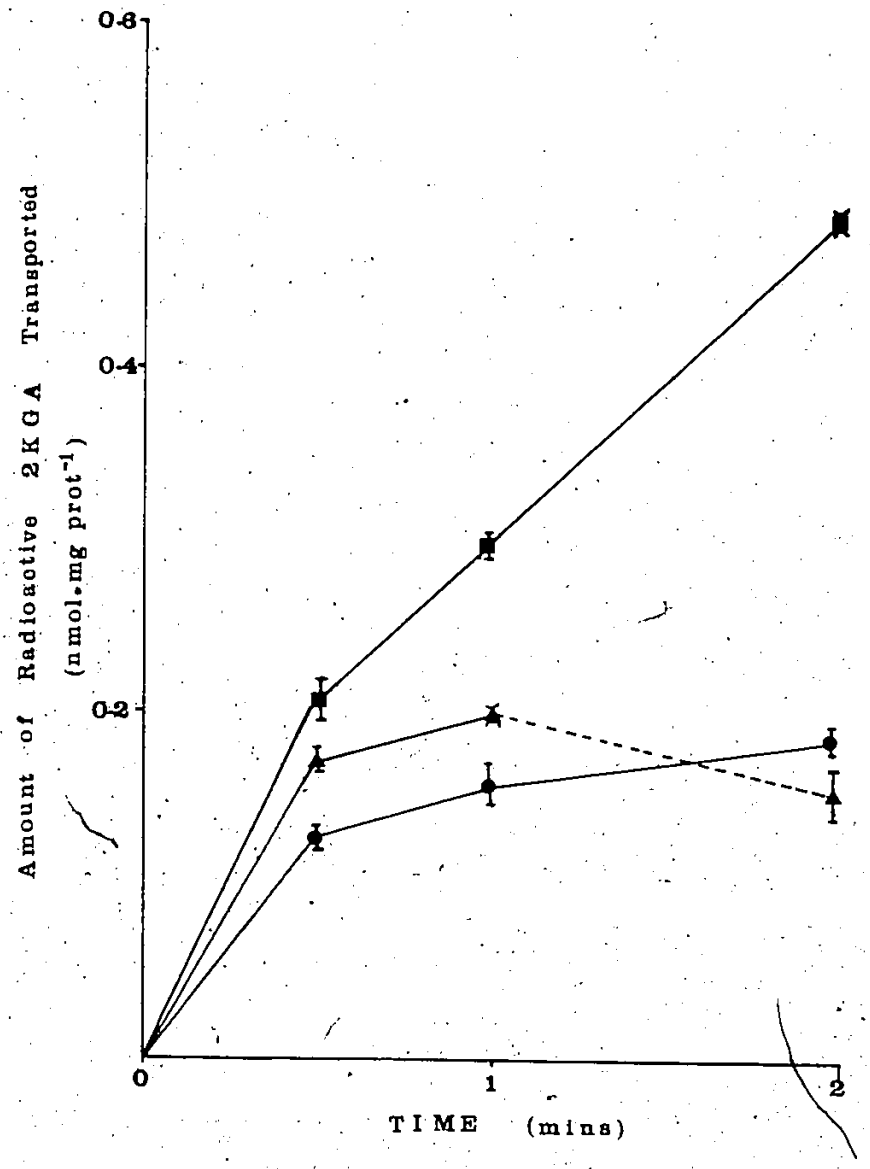
0·6
0·4
0·2
0
1
2
TIME (mins)
Amount of Radioactive 2KGA Transported
(nmol.mg prot^{-1})

initial rate of 2KGA transport in these vesicles. The stimulation by L-malate/FAD provides evidence for the presence of a membrane bound L-malate dehydrogenase in P. putida. The presence of an FAD-dependent L-malate dehydrogenase in Azotobacter vinelandii (150) and P. aeruginosa (74) have previously been reported. A significant stimulation of 2KGA transport was also observed when the vesicles were provided with other electron donors (Table 3). 2DOG is a known substrate for glucose dehydrogenase in P. aeruginosa (122), while 3FG (133), glucose and gluconate (72) are substrates for glucose dehydrogenase and gluconate dehydrogenase in P. putida. These results suggest that 2KGA transport is coupled to electron donor oxidation via the respiratory chain which, according to the chemiosmotic theory (55,56,57), would generate the necessary Δp required for active transport systems. In addition to electron donor stimulation, another criterion for active transport processes in the accumulation of substrates against concentration gradients (22). The data in Table 4 shows that in the absence of electron donors, 2KGA merely equilibrates across the membrane. Provision of various electron donors enhanced substrate accumulation by the vesicles to different extents. The efficiency of an electron donor in energizing transport could depend on factors such as its rate of oxidation and the mechanism of transport of the electron donor and its oxidative products. For example the conversion of glucose or gluconate to 2KGA will result in isotope dilution of the radiolabelled 2KGA. Thus the 2KGA concentration ratios reported in Table 4

Table 3

The Effect of Various Electron Donors on the Initial Rate of 2KGA Transport in Vesicles Prepared from Glucose-Grown P. putida.

Electron Donors Added (Final Concentration)	Initial Rate of Transport (nmol.mg prot.$^{-1}$min^{-1})
None	0.30
PMS (0.1mM)/Ascorbate (20 mM)	0.50
L-Malate (10 mM)/FAD (50 µM)	0.45
D-Glucose (100 µM)	0.85
D-Gluconate (100 µM)	1.10
2DOG (10 mM)	1.70
3FG (260 µM)	0.60

The reaction mixture contained 50 µmol potassium phosphate buffer, pH 6.6, 12 µmol $MgSO_4.7H_2O$, 0.98 mg protein and the above stated final concentrations of electron donors. After 5 min incubation at 30°C, the reaction was initiated by addition of 144.9 µM D-[U-^{14}C]2KGA. Total reaction volume was 1.0 mL. At 30, 60 and 120 s, 0.1-mL aliquots were filtered, washed, and the amount of 2KGA transported determined (See MATERIALS AND METHODS section). Results are the averages of duplicate assays.

Table 4

The Effect of Various Electron Donors on the Accumulation of 2KGA Transport in Vesicles Prepared from Glucose-Grown P. putida.

Electron Donors Added (Final Concentration)	Intravesicular Concentration of 2KGA (μM)	$\frac{[2KGA]_{int}}{[2KGA]_{ext}}$
None	143	0.99
PMS (0.1 mM)/Ascorbate (20 mM)	142	0.98 (2.05)
L-Malate (10mM)/FAD (50 μM)	207	1.43
D-Glucose (100 μM)	369	2.55
D-Gluconate (100 μM)	256	1.56
2DOG (10 mM)	536	3.70
3FG (260 μM)	269	1.86

Reaction conditions were identical to those described in the footnote to Table 3, except the intravesicular 2KGA was measured 10 min after the reaction was initiated. Results are the averages of duplicate assays.
The accumulation of 2KGA is based on initial external 2KGA of 144.9 μM and an intravesicular volume of 3.6 $\mu L \cdot mg\ protein^{-1}$.
Note: The number in parenthesis is based on measurements made 1 min after the reaction was initiated.

using glucose and gluconate as electron donors may be underestimated. Furthermore, the transport of glucose, gluconate, 3FG and 2DOG have been shown to be linked to respiration (72), and could accumulate in response to a Δp generated by their oxidation. If these substrates are transported by a proton-symport mechanism, the Δp will be dissipated and may no longer be sufficient to effect maximum 2KGA accumulation. It is interesting to note that no accumulation was observed with PMS/ascorbate after 10 min incubation with labelled substrate (Table 4). As illustrated in Figure 19, the initial stimulation by PMS/ascorbate was followed by a rapid net efflux of labelled 2KGA so that the steady-state value of 0.98 obtained for substrate accumulation after 10 min was considerably less than the value of 2.05 obtained in the first 60 s. The reason for this efflux is not known.

A detailed kinetic analysis of 2KGA transport was performed with external substrate concentrations in the range of 10.4 µM to 144.9 µM. In the absence of electron donors, vesicles from glucose-grown cells displayed saturation kinetics for 2KGA transport with average apparent Km and Vmax of 111.0±2.9 µM and 0.55±0.04 nmol.mg protein^{-1}.min^{-1} (Figure 20). With PMS/ascorbate or L-malate/FAD present, the average apparent Km values were significantly reduced to 50.2±2.1 µM and 34.8±2.9 µM, respectively, while the Vmax remained unchanged. (Figure 20). These results are consistent with an increased binding

Figure 20

Double Reciprocal Plots of 2KGA Transport in Membrane Vesicles Prepared from Glucose-Grown P. putida in the Presence or Absence of Electron Donors.

Legend:

—●—●— No Electron Donor

—▲—▲— PMS (0.1 mM)/Ascorbate (20 mM)

—■—■— L-Malate (10 mM)/FAD (50 μM)

Experimental conditions are given in the legend to Figure 18. The line represents the best fit line derived from linear regression analysis of the kinetic data. Each point is the average of duplicate determinations.

Average apparent Km values (3 different vesicle preparations) are 111.0±2.9 μM in the absence of electron donor; 50.2±2.1 μM in the presence of PMS/Ascorbate and 34.8±2.9 μM in the presence of L-malate/FAD. The average apparent Vmax value in the presence or absence of electron donors is 0.55±0.04 nmol.mg protein^{-1} min.$^{-1}$.

Figure 20

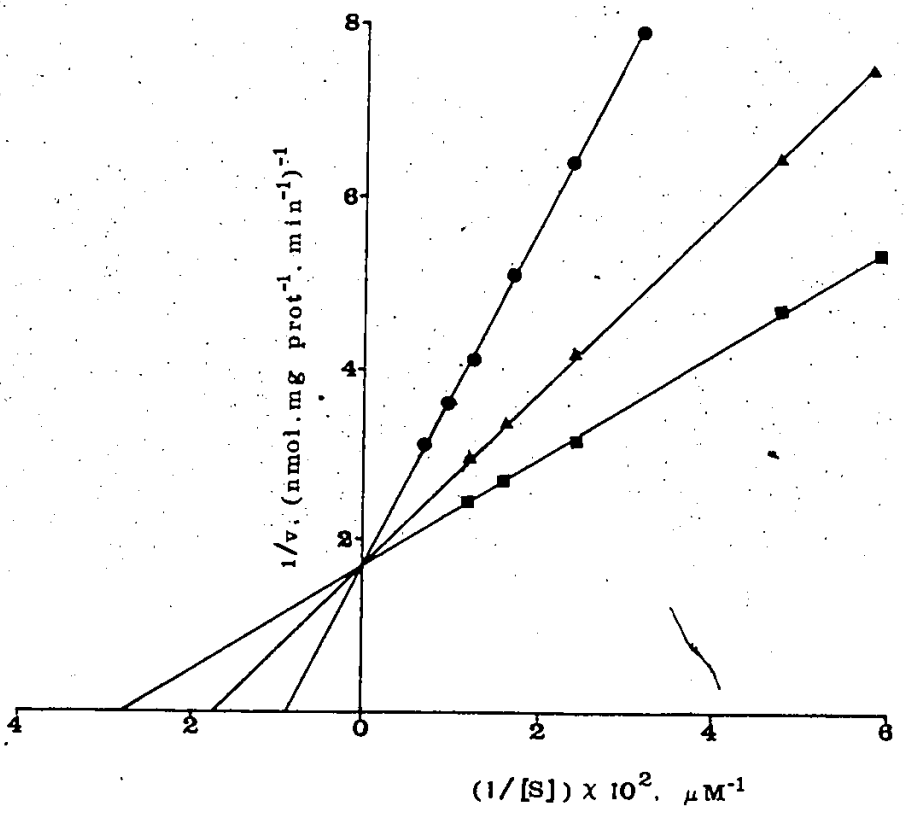

affinity of 2KGA for its carrier in the presence of electron donors. Similar observations have been reported for dansyl-galactoside binding to E. coli vesicles (151) as well as glucose and gluconate transport in vesicles from P. putida (72) in the presence and absence of electron donors. To obtain further evidence for the coupling of 2KGA transport to respiration, studies were carried out to investigate the effect of electron chain inhibitors and uncoupler on the transport system. As anticipated the compounds tested had no effect on 2KGA transport in the absence of electron donor (Table 5). Under these conditions transport occurs by a facilitated diffusion process both in the presence and absence of the inhibitors. In the presence of L-malate/FAD, the transport system is coupled to L-malate oxidation and 2KGA accumulates against a concentration gradient. Thus the provision of antimycin A, which blocks electron transfer from L-malate to oxygen between cytochromes b and c, and rotenone, which blocks between the primary dehydrogenase and coenzyme Q, decrease the initial rate of transport and accumulation of 2KGA. A similar effect is observed with DNP, an uncoupler which collapses the Δp generated by L-malate oxidation. The non-inhibitory effect of cyanide could be due to the presence of a cyanide insensitive O-type cytochrome in P. putida. This type of cytochrome has been identified in P. aeruginosa (152). Lui and Webster have also shown that a purified oxygenated cytochrome o obtained from a strain of Vitrcescilla sp does not react with cyanide (153). The reason for the stimulation of the initial rate

Table 5

The Effect of Repiratory Chain Inhibitors and Uncoupler on the Initial Rate of 2KGA Transport in Vesicles from Glucose-Grown P. putida.

Compounds Added (Final Concentrations)	Initial Rate of 2KGA Transport (nmol.mg prot.$^{-1}$ min.$^{-1}$) (a)	(b)	
None	0.44	0.35	(1.72)
Antimycin A (0.24 mM)	0.45	0.24	(0.98)
Rotenone (0.24 mM)	0.42	0.24	(0.95)
2,4-DNP (30 mM)	0.40	0.22	(0.90)
KCN (20 mM)	0.44	0.44	(1.79)

(a): 124.2 µM D-[U-^{14}C]2KGA; - L-malate/FAD
(b): 82.8 µM D-[U-^{14}C]2KGA; + L-malate/FAD
Numbers in parenthesis refer to substrate accumulation ratios, i.e., [S]int/[S]ext, measured 10 min after initiating the reaction, and is based on an intravesicular volume of 3.6 µL.
Reaction mixtures contained 50 µmol potassium phosphate buffer, pH 6.6, 12 µmol $MgSO_4$, 1.0 mg protein, the above concentration of inhibitor and when present, 10 mM L-malate/50 µM FAD. The mixture was preincubated with shaking and oxygen gassing at 30°C for 10 min before addition of known concentrations of radioactive 2KGA. Total reaction volume was 1.0 mL. The initial rates of transport were determined as described in the footnote to Table 3. Results are the averages of duplicate assays. Antimycin A, Rotenone and DNP were made up in absolute ethanol. The effects of ethanol were corrected for where appropriate.

of transport by cyanide is not known.

To further characterize the 2KGA transport protein, the effect of fluorinated 2KGA analogues on this system was investigated. The use of fluorocarbohydrates as biochemical probes is now fairly well established (154). These compounds have been widely used to probe the specificity of the glucose carrier in human erythrocytes (155, 156) and hamster intestine (157) as well as carbohydrate metabolism in E. coli (158) and P. putida (159). The fundamental reasoning is that fluorine may mimic hydroxy-group electronegativity, especially with respect to size and the ability to form hydrogen bonds. As a result of this, fluorinated substrate analogues, in which a specific hydroxyl group of the substrate has been replaced by a fluorine atom, may retain the biological activities of the natural substrate. The specificity of a transport system can be determined by comparing the affinity of various fluorinated and deoxygenated substrate analogues on the system. In membrane vesicles from glucose-grown P. putida both 3F2KGA and 4F2KGA competitively inhibited 2KGA transport with K_i values of 160 μM and 50 μM respectively (Figures 21 and 22), suggesting that 2KGA and its fluorinated analogues are transported by a common system. 4F2KGA, however, binds more effectively to the carrier than 3F2KGA. This may be a consequence of the involvement of the C-3 hydroxyl group of 2KGA in hydrogen bond interactions between the substrate and the carrier during the trans-

Figure 21

Dixon Plot of 2KGA Transport from Glucose-Grown P. putida in the Presence of Known 3F2KGA Concentrations.

Legend:

—●—●— 154 µM 2KGA

—▲—▲— 95 µM 2KGA

—■—■— 47.5 µM 2KGA

$\bar{v}$ – Initial Rate of 2KGA Transport

1.0 mg of the vesicle preparation was incubated with 50 mM potassium phosphate buffer, pH 6.6, 12 mM $MgSO_4.7H_2O$, and known concentrations of 3F2KGA at 30°C for 10 min, with continuous gassing with oxygen. The reaction was initiated by adding the appropriate concentration of radioactive 2KGA. The final volume was 1.0 mL. The amount of 2KGA transported was assayed in duplicate as described for Table 3.

An average K_i value of 160 µM was obtained for two different vesicle preparations.

Figure 21

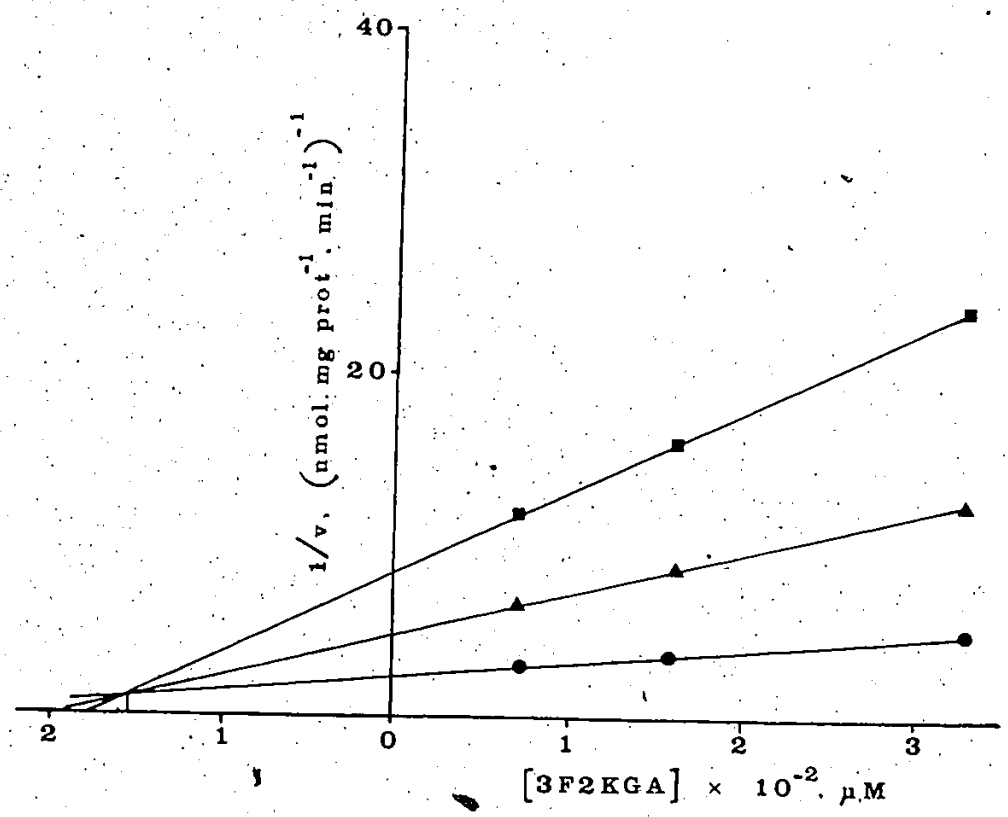

Figure 22

Dixon Plot of 2KGA Transport from Glucose-Grown P. putida in the Presence of Known 4F2KGA Concentrations.

Legend:

—●—● 154 μM 2KGA

—▲—▲ 95 μM 2KGA

—■—■ 47.5 μM 2KGA

v - Initial Rate of 2KGA Transport

1.0 mg of the vesicle preparation was incubated with 50 mM potassium phosphate buffer, pH 6.6, 12 mM $MgSO_4.7H_2O$, and known concentrations of 4F2KGA at 30°C for 10 min, with continuous gassing with oxygen. The reaction was initiated by adding the appropriate concentration of radioactive 2KGA. The final volume was 1.0 mL. The amount of 2KGA transported was assayed in duplicate as described for Table 3.

An average K_i value of 50 μM obtained for two different vesicle preparations.

Figure 22

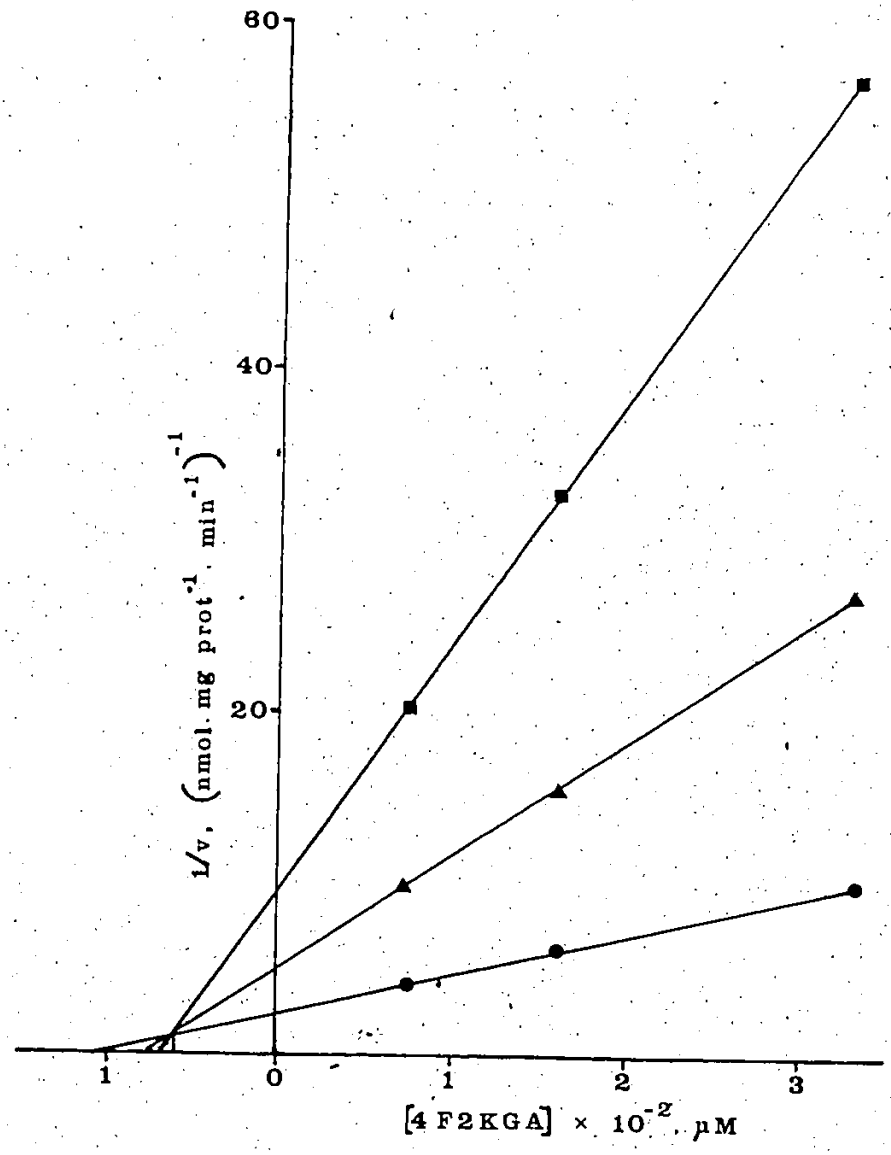

location process. If the hydrogen bond extends from the hydrogen of the C-3 hydroxyl group to an electronegative group on the carrier, then replacing the hydroxyl group with a fluorine atom would prevent this interaction and result in a lower affinity of 3F2KGA for the carrier. The high affinity of 4F2KGA for the carrier can be explained in two ways. The C-4 hydroxyl group of 2KGA may not interact with the carrier to a significant extent so that replacing it with flourine does not affect the affinity of the substrate. On the other hand, a hydrogen bond may extend from the oxygen atom of the hydroxyl group to a hydrogen atom on the carrier. In this case, on replacing the hydroxyl group with a fluorine atom, the hydrogen bond interaction will now occur between the fluorine of 4F2KGA and the hydrogen on the carrier. In order to draw unambiguous conclusions about possible hydrogen bonding between 2KGA and the carrier protein, a comparison between the effects of 3F2KGA, 4F2KGA and the corresponding deoxysugars on 2KGA transport would have to be made. Unfortunately, the appropriate deoxysugar analogues are not available.

Like glucose-vesicles, the initial rate of 2KGA transport in vesicles prepared from succinate-grown cells increased with increased substrate concentrations (Table 6). However, a double reciprocal plot of the kinetic data obtained from these studies showed that 2KGA transport in these vesicles occurred by a non-specific physical diffusion process with a Km value of ∞ (Figure 23). Furthermore no stimulation of 2KGA transport was observed when the vesicles

Table 6

Transport of 2KGA in Vesicles Prepared from Succinate-Grown *P. putida*.

2 KGA (μM)	Initial Rate of 2KGA Transport (nmol.mg prot.$^{-1}$min.$^{-1}$)
23.8	0.05
47.5	0.10
95.0	0.18
142.6	0.31
190.1	0.41

Reaction conditions were identical to those described for Table 3. The reaction mixture contained 50 μmol potassium phosphate buffer, pH 6.6, 12 μmol $MgSO_4.7H_2O$ and 0.98 mg protein. After 5 min incubation at 30°C the reaction was initiated by adding the appropriate amount of radioactive 2KGA. The initial rates of transport were determined as previously described (See footnote to Table 3). Results are the averages of duplicate determinations.

Figure 23

Double Reciprocal Plot of 2KGA Transport in Membrane Vesicles Prepared from Succinate-Grown P. putida.

Legend:

[S] - 2KGA concentration

v - Initial rate of 2KGA transport

Experimental conditions are given in the footnote to Table 6

Km values of ∞ were obtained for 3 different vesicle preparations.

Figure 23

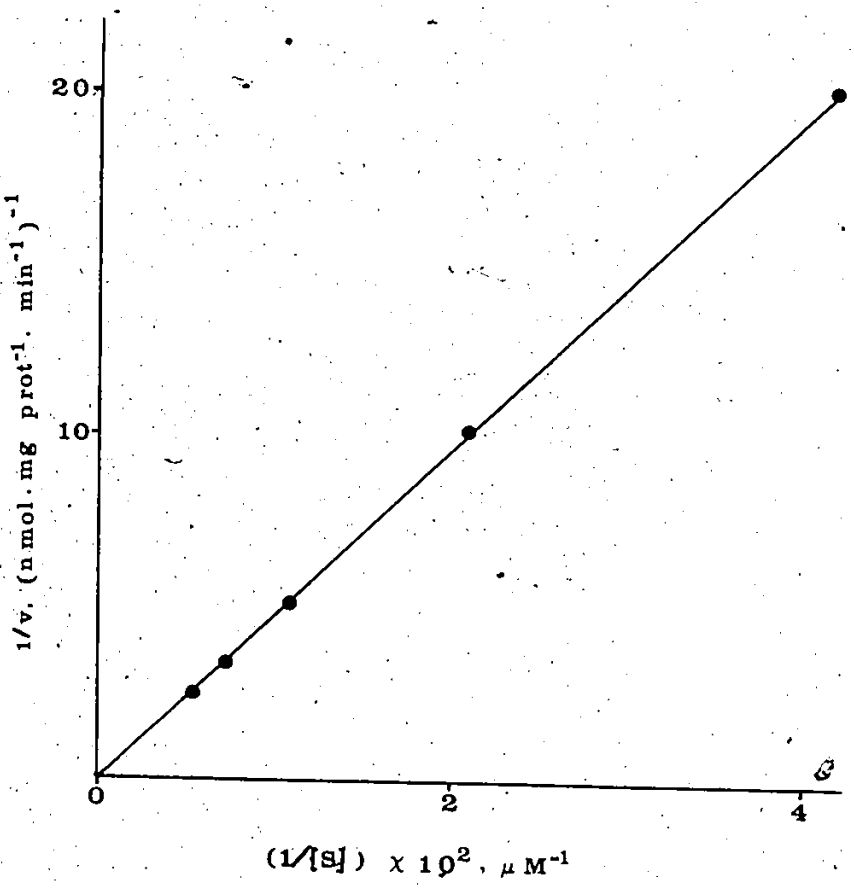

were provided with electron donors (Data not shown). These results suggest that the 2KGA carrier is repressed by growth of P. putida on succinate. Similar observations have been reported for the glucose carrier in vesicles from succinate-grown P. putida (72). The gluconate carrier in these organisms appears to remain constitutive (72).

Since all the evidence presented so far suggest that 2KGA transport is coupled to the electron transport chain, studies were undertaken to measure the Δp generated by vesicles during electron donor oxidation. The magnitude of $\Delta\Psi$ and ΔpH was determined by flow dialysis using the distribution of radiolabelled $TPMP^+$ and acetate respectively. Figure 24 illustrates a typical flow dialysis experiment carried out with [U-^{14}C]$TPMP^+$. The radioactive $TPMP^+$ added to the upper chamber diffused into the lower chamber and appeared in the dialysate. The amount of radioactivity in the dialysate increased linearly until equilibrium was established between the upper and lower chambers, and then decreased at a slow rate due to dilution with the buffer being pumped through the lower chamber (closed circles). Immediatedly after PMS/ascorbate was added to the upper chamber, the vesicles began to accumulate $TPMP^+$, and its concentration in the dialysate decreased drastically. This observation is consistent with the principle that when a $\Delta\Psi$ is generated by the oxidation of electron donors, $TPMP^+$ will redistribute until electrochemical equilibrium is regained. DNP collapsed $\Delta\Psi$ by rendering the membrane permeable to protons. Thus

Figure 24

Flow Dialysis Measurement of Electron Donor Dependent $TPMP^+$ Uptake in Vesicles from Glucose-Grown P. putida.

Legend:

—●—● Equilibration of $TPMP^+$

—▲—▲— Uptake of $TPMP^+$ after addition of Electron Donor (ED) which was a mixture of 9 µL PMS (0.1 mM) and 37 µL Ascorbate (20 mM)

—o—o— Uptake of $TPMP^+$ after addition of ED and 20 µL DNP (2 µM)

Arrows indicate point of addition of ED or DNP

Membrane vesicles (3.0 mg protein), suspended in 0.82 mL of 0.05 M potassium phosphate buffer, pH 6.6, containing 0.01 M $MgSO_4$ were added to the upper chamber. 20 µL of $TPMP^+$ (125 µM, 9 mCi/mmol) was added through the aperture in the top well followed by the addition of ED and DNP at the appropriate times. For $TPMP^+$ equilibration, 46 µL of water was added instead of ED. DNP was made up in 50% ethanol. Addition of 20 µL of 50% ethanol instead of DNP did not cause $TPMP^+$ release from the vesicles.

For details of experimental set up see MATERIALS AND METHODS section.

$\Delta\Psi$= -72.6 mV

Figure 24

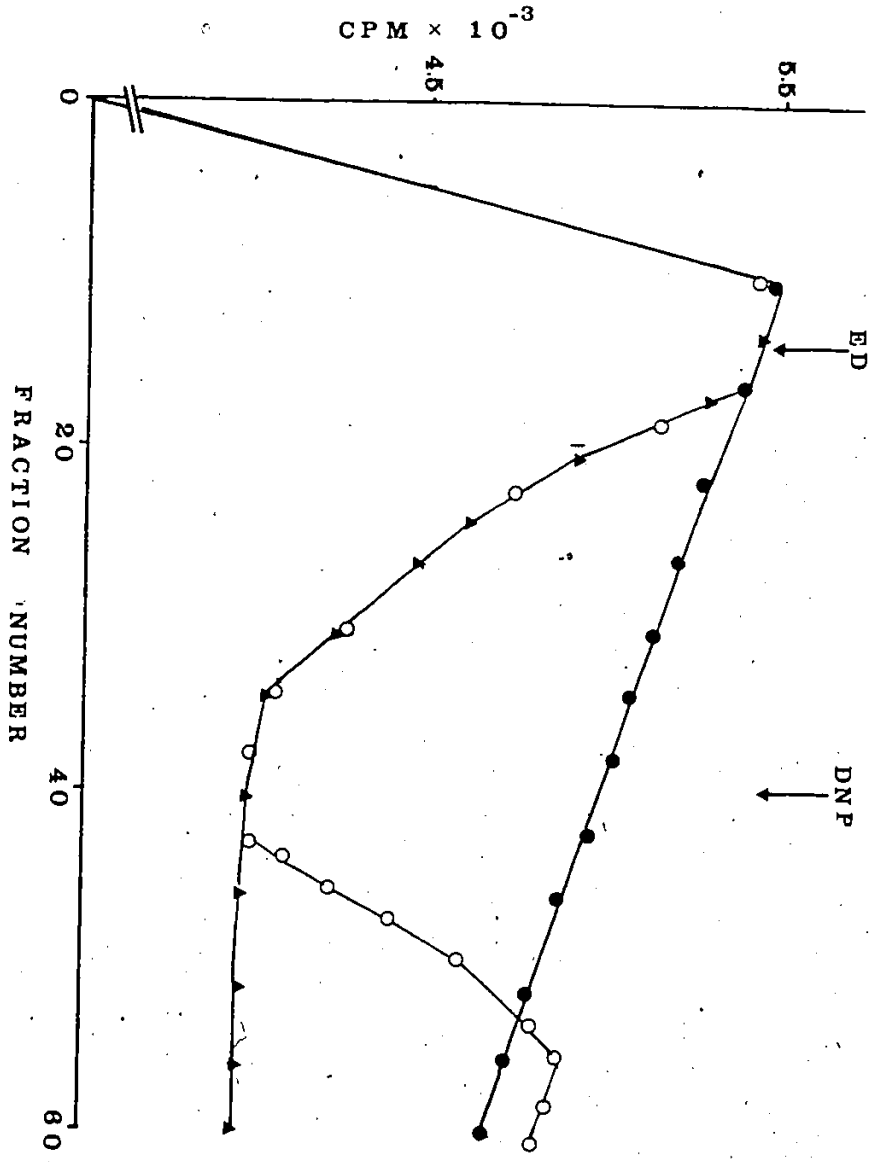

$TPMP^+$ is released from the vesicles into the medium, and the external concentration virtually returns to the control levels. By using the difference in equilibrium concentrations of $TPMP^+$ observed in the dialysate before and after addition of PMS/ascorbate (i.e., fraction 34), the amount of $TPMP^+$ accumulated by the vesicles was calculated (see APPENDIX VI). ΔpH was determined in a similar manner using the distribution of sodium[1-^{14}C]acetate. Again, acetate accumulation was observed immediately after the addition of PMS/ascorbate (Figure 25). The oxidation of PMS/ascorbate generated a ΔpH, internal alkaline, across the membrane. This caused the equilibrium between the undissociated and dissociated species of acetate to be displaced towards the non-permeable ionic form which accumulated within the vesicular compartment. Acetate accumulation was calculated from fraction 26 (See APPENDIX VI). The flow dialysis pattern obtained with some of the natural electron donors differed slightly from that obtained with PMS/ascorbate. With L-malate/FAD for example, acetate accumulation by glucose-vesicles was observed at approximately 8 min after the electron donor was added (Figure 26), thus ΔpH was calculated from fraction 38. (Note that with PMS/ascorbate as electron donor, maximum acetate accumulation was observed in fraction 26). In this set of experiments, the possibility of L-malate buffering the system must be taken into consideration. L-malate is a weak acid with a pK_2 of 5.2, and is present in the system at a fairly high concentration of 10

Figure 25

Flow Dialysis Measurement of Electron Donor Dependent Acetate Uptake in Vesicles from Glucose-Grown P. putida.

Legend:

—●—●— Equilibration of Acetate

—▲—▲— Uptake of Acetate after addition of Electron Donor (ED) which was a mixture of 9 µL PMS (0.1 mM) and 37 µL Ascorbate (20 mM)

—o—o— Uptake of Acetate after addition of ED and 20 µL DNP (2 µM)

Arrows indicate point of addition of ED or DNP.

Membrane vesicles (3.0 mg protein), suspended in 0.80 mL of 0.05 M potassium phosphate buffer, pH 6.6, containing 0.01 M $MgSO_4$ were added to the upper chamber. 40 µL of [1-^{14}C]Acetate (44.3 µM, 54.2 mCi/mmol) was added through the aperture in the top well followed by the addition of ED and DNP at the appropriate times. For Acetate equilibration, 46 µL of water was added instead of ED. DNP was made up in 50% ethanol. Addition of 20 µL of 50% ethanol instead of DNP did not cause Acetate release from the vesicles.

For details of experimental set up see MATERIALS AND METHODS section.

$\Delta pH = -73.5$ mV

Figure 25

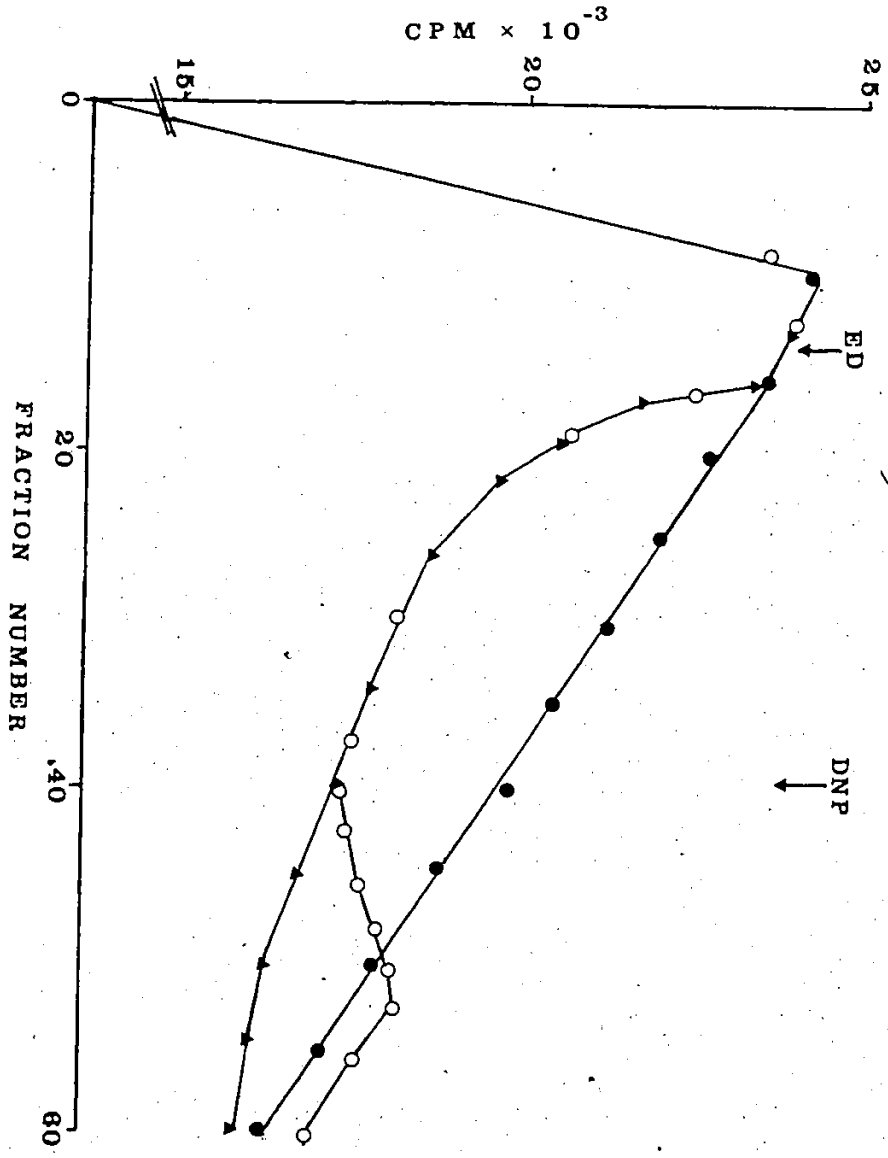

Figure 26

Flow Dialysis Measurement of Electron Donor Dependent Acetate Uptake in Vesicles from Glucose-Grown *P. putida*.

Legend:

—●—●— Equilibration of Acetate

—○—○— Uptake of Acetate after addition of Electron Donor (ED) which was a mixture of 23 µL L-malate (10 mM) and 23 µL FAD (50 µM)

Arrows indicates point of addition of ED

Experimental conditions are given in the Legend to Figure 25

$\Delta pH = -69$ mV

Figure 26

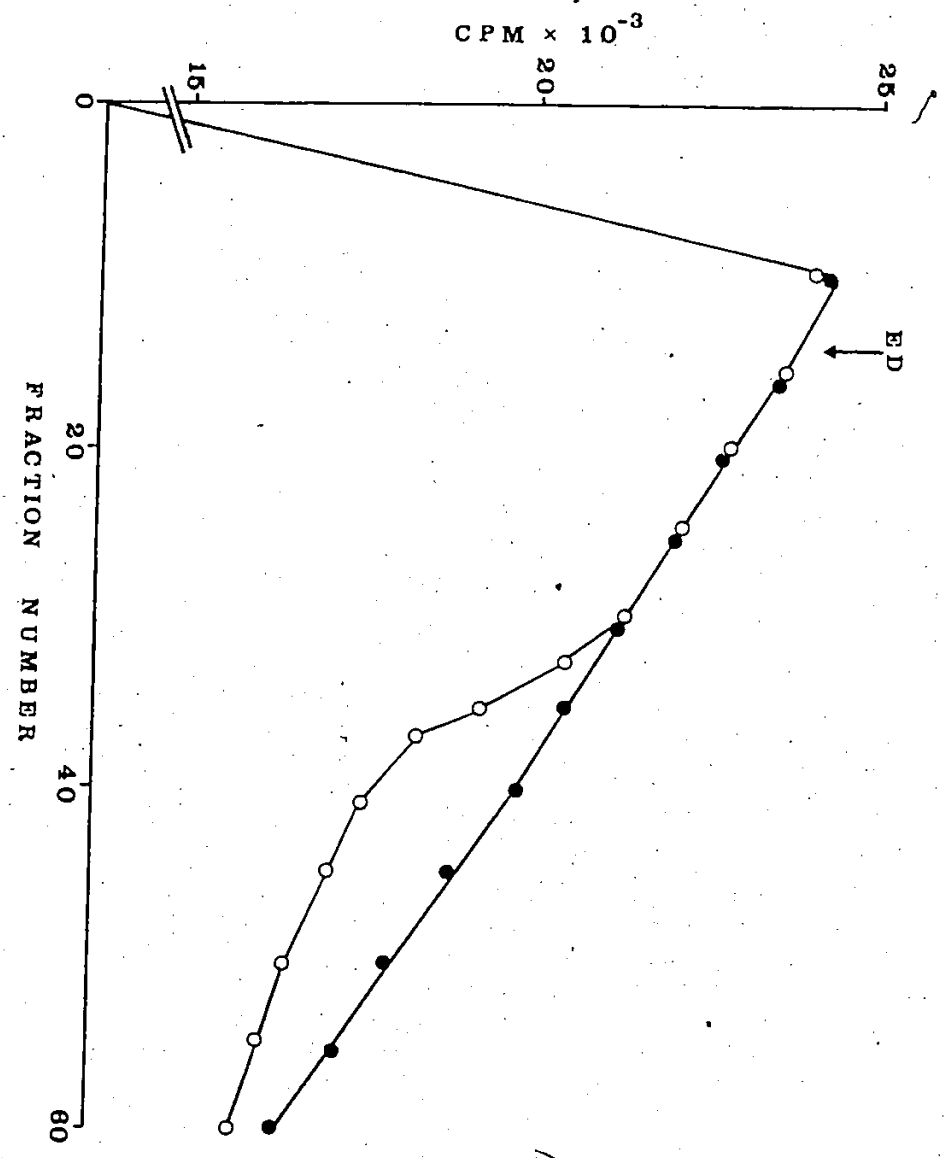

mM. By acting as a buffer L-malate could maintain a constant pH during its oxidation until its buffering capacity is exceeded. Further proton extrusion at this point would generate a pH gradient, inside alkaline, which can be detected from the distribution of acetate. Moreover $TPMP^+$ accumulation by glucose-vesicles occurred immediately after the provision of L-malate (Data not shown), indicating that the delay in acetate accumulation is not due to a lag period in L-malate oxidation by these vesicles. It is also interesting to note that acetate accumulation during glucose and gluconate oxidation by succinate vesicles is initially similar (Figure 27). However, 9 min after the addition of glucose, the ΔpH collapsed and acetate was released. At approximately the same time, acetate accumulation started to increase with gluconate as electron donor, and reached a maximum in 13 min (fraction 40). Thus the ΔpH generated with glucose and gluconate as electron donors were calculated from fractions 30 and 40 respectively.

The $\Delta\Psi$ and ΔpH values obtained for glucose- and succinate-vesicles in the presence of various electron donors are given in Table 7. With PMS/ascorbate as electron donor Δp values of -145 mV and -140 mV were obtained for glucose- and succinate-vesicles respectively. With natural electron donors, however, there were significant variations between the Δp values obtained for glucose and succinate vesicles. It is apparent from the above observation that results obtained with natural electron donor are much more difficult to interpret than those obtained with the

Figure 27

Flow Dialysis Measurement of Electron Donor Dependent Acetate Uptake in Vesicles from Succinate-Grown *P. putida*.

Legend:

—●—●— Equilibration of Acetate

—○—○— Uptake of Acetate after addition of Electron Donor (ED), 46 µL Glucose (2.5 mM): ΔpH = -50 mV

—△—△— Uptake of Acetate after addition of Electron Donor (ED), 46 µL Gluconate (2.5 mM): ΔpH = -70.5 mV

Arrows indicates point of addition of ED

Experimental conditions are given in the Legend to Figure 25

Figure 27

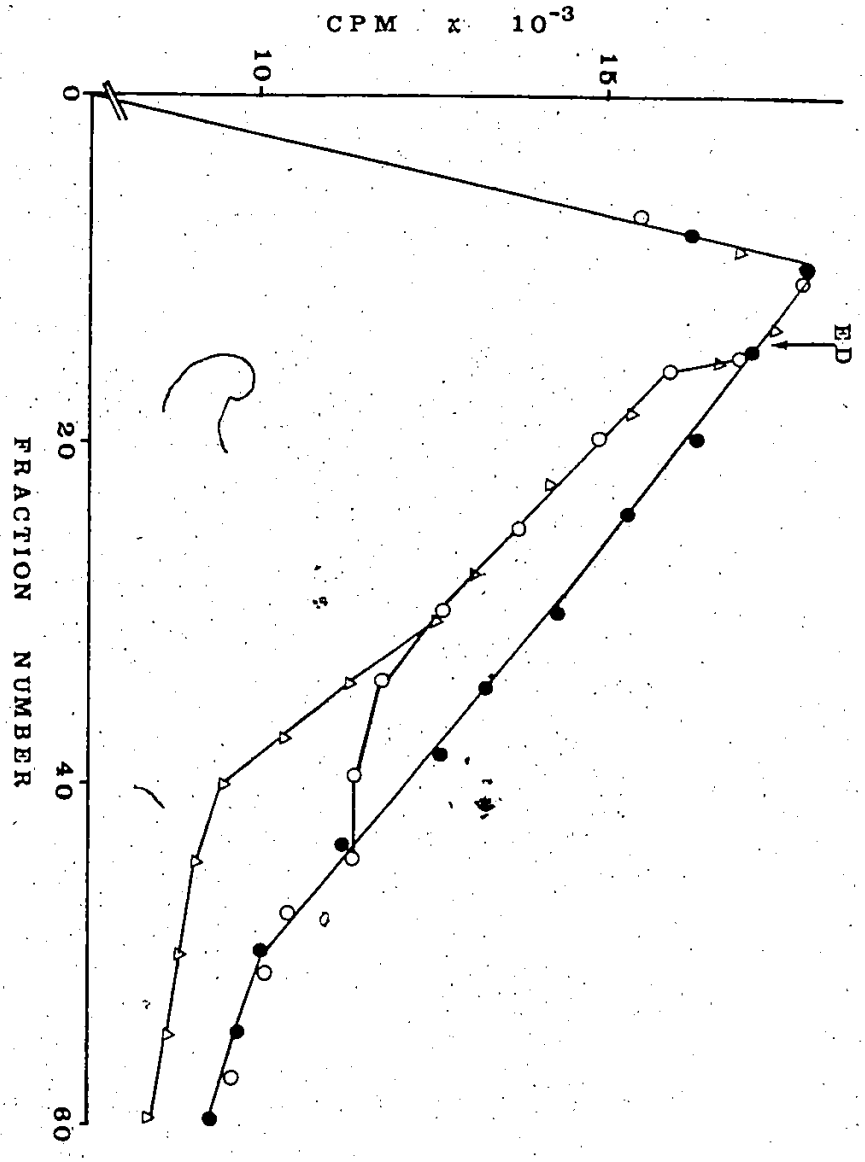

Table 7

Summary of $\Delta\psi$, ΔpH and Δp Values Obtained for Vesicles Prepared from Glucose- and Succinate-Grown *P. putida*.

Electron Donors Added (Final Concentration)	Vesicles from Glucose-Grown Cells			Vesicles from Succinate-Grown Cells		
	$\Delta\psi$	ΔpH	Δp	$\Delta\psi$	ΔpH	Δp
PMS (0.1 mM)/ Ascorbate (20mM)	-71	-74	-145	-70	-70	-140
L-malate (10mM)/ FAD (50 μM)	-60	-69	-129	0	0	0
Glucose (2.5 mM)	-47	-68	-115	-33	-49	-82
Gluconate (2.5mM)	-62	0	-62	-41	-71	-112

Experimental conditions are given in the legends to Figures 25 - 27.

$\Delta\psi$ and ΔpH values are in mV, and were calculated from $TPMP^+$ and acetate accumulation ratios respectively (See APPENDIX VI for sample calculations).

Δp is the sum of $\Delta\psi$ and ΔpH and is in mV.

The values given are the averages of duplicate determinations.

artificial electron donor. The magnitude of $\Delta\Psi$ and ΔpH probably depends on the rate of oxidation and/or the mechanism of transport of the natural electron donors in the two sets of vesicles. With reference to equation (3), i.e., $\log([S]_{in}/[S]_{out}) = [(n+m)\Delta\Psi - nZ\Delta pH]/Z$; if glucose (charge, m = 0), is transported by an electrogenic symport reaction (e.g., the neutral substrate is transported with one or more protons) with a ratio of proton to substrate of 1:1, then the charge on the proton, n = +1. Equation (3) reduces to $\log([S]_{in}/[S]_{out}) = \Delta\Psi/Z - \Delta pH = \Delta p/Z$. Considering the transport of gluconate (charge, m = -1) by an electroneutral symport mechanism (e.g., the transport of a negatively charged ion with protons such that there is no overall charge transfer), n = +1 and equation (3) reduces to $\log([S]_{in}/[S]_{out}) = \Delta pH$. Thus the transport of substrate can be coupled to the total Δp in electrogenic symport reactions or to only the ΔpH in electroneutral symport reactions. The transport of glucose, gluconate (72) and their oxidative product 2KGA, have been shown to be coupled to electron donor oxidation and presumably occurs by either an electrogenic or an electroneutral proton symport mechanism. In addition, the mechanism of transport of glucose and 2KGA differ in glucose- and succinate vesicles (72), since the glucose and 2KGA carriers are repressed in succinate-grown cells. Thus depending on the mechanism of transport of glucose, gluconate or their oxidative product, 2KGA in a particular set of vesicles, a partial dissipation of Δp may occur as a result of protons moving back into the

vesicles with these carbohydrates. It is therefore difficult to understand the results obtained with glucose and gluconate as electron donors since data interpretation is complicated by the fact that various oxidation and transport steps occur simultaneously in vesicles provided with these electron donors. Very striking, is the observation that no Δp was detected with L-malate as electron donor in succinate-vesicles while a Δp of -129 mV was obtained with glucose-vesicles (Table 7). Evidence will be presented later to show that this is probably due to the obligatory couple of L-malate transport to proton uptake via the L-malate carrier in succinate-vesicles.

In order to determine whether the magnitude of $\Delta\Psi$ and ΔpH was affected by the rate of oxidation of the natural electron donors, the dehydrogenase and oxidase activities of the electron donors in glucose- and succinate-vesicles were compared. Using DCIP and potassium ferricyanide as artificial electron acceptors, it was demonstrated that glucose and malate dehydrogenase activities remained virtually the same in the two sets of vesicles but the activity of gluconate dehydrogenase in succinate-vesicles was approximately 10% of that obtained for glucose-vesicles (Table 8). This suggests that the residual gluconate dehydrogenase activity in succinate-vesicles is still sufficient to generate a $\Delta\Psi$ and ΔpH in these vesicles (Table 7). Subsequent studies in which oxygen consumption was measured showed that both glucose- and succinate-vesicles have active glucose and L-malate oxidases (Table 9). Like

Table 8

Dehydrogenase Activities in Vesicles from Glucose- and Succinate-Grown *P. putida*.

Substrate Concentration	Dehydrogenase Activity (nmol DCIP or Fe^{3+} .mg protein.$^{-1}$min.$^{-1}$)			
	Vesicles from Glucose-Grown Cells		Vesicles from Succinate-Grown Cells	
	DCIP	Fe^{3+}	DCIP	Fe^{3+}
D-Glucose (6.7mM)	140	315	110	245
D-Gluconate (6.7mM)	70	175	0	17.5
L-malate (10 mM)+ FAD (50 μM)	35	19.6	45.5	21

Dehydrogenase activity was determined by measuring the change in absorbance of the electron acceptors, DCIP or ferricyanide at 25°C and pH 6.6 at 600 and 420 nm, respectively (See MATERIALS AND METHODS). The results are the averages of duplicate assays.

Table 9

Oxidase Activities in Vesicles from Glucose- and Succinate-Grown *P. putida*.

Substrate Concentration	Oxidase Activity ($nmol\ O_2 . mg\ protein.^{-1}\ min.^{-1}$)	
	Vesicles from Glucose-Grown Cells	Vesicles from Succinate-Grown Cells
D-Glucose (6.7 mM)	376.0	241.0
D-Gluconate (6.7 mM)	110.5	8.2
L-malate (10 mM) + FAD (50 μM)	38.5	50.0

Oxidase activity was measured at 30°C with an oxygen electrode (See MATERIALS AND METHODS). The results are the averages of duplicate assays.

gluconate dehydrogenase, the gluconate oxidase activity in succinate vesicles was drastically reduced (Table 9). Thus the discrepancies observed between the Δp values for glucose- and succinate-vesicles cannot be attributed to the rate of electron donor oxidation in these vesicles.

Ramos et al. (65) have previously reported that the composition of Δp in energized E. coli vesicles depended on pH_o. At a pH_o of 5.5, a ΔpH of -110 mV constituted the major component of Δp (-180 mV). As pH_o was increased to 7.5, ΔpH decreased to zero, while $\Delta\Psi$ remained at approximately -75 mV. It is of interest to note that at an intermediate pH_o of 6.6, $\Delta\Psi$ (-71 mV) and ΔpH (-74 mV) contributed equally to Δp in P. putida vesicles provided with PMS/ascorbate (Table 7). In conclusion, the oxidation of appropriate electron donors by vesicles prepared from P. putida generates a Δp of sufficient magnitude to support active transport.

Ramos and Kaback (83) carried out a series of transport studies in which they manipulated ΔpH and $\Delta\Psi$ values with the aid of uncouplers and ionophores. They concluded that at pH_o of 5.5, the transport of one class of compounds (e.g., lactose, glycine and succinate) was driven primarily by Δp, while another class (e.g., glucose-6-phosphate and gluconate) was driven primarily by a ΔpH. In view of this, experiments were designed to establish which component of Δp drives 2KGA transport in these studies, i.e., at pH_o of 6.6. Figure 28 illustrates the effects of ionophores and CCCP on 2KGA transport in the presence of L-malate/FAD. With

Figure 28

The Effect of Ionophores and CCCP on 2KGA Transport in Vesicles from Glucose-Grown P. putida.

Legend:

—●—●— 2KGA only

—◆—◆— 2KGA + ED

—o—o— 2KGA + ED + Valinomycin (5.0 μM)

—▲—▲— 2KGA + ED + Nigericin (1.0 μM)

—△—△— 2KGA + ED + CCCP (1.0 μM)

Vesicles from glucose-grown P. putida (1.2 mg protein) were suspended in 50 mM potassium phosphate buffer, pH 6.6, 12 mM $MgSO_4$ and 10 mM L-malate/50 μM FAD. The mixture was incubated at 30°C for 10 min in the presence or absence of known concentrations of ionophores or CCCP. Transport was initiated by the addition of 82.78 μM D-[U-^{14}C]2KGA in a final volume of 1.0 mL. At time intervals 0.1-mL aliquots were filtered, washed, and the amount of 2KGA transported determined (See MATERIALS AND METHODS section). Valinomycin, nigericin and CCCP were made up in absolute ethanol. 2 μL of ethanol was added to the control instead of ionophore or uncoupler to correct for the effect of ethanol. Each point is the average of duplicate determinations.

The variation observed between the percent inhibition values of two different vesicle preparations is less than 4%.

Figure 28

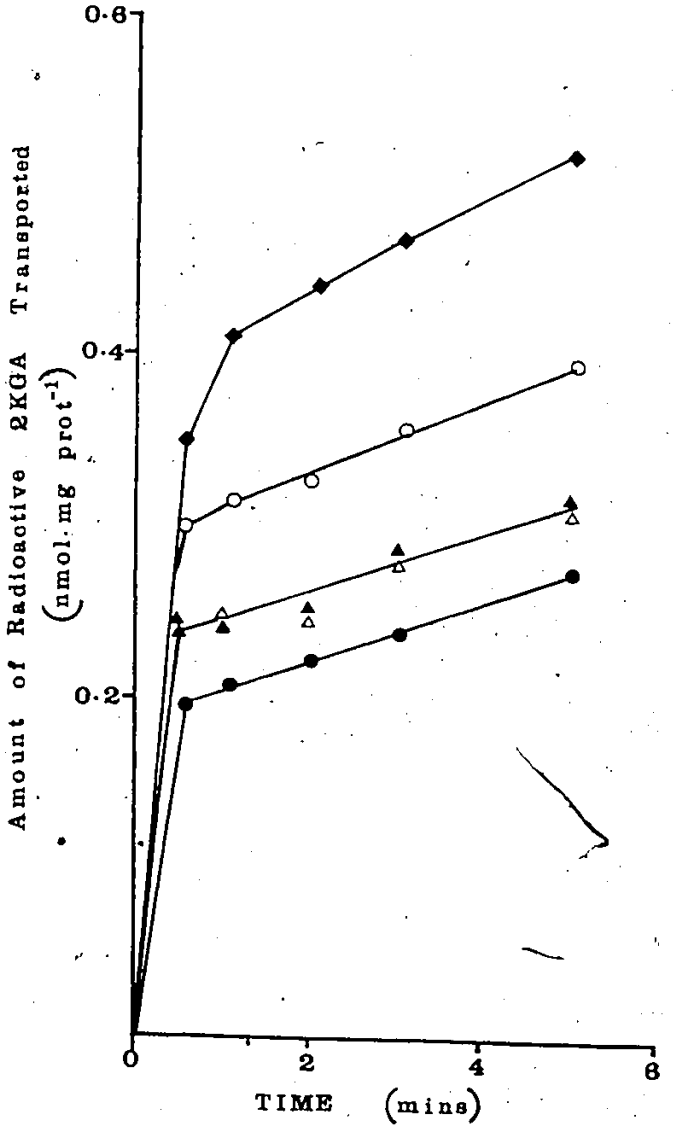
0·6
0·4
0·2
0
2
4
6
Amount of Radioactive 2KGA Transported
(nmol.mg prot^{-1})
TIME (mins)

valinomycin, which collapses $\Delta\Psi$ by catalyzing a K^+ uniport, only a 38% inhibition of 2KGA accumulation was observed. However, when ΔpH was collapsed by adding nigericin (which catalyzes a K^+-H^+ exchange), a 73% inhibition of 2KGA accumulation occurred. CCCP collapses both the $\Delta\Psi$ and ΔpH and is expected to inhibit 2KGA accumulation 100%. However, CCCP produced an inhibition pattern similar to that obtained with nigericin. Increasing the concentration of CCCP to 5.0 µM had no further effect on 2KGA accumulation. The reason for this is not known. The above results indicate that at pH 6.6, the major component of Δp which drives 2KGA transport is the ΔpH. Similar results were obtained when PMS/ascorbate was used as electron donor (Data not shown). Subsequent experiments were carried out to determine the effect of an artificially generated $\Delta\Psi$ on 2KGA transport. Addition of valinomycin to K^+-loaded vesicles elicited a rapid accumulation of $TPMP^+$ (Figure 29). A concentration gradient for $TPMP^+$ of approximately 7 (equivalent to a $\Delta\Psi$ of -49 mV) was obtained under these conditions. This is consistent with the contention that valinomycin catalyzes an electrogenic efflux of K^+ from K^+-loaded vesicles, thus generating a $\Delta\Psi$ which can be detected by the distribution of $TPMP^+$. When 2KGA transport was measured under similar conditions, no substrate accumulation was observed (Figure 29). It is apparent from this observation that a $\Delta\Psi$ alone cannot drive 2KGA transport. These results conflict with those reported by Hirata et al. (110), in which a transient accumulation of

Figure 29

Transport of $TPMP^+$ and 2KGA in K^+-Loaded Vesicles Prepared from Glucose-Grown P. putida.

Legend:

—◇—◇— Equilibration of $TPMP^+$

—◆—◆— Uptake of $TPMP^+$ after addition of valinomycin (2 µg)

—○—○— Equilibration of 2KGA

—●—●— Uptake of 2KGA after addition of valinomycin (VAL) (2 µg)

Arrows indicate point of addition of valinomycin (VAL).

K^+-loaded vesicles were prepared as described in the MATERIALS AND METHODS section. Reaction mixtures contained the following (final concentrations) in a final volume of 1.0 mL: 100 mM Tris.maleate (pH 7), 13 mM $MgSO_4$, 280 mM sucrose and either 208 µM [^{14}C]-$TPMP^+$ (4.8 mCi/mmol) or 103.5 µM D-[U-^{14}C]2KGA (3.2 mCi/mmol). The mixture was incubated at 30°C for 10 min and 2 µL valinomycin added to a final concentration of 2 µg/mL where indicated by the arrow. At time intervals 0.1 mL aliquots were filtered and washed twice with 2 mL of 0.4 M sucrose containing 5 mM $MgSO_4$. The amount of labelled substrate transported was determined as described in MATERIALS AND METHODS. Valinomycin was made up in absolute ethanol. Effect of ethanol was corrected for by adding 2 µL ethanol to the control instead of valinomycin. Each point is the average of duplicate determinations.

Figure 29

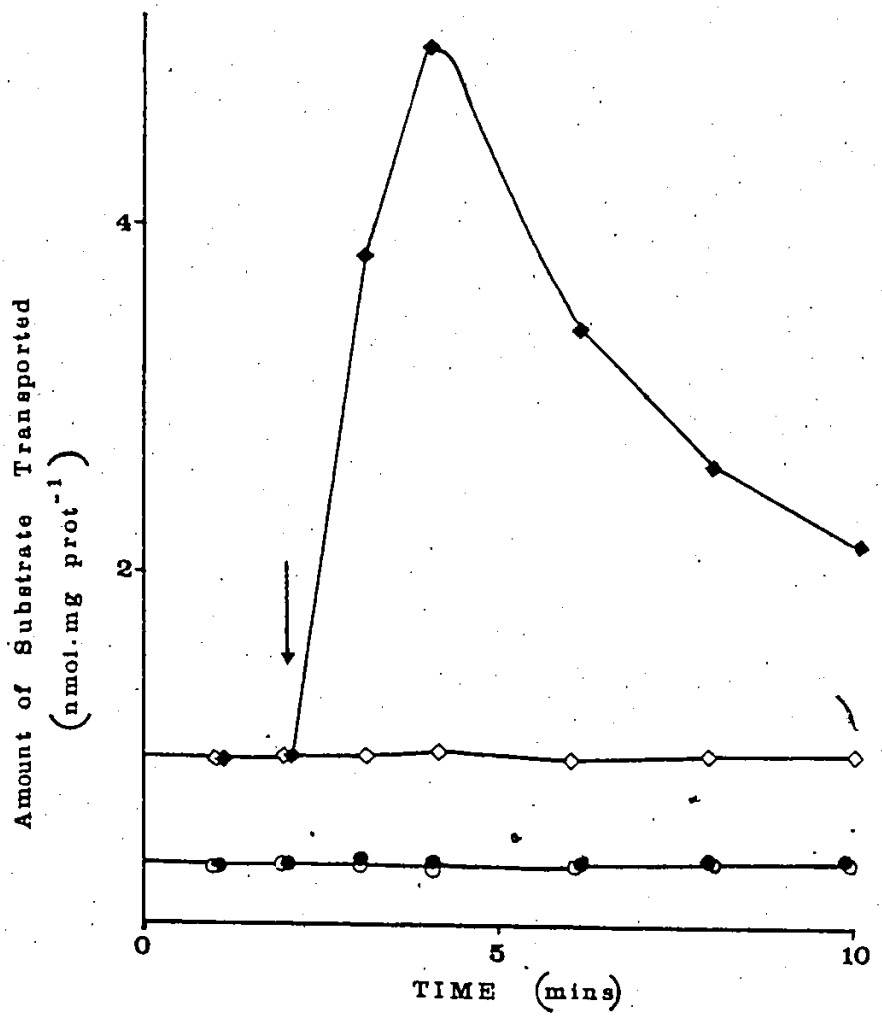
Amount of Substrate Transported
(nmol.mg prot^{-1})
4
2
0
5
10
TIME (mins)

lactose, TMG and several amino acids was observed in E. coli vesicles under similar conditions. This is probably due to the fact that unlike 2KGA, all the substrates tested accumulate in response to Δp, presumably by an electrogenic proton symport mechanism. Thus with a $\Delta\psi$ present, a solute/proton symport could occur such that a situation similar to $TPMP^+$ accumulation against $\Delta\psi$ is created. This would result in solute accumulation, accompanied by alkalinization of the external medium. This is supported by the observation that CCCP, which would undoubtedly prevent alkalinization of the external medium, totally blocked solute accumulation (110).

In conjunction with other studies carried out in this laboratory (131, 145, 148), it is now obvious that during the transport of glucose, gluconate and 2KGA by P. putida the substrates interact with proteins in both the outer and cytoplasmic membranes. Attempts to isolate periplasmic binding proteins in this organism were however, unsuccessful (145). In these studies the activity of the binding protein was assayed by equilibrium dialysis using a substrate concentration of 2.5 μM (145). In the present study, periplasmic binding proteins were isolated by the osmotic shock procedure of Stinson et al. (40) and tested for glucose binding activity by equilibrium flow dialysis at various substrate concentrations. The crude shock extracts bound negligible amounts of labelled glucose in the range of 0.04-0.13 nmol glucose.mg protein^{-1}, when assayed at glucose

concentrations ranging from 2.5-10 μM. The glucose binding activites obtained were approximately 10-fold lower than that reported for P. aeruginosa (46). The small amount of binding activity detected was probably due to non-specific binding of glucose to the protein since similar binding activities were obtained with proteins that were denatured by heating at 70°C for 1 h. Thus glucose binding proteins are probably absent from P. putida.

As mentioned earlier the failure to detect a Δp in succinate-vesicles during L-malate oxidation is presumably due to L-malate/proton symport. In a previous study it was shown that L-malate was transported actively by succinate-vesicles of P. putida with a Km value of 14.3 mM and a Vmax of 313 nmol.mg protein^{-1}.min^{-1} (131). A detailed kinetic analysis of L-malate transport in glucose-vesicles showed that in this case, the uptake of L-malate was by non-specific diffusion with a Km of ∞ (Figure 30). This was confirmed by the observation that L-malate transport in glucose-vesicles was not coupled to the oxidation of electron donors (Table 10). Contrary to this observation, provision of succinate-vesicles with electron donors resulted in a stimulation of the initial rate of L-malate transport. This is consistent with the increased binding affinity of L-malate for the carrier protein in the presence of electron donors. The inhibition observed with succinate (Table 10) is a consequence of succinate acting as a competitive inhibitor of L-malate transport in P. putida (70). Thus the failure to detect a Δp in succinate-vesicles

Figure 30

Double Reciprocal Plot of L-Malate Transport in Membrane Vesicles from Glucose-Grown P. putida.

Legend:

[S] - L-malate concentration

v - Initial rate of L-malate transport

The reaction mixture contained 50 µmol potassium phosphate buffer, pH 6.6, 12 µmol $MgSO_4.7H_2O$, and 0.98 mg protein. After pre-incubation at 30°C for 5 min, the reaction was initiated by adding the appropriate amount of L-[U-^{14}C]malate (sodium salt; 0.12 mCi/mmol). Total reaction volume was 1.0 mL. The initial rates of transport were measured as previously described. (See footnote to Table 3).

The initial rates of transport were measured in duplicate as previously described, (See footnote to Table 3).

Km values of ∞ were obtained for two different vesicle preparations.

Figure 30

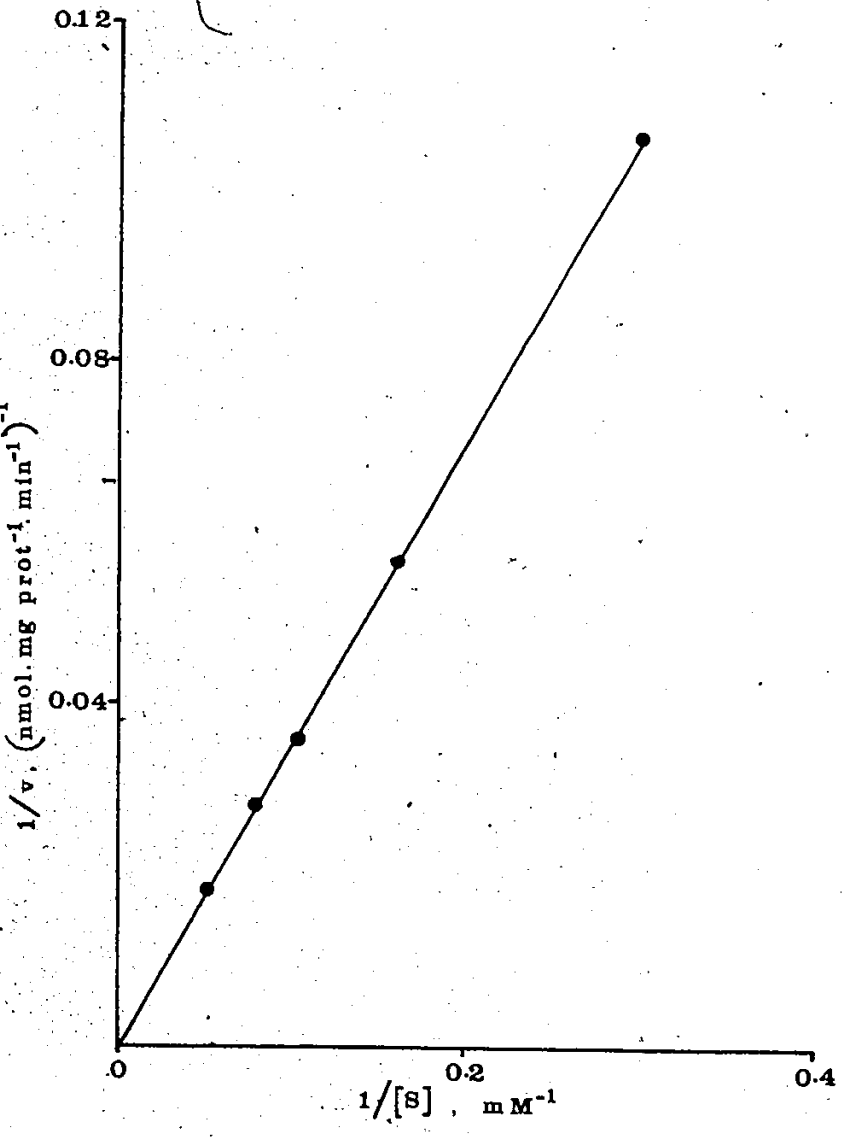

Table 10

The Effect of Various Electron Donors on the Initial Rate of L-Malate Transport in Vesicles from Glucose- or Succinate-Grown *P. putida*.

Electron Donor Added (Final Concentration)	Initial Rate of L-Malate Transport (nmol .mg protein.$^{-1}$ min.$^{-1}$)	
	Vesicles from Glucose-Grown Cells	Vesicles from Succinate-Grown Cells
None	54	170
Ascorbate (20 mM)/ PMS (0.1mM)	50	205
Succinate (10 mM)/ FAD (50 µM)	50	85
D-Glucose (10 mM)	54	215
2DOG (10 mM)	56	185

The reaction mixture contained 50 µmol potassium phosphate buffer, pH 6.6, 12 µmol $MgSO_4 \cdot 7H_2O$, 0.98 mg protein and the above stated final concentrations of electron donors. The mixture was preincubated at 30°C for 5 min and the reaction initiated by adding 17.9 µM L-[U-^{14}C]malate (sodium salt; 0.12 mCi/mmol). The initial rates of transport were determined as described in the footnote to Table 3.

may be due to the presence of the L-malate carrier in these vesicles. If L-malate is transported by an electrogenic proton symport mechanism, it would accumulate against both a $\Delta\Psi$ and a ΔpH, with a concomitant dissipation of Δp. To confirm this, L-malate-promoted pH changes were measured in lightly buffered medium as previously described (79, 86). Provision of an aerobic suspension of succinate-vesicles with L-malate resulted in an alkaline pH change (Figure 31). The alkaline pH shift was inhibited in the presence of DNP, suggesting that alkalinization of the medium was caused by movement of protons across the membrane. This provides evidence for an obligatory coupling of L-malate transport to proton uptake in these vesicles. The small pH shift in the buffer control (i.e., in the absence of vesicles) could be due to the effect of L-malate on the pH of the solution. A similar pH shift was also observed with glucose vesicles which lack the L-malate carrier. Data obtained from the kinetic analysis of L-malate-induced proton uptake is shown in Table 11. The initial rates of proton uptake were obtained by converting the pH changes into nmol H^+ using an experimentally determined conversion factor derived from the addition of known amounts of HCl to the vesicle suspension. A double reciprocal plot of the initial rates of proton uptake against L-malate concentration gave an apparent Km of 16 mM and an apparent Vmax of 667 nmol.mg protein.$^{-1}$ min^{-1} (Figure 32). In conjunction with the apparent Km and Vmax of 14.3 mM and 313nmol.mg protein^{-1}.min^{-1} obtained for L-malate transport in succinate-vesicles (131), a

Figure 31

L-Malate-Promoted pH Changes in Lightly Buffered Medium by Vesicles from Glucose- or Succinate-Grown P. putida under Aerobic Conditions.

Legend:

The reaction mixture, consisting of 100 mM-KCl-2 mM-glycylglycine buffer, pH 7.0, 10 mM $MgSO_4$, 7.25 mg protein, 50 µM FAD and when present, 100 µM DNP was incubated at 30°C. The cell suspension was stirred continuously by a stream of oxygen. After 20 min preincubation, the pH of the suspension was adjusted to 6.69 with small amounts of 0.1 M HCl or KOH and the reaction initiated by adding 10 mM L-malate (pH 6.69) to a final volume of 5 mL. Arrows indicate the point of addition of L-malate. A downward deflection represents an alkaline pH.

Figure 31

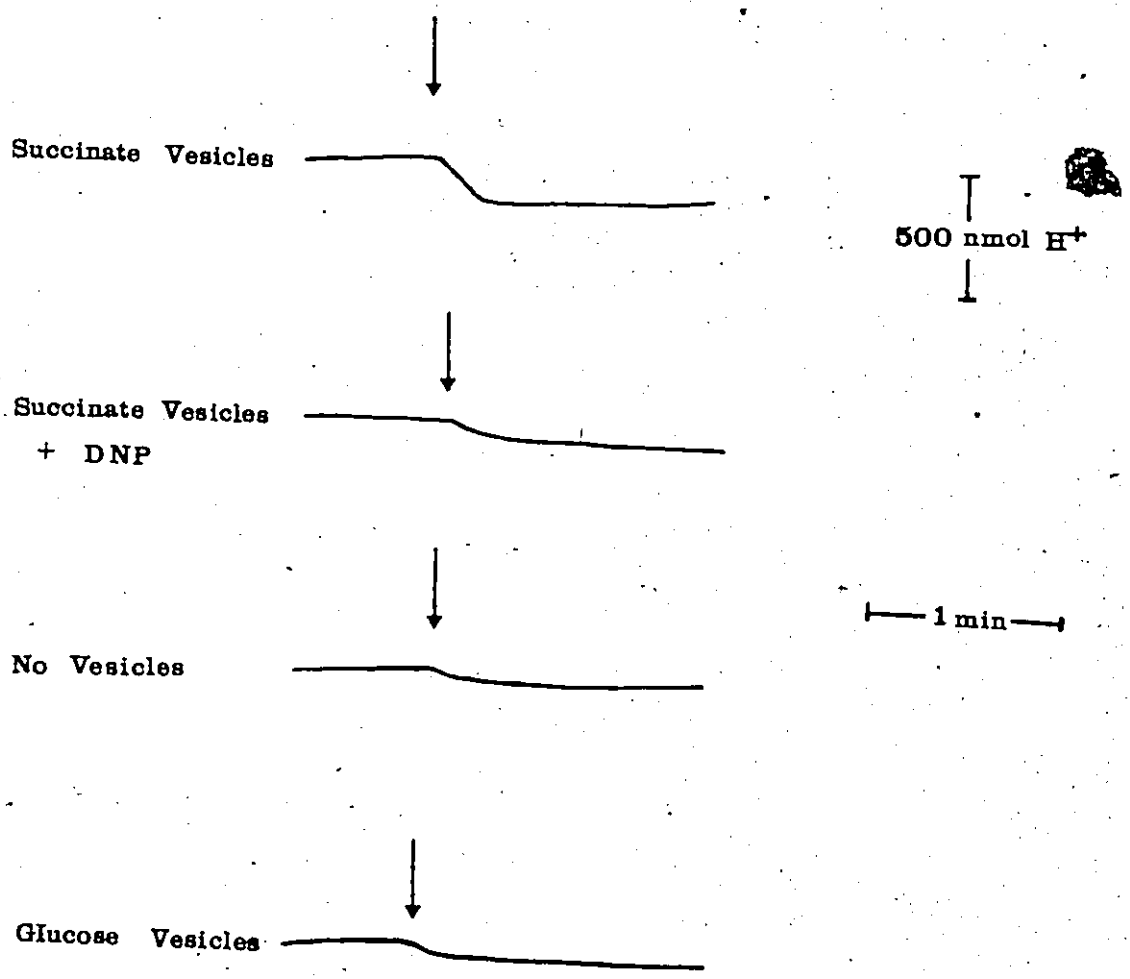
Succinate Vesicles
500 nmol H+
Succinate Vesicles
+ DNP
1 min
No Vesicles
Glucose Vesicles

Table 11

L-Malate-Induced Proton Uptake in Lightly Buffered Medium by Vesicles from Succinate-Grown *P. putida*.

L-Malate mM	Initial Rate of H^+ Transport (nmol .mg prot.$^{-1}$min.$^{-1}$)
2	69
5	152
10	250
20	349

Reaction conditions are given in the Legend to Figure 31. pH changes were converted into nmol of H^+ by using an experimentally determined conversion factor derived from the addition of known amounts of HCl to the cell suspension. Results are the averages of duplicate assays.

Figure 32

Double Reciprocal Plot of L-Malate-Induced Proton Uptake in Lightly Buffered Medium by Vesicles from Succinate-Grown *P. putida*.

Legend:

[S] - L-Malate concentration

v Initial rate of H^+ transport

Kinetic Data derived from Table 11

Average apparent Km and Vmax values obtained for two different vesicle preparations are 16 mM and 667 nmol.mg protein.$^{-1}$ min.$^{-1}$, respectively.

Figure 32

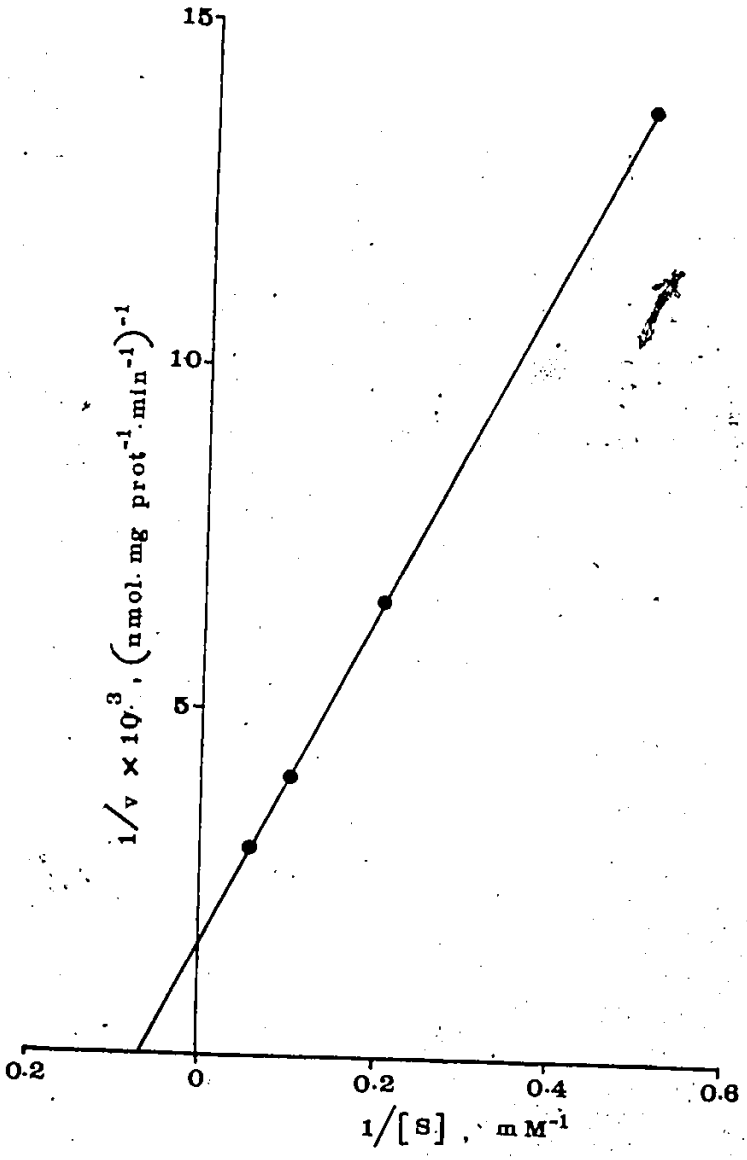

H^+/L-malate Vmax ratio of 2.1 was obtained. A Vmax ratio of 2.2 was obtained when the experiment was repeated under anaerobic conditions. These results suggest that L-malate is transported by an electroneutral proton symport mechanism in response to a ΔpH. However, the failure to detect a $\Delta\Psi$ as well as a ΔpH with vesicles oxidizing L-malate indicates an electrogenic proton symport mechanism for L-malate transport. It is possible that the rates of H^+ uptake were underestimated due to acidification of the medium caused by a simultaneous L-malate oxidation. Thus the values obtained could be the difference between H^+ uptake with L-malate and H^+ extrusion during L-malate oxidation.

As previously illustrated in Table 10, the initial rate of L-malate transport was stimulated by electron donors. L-malate accumulation after 10 min however remained at approximately 2.6 both in the presence and absence of electron donors. It appears from this observation that the energy for L-malate accumulation is derived from its own oxidation. What remains to be established is whether L-malate is oxidized extra-vesicularly and then transported as oxaloacetate, or if the oxidation occurs subsequent to L-malate transport. The non-inhibitory effect of a 10-fold oxaloacetate concentration on L-malate transport suggests that L-malate was not transported as oxaloacetate (Data not shown). The dicarboxylate carrier of *E. coli* has also been shown to be insensitive to oxaloacetate (105). By testing the effect of various dicarboxylic acids on fumarate and succinate transport these workers concluded that substitu-

tion at the α-carbon had major effects on the affinity of the substrate for the carrier (105). In other words oxaloacetate fails to inhibit transport because its α-carbon configuration renders it an unsuitable substrate for the dicarboxylate carrier. Contrary to expectations that L-malate would accumulate only under conditions where L-malate oxidation occured, L-malate concentration ratios of 2.6 and 1.9 were obtained under aerobic and anaerobic conditions, respectively. Thus it seems that L-malate accumulated as a result of its continued metabolism under anaerobic conditions. To gain further insight into this system, the intra- and extra-vesicular materials were analysed by HPLC after incubating succinate-vesicles with L-malate. Under aerobic conditions, L-malate and oxaloacetate were detected in the extra-vesicular medium (Figure 33). The oxaloacetate peak increased with time as the L-malate peak decreased, indicating that L-malate was converted to oxaloacetate extra-cellularly. Under anaerobic conditions, the rate of L-malate oxidation decreased and oxaloacetate appeared in the medium at a much slower rate (Figure 34). Similar results were obtained with glucose-vesicles (Data not shown). In the control sample, vesicles were excluded and no oxaloacetate was formed. When the intravesicular components were analyzed under aerobic conditions, a compound which chromatographed with a retention time identical to that of succinate was detected (Figure 35). This suggests that L-malate is converted to

Figure 33

HPLC Analysis of Extra-Vesicular Materials During L-Malate Transport in Membrane Vesicles from Succinate-Grown P. putida under aerobic conditions.

Legend:

1. Solvent front
2. Phosphate
3. Oxaloacetate
4. L-malate

Reaction mixtures contained 50 mM potassium phosphate buffer, pH 6.6, 10 mM $MgSO_4$, 50 µM FAD and 4 mg protein. The suspension was incubated at 30°C and gassed continuously with oxygen for 20 min before adding 10 mM L-malate to a final volume of 4.0 mL. At time intervals 0.5-mL samples were filtered, and 10 µL of the filtrate was analysed by HPLC as described in MATERIALS AND METHODS. Samples were run at ambient temperature.

Fluent - 0.007N H_2SO_4
Flow Rate - 0.5 mL/min
Chart Speed - 0.2 inch/min
Attenuation - 4 X
Detector - Differential Refractometer

Figure 33

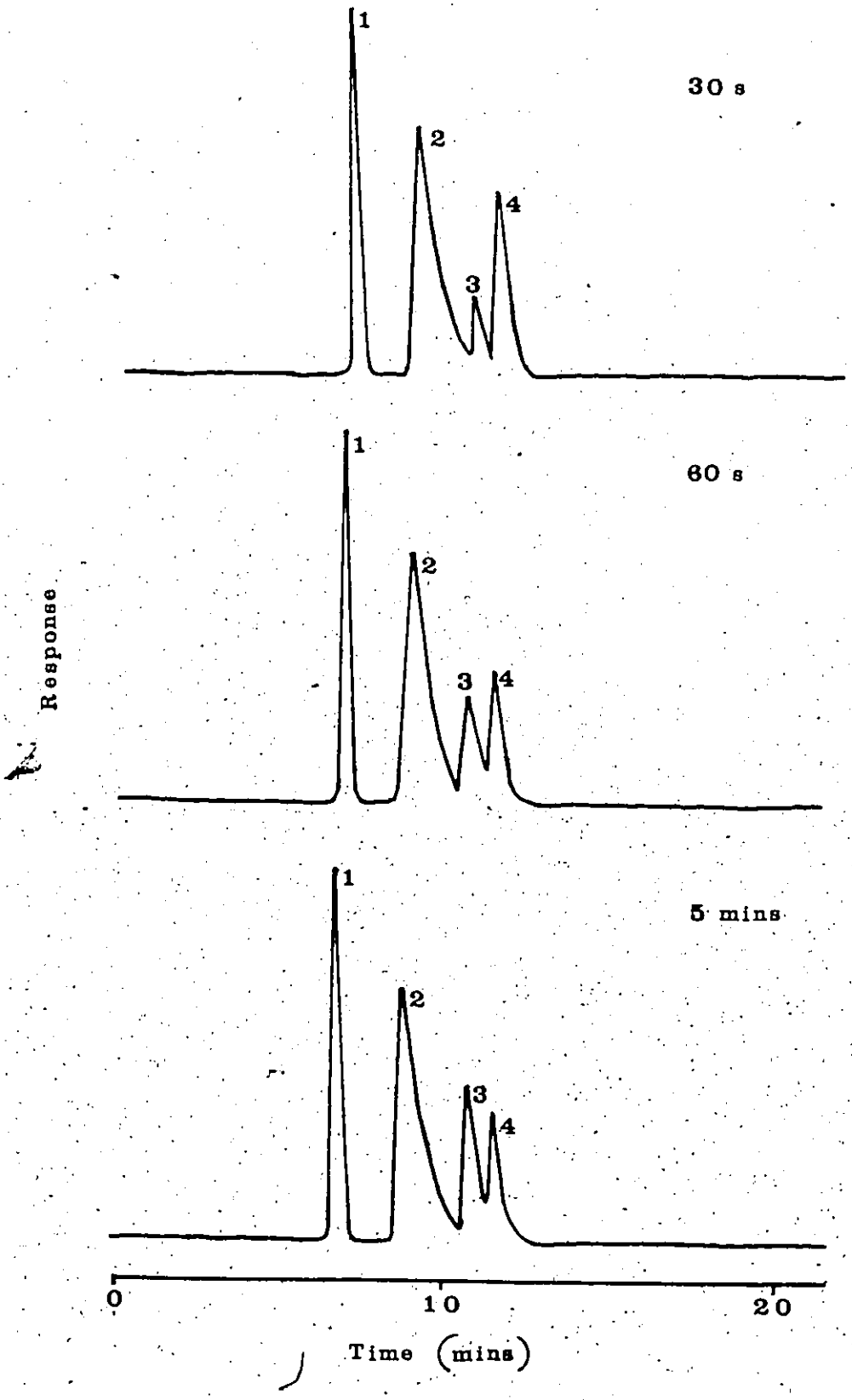

Figure 34

HPLC Analysis of Extra-Vesicular Materials During L-Malate Transport in Membrane Vesicles from Succinate-Grown *P. putida* under Anaerobic Conditions.

Legend:

1. Solvent front
2. Phosphate
3. Oxaloacetate
4. L-malate

Reaction conditions are identical to those given in the legend to Figure 33 except the suspension was gassed continuously with nitrogen for 20 min before adding L-malate, which had also been gassed with nitrogen for 20 min. Membrane vesicles were excluded from the control.

Sample Volume - 10 µL

Attenuation - 4 X

Figure 34

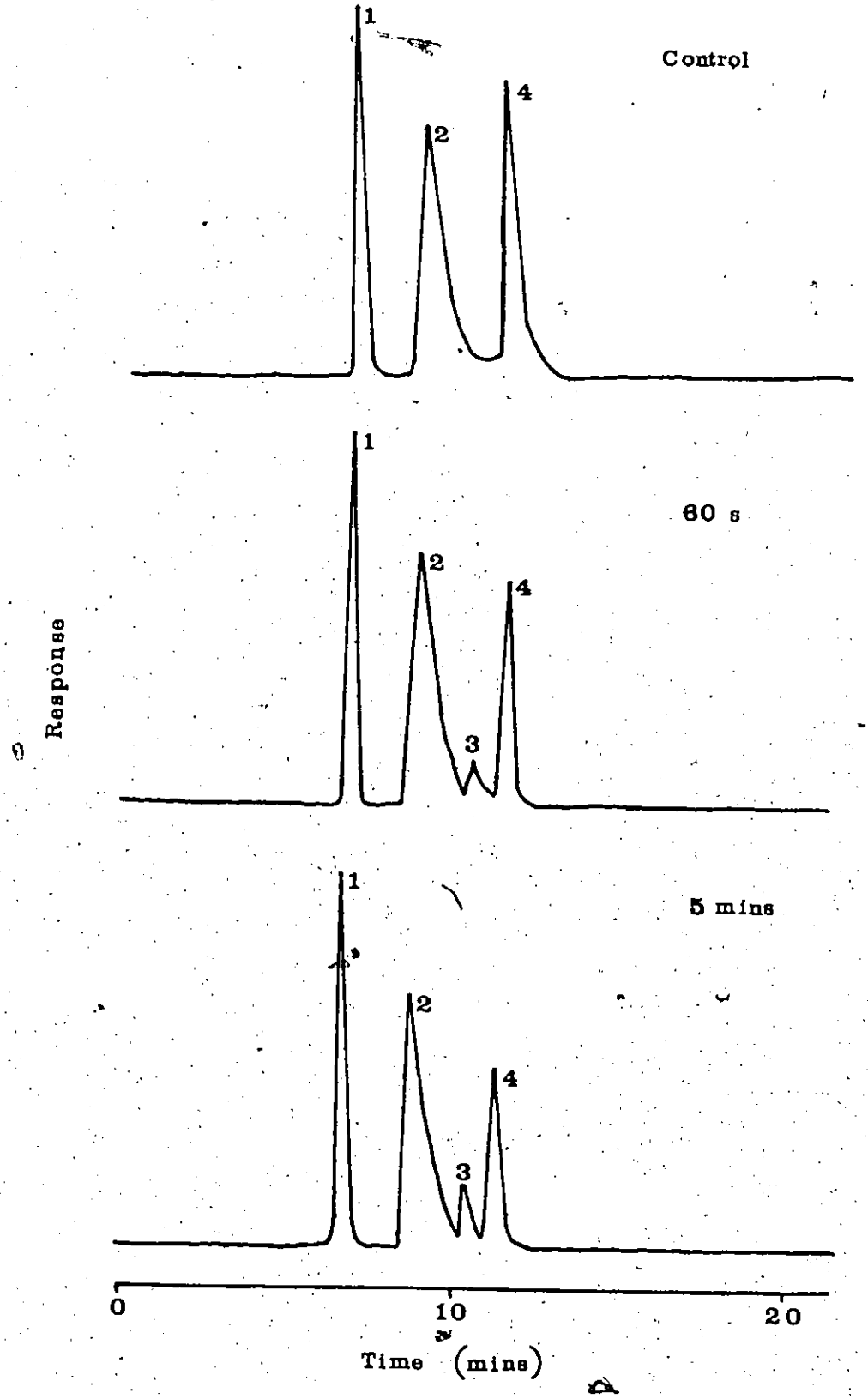

Figure 35

HPLC Analysis of Intra-Vesicular Materials During L-Malate Transport in Membrane Vesicles from Succinate-Grown P. putida under Aerobic Conditions.

Legend;

1. Solvent front
2. Phosphate
3. Oxaloacetate
4. L-malate
5. Succinate

Reaction conditions are given in Figure 33. At time intervals 0.5-mL samples were filtered and washed twice with 3 mL of 0.1 M LiCl. The intra-vesicular contents were extracted and analyzed as described in MATERIALS AND METHODS. Samples were run at ambient temperature.

Sample Volume - 20 µL

Attenuation - 2 X

Figure 35

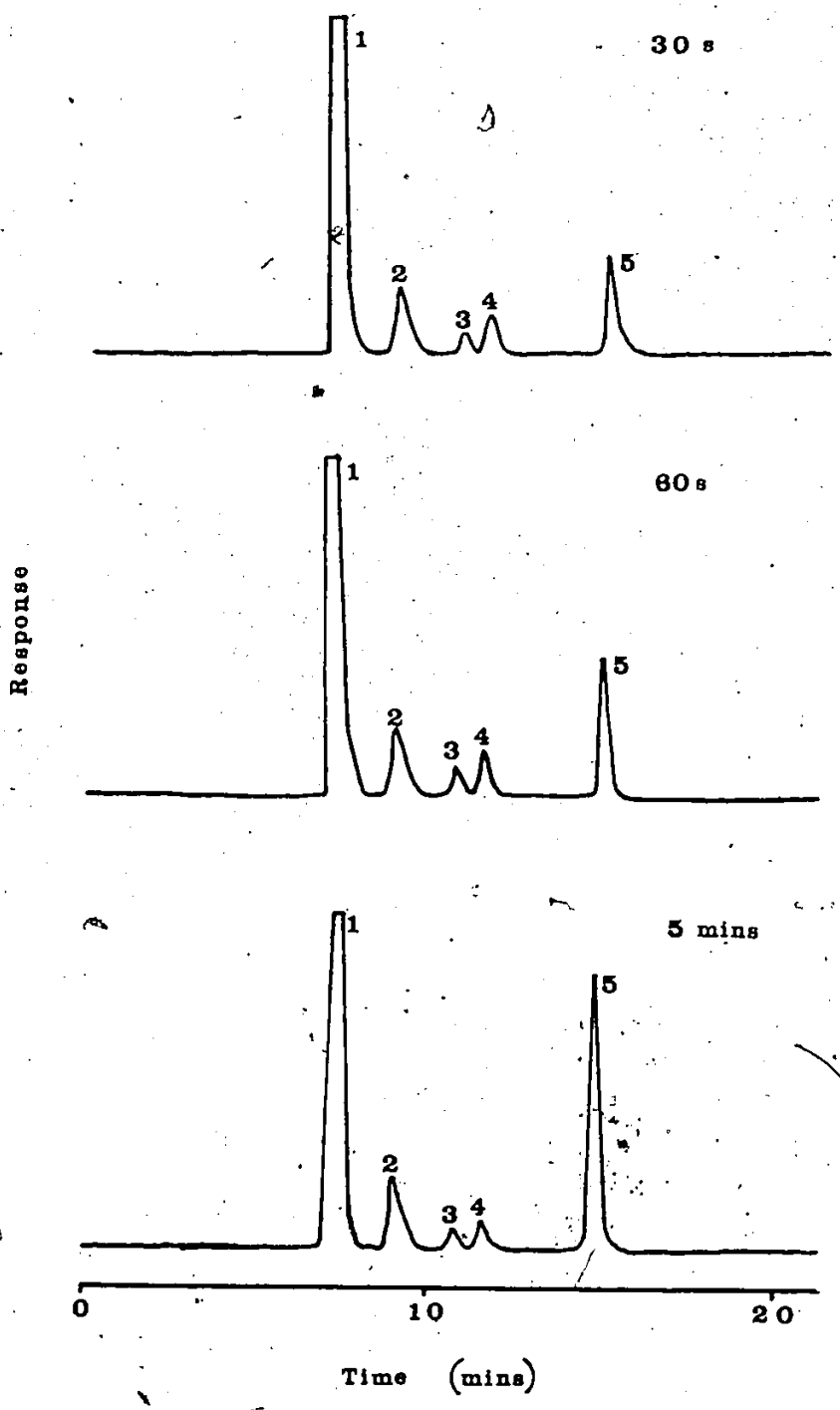

succinate intra-vesicularly. Similar results were obtained when the experiment was repeated under anaerobic conditions (Data not shown). The intra- and extra-vesicular substrate concentrations were calculated from the peak areas and are summarized in Table 12. The results suggest that L-malate accumulates as succinate with a concentration ratio of approximately 3, assuming an external L-malate concentration of 10 mM. The fact that a significant amount of L-malate was converted to oxaloacetate must, however, be taken into consideration. A similar pattern was observed with glucose vesicles, though in this case the intra-vesicular succinate concentration obtained after 5 min was 10 mM (Data not shown). This gives a concentration ratio of 1.05. The slow rate of succinate formation in glucose-vesicles is a result of the slow rate of L-malate transport in these vesicles. As can be observed in Figures 33 and 34, poor peak resolutions were obtained for the separation of solutes. Thus the solute concentrations (See Table 12), calculated from the peak areas, cannot be considered as accurate quantitative estimations. They however enable a qualitative comparison of the intra- and extra-vesicular contents.

It is apparent from the above observations that L-malate metabolism was not eliminated in these studies. In addition to conversion of L-malate to oxaloacetate via a membrane bound FAD-linked L-malate dehydrogenase (131), L-malate is also converted to a compound identified as succinate intra-vesicularly. Conversion of L-malate to succinate requires the presence of both fumarase and

Table 12

HPLC Analysis of Extra- and Intra-Vesicular Materials During L-Malate Transport in Membrane Vesicles from Succinate-Grown P. putida under Aerobic Conditions.

	Time	Oxaloacetate (mM)	Malate (mM)	Succinate (mM)
External Medium	30 s	1.3	6.2	0
	60 s	4.0	3.2	0
	5 min	4.8	2.9	0
Intravesicular Content	30 s	1.7	2.5	10.2
	60 s	1.7	3.0	12.1
	5 min	1.9	2.0	30.0

Experimental conditions are given in the legends to Figure 33 - 35.

The intra- and extra-vesicular concentrations were calculated from the peak areas as described in MATERIALS AND METHODS.

The results are the averages of duplicate determinations.

succinate dehydrogenase in these vesicles. Moses (131) demonstrated the presence of succinate dehydrogenase in membrane vesicles from succinate-grown P. putida. There is however, no evidence for the presence of fumarase in these vesicles. Furthermore, the failure to detect fumarate strongly suggests that fumarase is absent in the vesicle preparation. Thus it seems unlikey for the vesicles to catalyze the formation of succinate from L-malate. The possibility of the intra-vesicular conversion of L-malate to a compound other than succinate, but which coincidentally chromatographs with the retention time of succinate cannot be ruled out.

CHAPTER IV

SUMMARY AND CONCLUSIONS

2KGA was transported by a saturable process in glucose- and succinate-grown cells of P. putida. Studies with membrane vesicles indicated that 2KGA transport was catalyzed by an inducible/repressible carrier protein in the cytoplasmic membrane of these organisms. The transport system was coupled to electron donor oxidation via the electron transport chain, indicating that 2KGA transport occurs by a proton-linked active transport mechanism. Both 3F2KGA and 4F2KGA were competitive inhibitors of the 2KGA carrier protein.

Membrane vesicles from glucose- and succinate-grown cells oxidizing PMS/ascorbate generated a Δp at pH 6.6, composed of a $\Delta\Psi$ and a ΔpH of approximately equal magnitude. Similar results were obtained for membrane vesicles from glucose-grown cells oxidizing L-malate. However, no Δp was detected for membrane vesicles from succinate-grown cells provided with L-malate. This could be attributed to an obligatory coupling of the L-malate transport system to proton uptake. Evidence for this is provided by the observation that during L-malate transport, an alkaline pH shift occurred with succinate-vesicles but not with glucose-vesicles. In addition, L-malate transport was stimulated in the presence of electron donors only in succinate-vesicles, suggesting that L-malate was transported by a proton-linked

active transport system in these vesicles. Thus a Δp generated as a result of L-malate oxidation is dissipated when protons move back into the vesicles with L-malate. In glucose vesicles, the L-malate carrier is absent, and protons pumped out as a result of L-malate oxidation do not move back into the vesicles. Determination of the Δp generated by glucose- or succinate-vesicles oxidizing glucose and gluconate was complicated by the transport of these electron donors and/or their oxidative products, resulting in inconsistent values of Δp.

Results obtained with valinomycin, nigericin, and CCCP suggest that 2KGA transport is coupled predominantly to the ΔpH component of Δp at pH 6.6. Thus from equation (3), i.e., $\log([S]_{in}/[S]_{out}) = [(n+m)\Delta\Psi - nZ\Delta pH]/Z$, if the charge on the 2KGA, m, = −1; and the number of protons, n = +1; then n+m = 0 and $\log([S]_{in}/[S]_{out}) = -\Delta pH$. With a ΔpH value of −74 mV (i.e., 1.26 pH units) obtained with PMS/ascorbate (Table 7), an 18-fold accumulation of 2KGA is expected. However the maximum accumulation ratio of 2KGA obtained in this study was 3.7 fold. This is probably due to a rapid rate of efflux of 2KGA from the vesicles. Similar low substrate accumulation ratios have also been reported for glucose and gluconate transport in membrane vesicles prepared from P. putida (131, 148). It appears that vesicles prepared from P. putida in these studies do not accumulate substrate as effectively as membrane vesicles obtained from E. coli and other bacteria. However, the

increase in accumulation ratios obtained in the presence of electron donors in conjunction with the Δp produced by electron donor oxidation provide evidence for a proton-linked active transport mechanism for 2KGA transport in *P. putida*.

The observation that L-malate accumulates against a concentration gradient in the absence of electron donors in succinate-vesicles suggests that the driving force for L-malate accumulation is provided by a Δp generated by the oxidation of L-malate itself. Whether the oxidation takes place intra-cellularly as well as extra-cellularly is still uncertain. Subsequent to L-malate transport, L-malate is metabolized intra-cellularly. The identity of the product formed however, remains questionable. The appearance of a product other than oxaloacetate inside the vesicles is a very striking observation and indicates that the system is more complicated than anticipated. Thus a much more detailed analysis of the system must be performed before any definite conclusions can be drawn.

APPENDIX I

Quench Correction Curve for [^{14}C]-Samples

Legend:

Samples counted were [^{14}C]-toluene quenched standards containing 190,000 dpm. (Nuclear Chicago). The instrument used was the Beckman LS 7500 Liquid Scintillation Counter. The H-number concept of quench correction was used (see manufacturer's instruction manual for theoretical discussion of this concept).

APPENDIX I

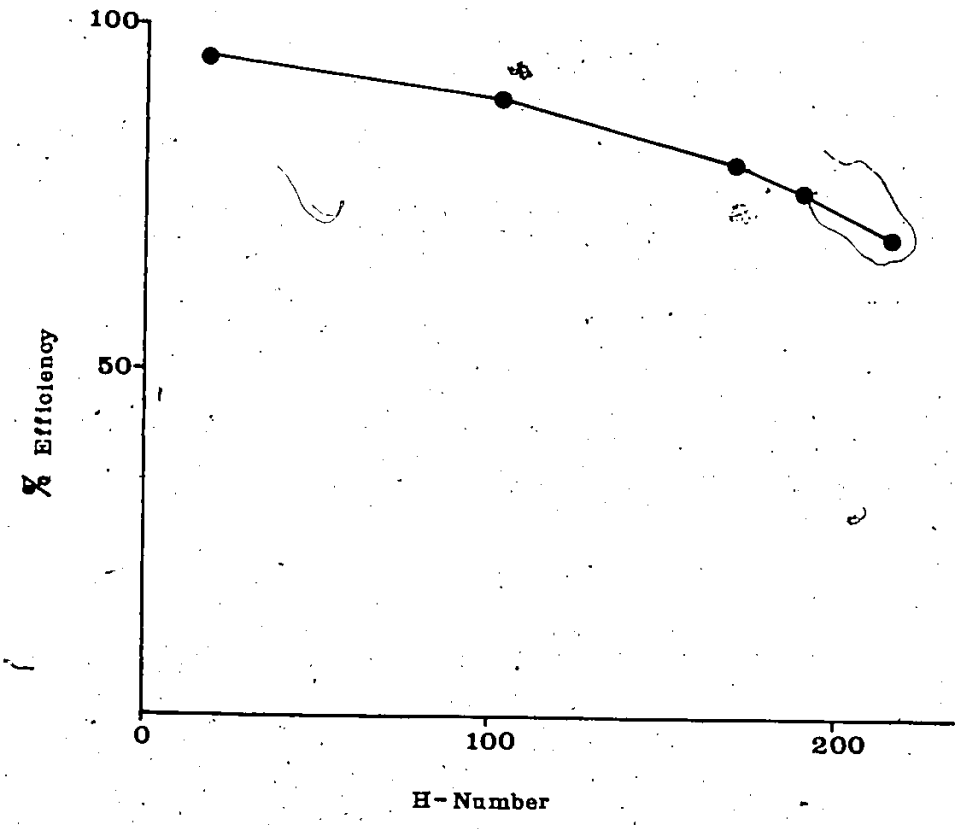

APPENDIX II

Calculation of the Amount of Radioactive Materials Transported by Whole Cells and Membrane Vesicles

From the quench correction curve (APPENDIX I) of % efficiency against H-number, the % efficiencies of the unknown samples were deduced from their H-numbers. The % efficiency (%E) is given by:

$$\%E = \frac{CPM}{DPM} \times 100$$

where CPM and DPM are the counts and disintegrations per minute respectively.

$$DPM = \frac{CPM}{E\%} \times 100$$

using the relationship;

1 nanocurie (nCi) of radioactivity = 2.22×10^3 DPM.

The amount of radiolabelled material transported in nCi (A), is given by;

$$A = \frac{CPM}{E\%} \times \frac{100}{2.22 \times 10^3} \text{ nCi}$$

If the specific activity of radioactive material used was X nCi/nmol, then the amount of radiolabelled material transported in nmol (B), is given by;

$$B = \frac{CPM}{E\%} \times \frac{100}{2.22 \times 10^3} \times \frac{1}{X} \text{ nmol}$$

If the reaction mixture contained Y mg of protein, the amount of radiolabelled material transported in nmol/mg

protein (C) is given by;

$$C = \frac{CPM}{E\%} \times \frac{100}{2.22 \times 10^3} \times \frac{1}{X} \times \frac{1}{Y} \quad \text{nmol/mg protein.}$$

For example, a 0.1 mL aliquot of a reaction mixture containing 0.95 mg protein in a total volume of 1.0 mL is counted. If CPM = 200

$$\%E = 95.0$$

$$X = 3.2 \text{ nCi/nmol}$$

Then the CPM of the total volume of 1.0 mL

$$= \frac{1.0 \text{ mL}}{0.1 \text{ mL}} \times 200 = 2{,}000$$

$$C = \frac{2{,}000}{95} \times \frac{100}{2.22 \times 10^3} \times \frac{1}{3.2} \times \frac{1}{0.95}$$

$$= \underline{0.312 \text{ nmol/mg protein}}$$

APPENDIX III

Determination of the Kinetic Parameters for Carrier-Mediated Substrate Transport.

a) Determination of Km and Vmax

For a one-substrate enzyme catalyzed reaction of the type;

$$E + S \underset{k_{-1}}{\overset{k_1}{\rightleftharpoons}} ES \xrightarrow{k_2} E + P \qquad \ldots\ldots\ldots\ldots\ldots\ldots (1)$$

Michaelis-Menton (160) defined the dissociated constant K_s for the enzyme-substrate complex (ES) as;

$$K_s = \frac{[E][S]}{[ES]} \qquad \ldots\ldots\ldots\ldots\ldots\ldots (2)$$

If the steady state treatment according to Briggs and Haldane (161) is applied to equation (1), one can derive the Michaelis-Menton equation relating reaction rates with substrate concentrations. This is given by the expression;

$$V_i = \frac{Vmax[S]}{[S] + Km} \qquad \ldots\ldots\ldots\ldots\ldots\ldots (3)$$

where $Km = (K_{-1} + K_2)/K_1$ and is known as the Michaelis-Menton constant; Vmax and V_i are the maximum and initial rates respectively; [S] is the substrate concentration. A linearized form of equation (3) is given by;

$$\frac{1}{V_i} = \frac{Km}{Vmax[S]} \cdot \frac{1}{[S]} + \frac{1}{Vmax} \qquad \ldots\ldots\ldots\ldots\ldots\ldots (4)$$

Plots of $1/v_i$ against $1/[S]$ give straight lines with

intercepts of 1/Vmax and slopes of Km/Vmax (140). These plots, known as double reciprocal plots, were used to determine apparent Km and Vmax for the carrier mediated 2KGA and L-malate transport.

b) Determination of Inhibition Constant, K_i

Inhibitors affect enzyme catalyzed reactions by increasing Km (competitive inhibition), decreasing Vmax (non-competitive inhibition) or changing both Km and Vmax (uncompetitive inhibition). A linearized form of equation for all three types of inhibition are derived from Michaelis-Menton equation for one-substrate reactions.

Competitive Inhibition

$$\frac{1}{V_i} = Km'\frac{(1 + [I]/K_i)}{Vmax[S]} + \frac{1}{Vmax} \quad \text{.....(5)}$$

where Km' is the apparent Km in the presence of inhibitor, [I] is the inhibitor concentration and K_i is the inhibition constant.

Non-Competitive Inhibition

$$\frac{1}{V_i} = Km'\frac{(1 + [I]/K_i)}{Vmax[S]} + \frac{1}{Vmax}(1 + [I]/K_i) \quad \text{.....(6)}$$

Uncompetitive Inhibition

$$\frac{1}{V_i} = \frac{Km'}{Vmax[S]} + \frac{(1 + [I]/K_i)}{Vmax} \quad \text{.....(7)}$$

In all three cases, plots of $1/v_i$ against $1/[S]$ at different inhibitor concentrations give straight lines which intercept on the x-axis (to the left of the vertical axis) for non-competitive inhibition, and on the y-axis for competitive inhibition. For uncompetitive inhibition, the lines run parallel to each other. The K_i values can be calculated from the slope and/or the intercept.

K_i values can also be determined from plots of $1/v$ against $[I]$ at different substrate concentrations; i.e., Dixon plots (141). These plots produce straight lines which intercept at a point on the left of the vertical axis. This point lies at $-K_i$, which can be read of directly. These were the plots used to determine K_i values for 3F2KGA and 4F2KGA inhibition of 2KGA transport.

APPENDIX IV

Equations for Linear Regression Analyses of Kinetic Data by the Least Square Method and Standard Deviations.

a) Linear Regression Analyses

$$M = \frac{[\Sigma x \Sigma y - N\Sigma xy]}{[(\Sigma x)^2 - N\Sigma x^2]}$$

$$C = \frac{[\Sigma x \Sigma xy - \Sigma x^2 \Sigma y]}{[(\Sigma x)^2 - N\Sigma x^2]}$$

where M and C are the slope and intercept of the best-fit line respectively. y and x are the reciprocals of the intial rate of transport and substrate concentration respectively. N is the number of x and y values.

b) Standard Deviation (SD)

$$SD = \sqrt{\frac{\Sigma(x - \bar{x})^2}{N}}$$

where x and $\bar{x}$ are determined and mean values respectively, and N is the number of independent runs.

APPENDIX V

Schematic Representation of a Flow Dialysis Apparatus (106).

APPENDIX V

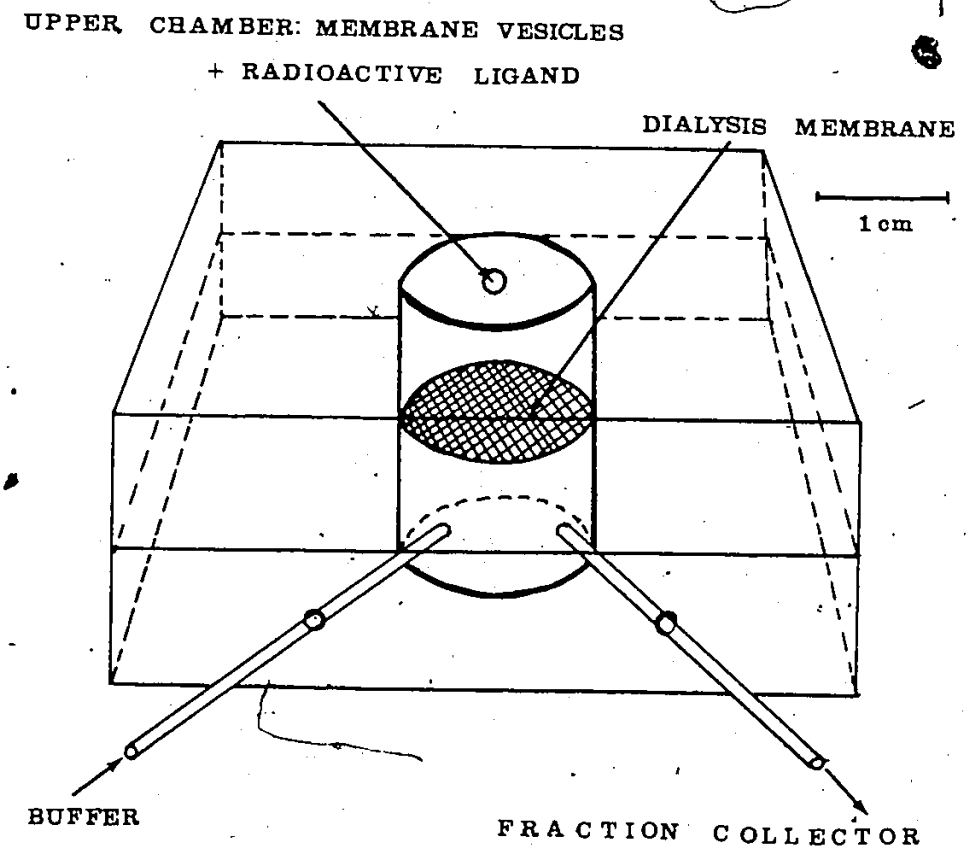
UPPER CHAMBER: MEMBRANE VESICLES
+ RADIOACTIVE LIGAND
DIALYSIS MEMBRANE
1 cm
BUFFER
FRACTION COLLECTOR

APPENDIX VI

Calculation of $\Delta\psi$, ΔpH and Δp values (106).

a). Calculatin of $\Delta\psi$ (Data derived from Figure 24)

At the inception of steady state (fraction 16), the amount of radioactivity in the dialysate is proportional to the concentration of $TPMP^+$ added at zero time

5498 cpm $\propto$ 125 µM

In the absence of PMS/ascorbate, fraction 34 contains 5074 cpm

5074 cpm = 92.3% of 5498 cpm

= 92.3% of 125 µM

= 115.4 µM

In the presence of PMS/ascorbate, fraction 34 contains 4195 cpm

4195 cpm = 76.3% of 5498 cpm

= 76.3% of 125 µM

= 95.4 µM

The amount of $TPMP^+$ accumulated by the vesicles in the presence of PMS/ascorbate (A), is given by:

A = (115.4 nmol/mL - 95.4 nmol/mL) x 0.886 mL

where 0.886 mL is the total volume of the upper chamber.

A = 17.7 nmol

Since a total of 3.0 mg protein was present in the upper chamber, the amount of $TPMP^+$ accumulated per mg protein (B), is given by

B = 17.7 nmol/3.0 mg protein

= 5.9 nmol/mg protein

The intravesicular volume = 3.6 µL/mg protein

$[TPMP^+]_{in}$ = 5.9 nmol/3.6 µL

= 1.64 nmol/µL

= 1640 µM

The external $TPMP^+$ concentration under these conditions is 95.4 µM. $\Delta\psi$ can be calculated from the Nernst equation;

$$\Delta\psi = -\frac{2.3RT}{F} \log \frac{[TPMP^+]_{in}}{[TPMP^+]_{out}}$$

where 2.3RT/F = 58.8 mV at room temperature.

$\Delta\psi$ = -58.8 log 1640/95.4

= -58.8 log 17.2

= -72.6 mV

b) Calculation of ΔpH (Data derived from Figure 25)

At the inception of steady state (fraction o), the amount of radioactivity in the dialysate is proportional to the concentration of acetate added at zero time.

2475 cpm $\propto$ 43.3 µM

In the absence of PMS/ascorbate, fraction 26 contains 2282 cpm.

2282 cpm = 92.2% of 2475 cpm

= 92.2% of 43.3 µM

= 39.9 µM

In the presence of PMS/ascorbate, fraction 26 contains 1875 cpm.

1875 cpm = 75.8% of 2475 cpm

= 75.8% of 43.3 μM

= 32.8 μM

Amount of acetate accumulated by the vesicles in the presence of PMS/ascorbate (A), is given by:

A = (39.9 nmol/mL - 32.8 nmol/mL) x 0.886 mL

where 0.886 mL is the total volume of the upper chamber

A = 6.3 nmol

The intravesicular acetate concentration is calculated as in (a); and

$[CH_3COOH]_{in}$ = 583 μM

The external acetate concentration under these conditions is 32.8 μM. ΔpH can be calculated directly from the Nernst equation;

$$\Delta pH \text{ (in mV)} = -\frac{2.3RT}{F} \log \frac{[\text{acetate}]_{in}}{[\text{acetate}]_{out}}$$

$$= -58.8 \log 583/32.8$$

$$= -58.8 \log 17.8$$

$$= -73.5 \text{ mV}$$

c) Calculation of Δp

$$\Delta p = \Delta\psi - \frac{2.3RT}{F}.\Delta pH$$

where Δψ is -72.6 mV and $2.3RT/F.\Delta pH$ = 73.5 mV (Obtained from (a) and (b) above)

Δp = -72.6 mV - 73.5 mV

= -146.1 mV

APPENDIX VII

Calculation of Oxygen Consumption for Oxygen Electrode Measurements

The oxygen electrode was calibrated so that a full scale deflection on the recorder was equivalent to 100% saturation on the oxygen meter, using 3.0 mL of air-saturated distilled water or potassium phosphate buffer. 100% saturation = 15 µL oxygen (See Instruction Manual).

The amount of oxygen consumed, expressed as µL/min, was calculated as follows:

$$\mu L\ (O_2)/min = [(X\%/min) \times 15]/100$$

where (X%/min) was the slope of the linear portion of the recorder tracing.

The volume of oxygen consumed under the experimental conditions was converted to standard temperature and pressure (STP) by the following expression:

$$\mu L(O_2)/min \text{ at STP} = \mu L(O_2)/min.273(P-Pw)/(760 \times T)$$

where P and Pw were the experimental and water vapour pressures respectively, and T was the experimental temperature (^{o}K).

The amount of oxygen expressed as µmol/min (n), was calculated from the ideal gas equation:

$$PV = nRT$$

where P = 101.3 kPa, T = 273 K, V = X µL/min abd R = 8.31 $kJ.K^{-1}.mol^{-1}$.

APPENDIX VIII

HPLC Chromatogram of a Standard Mixture of Dicarboxylic Acids.

Legend:

1. Solvent Front
2. Oxaloacetate (10 mM)
3. L-Malate (10 mM)
4. Succinate (10 mM)
5. Fumarate (10 mM)

Sample Volume = 5 µL
Flow Rate = 0.5 mL/min
Chart Speed = 0.2 inch/min
A; Attenuation = 4 X
B; Attenuation = 2 x

Samples were run at ambient temperature.

APPENDIX VIII

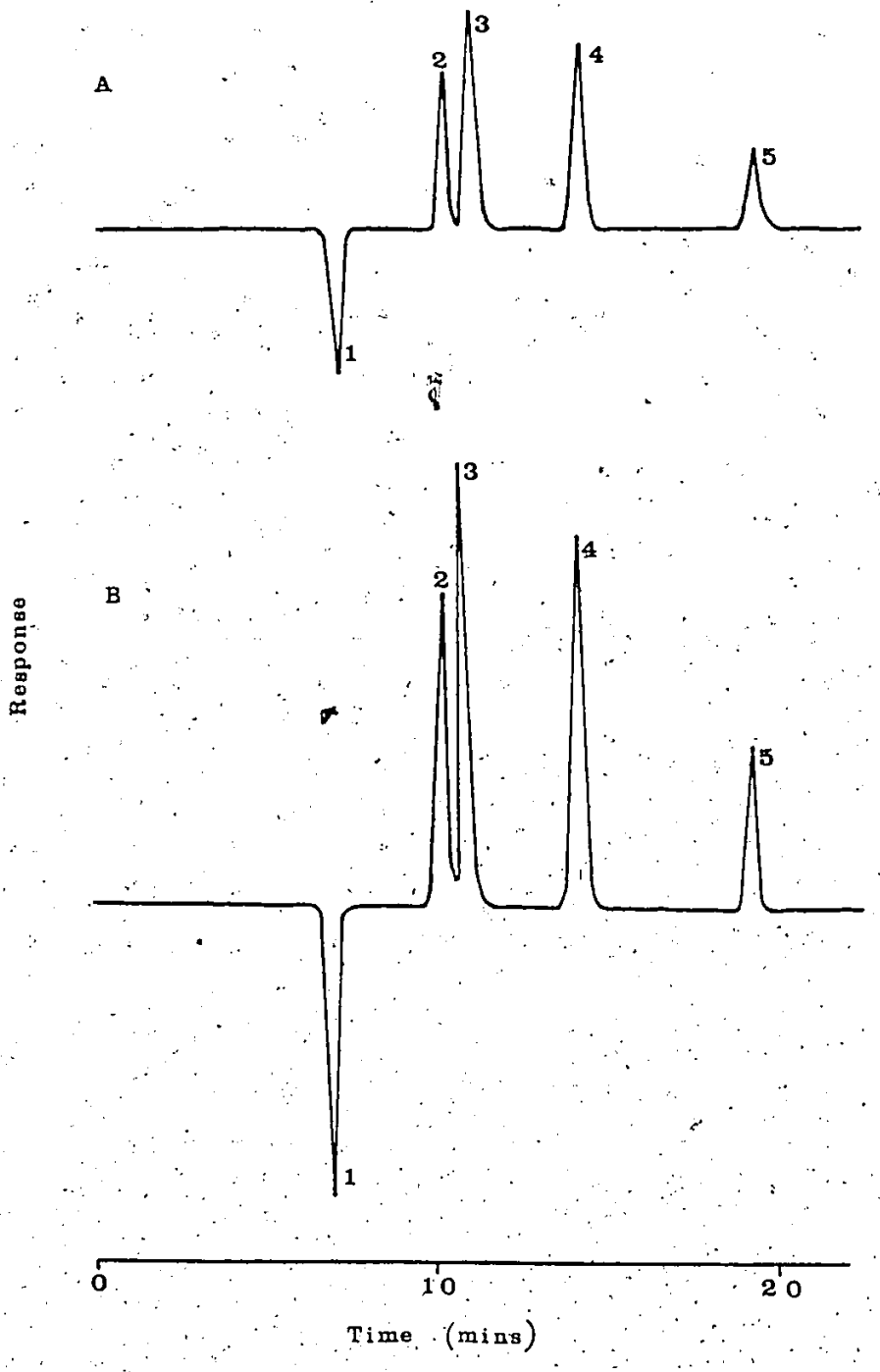

APPENDIX IX

Enzyme Commission Recommended Names, Numbers and Reactions Catalyzed by Key Enzymes Mentioned in the Text.

Recommended Name	Reaction Catalyzed	Number
1. Fumarate hydratase (Fumarase)*	L-malate = Fumarate + H_2O	EC 4.2.1.2
2. Gluconate-2-dehydrogenase (Gluconate dehydrogenase)*	D-gluconate + acceptor = 2-keto-D-gluconate + reduced acceptor	EC 1.1.99.3
3. Gluconokinase	D-gluconate + ATP = 6-phospho-D-gluconate + ADP	EC 2.7.1.12
4. Gluconolactonase (δ-gluconate lactonase)*	D-glucono-δ-lactone + H_2O = D-gluconate	EC 3.1.1.17
5. Glucose dehydrogenase	D-glucose + acceptor = D-glucono-δ-lactone + reduced acceptor	EC 1.1.99 A
6. Malate dehydrogenase (FAD)	L-malate + acceptor = oxaloacetate + reduced acceptor	EC 1.1.99.16
7. NADH dehydrogenase (cytochrome c oxidoreductase)*	NADH + acceptor = NAD^+ + reduced acceptor.	EC 1.6.99.3
8. Phosphogluconate dehydrogenase (decarboxylating)	6-phosphogluconate + $NADP^+$ = D-ribulose-5-phosphate + CO_2 + NADPH	EC 1.1.1.44

Recommended Name	Reaction Catalyzed	Number
9. Succinate dehydrogenase (FAD)	Succinate + acceptor = fumarate + reduced acceptor.	EC 1.3.99.1

NOTE: The name of the enzyme used in the text is shown by the asterisks when it differs from the Enzyme Commission recommended names.

APPENDIX X

Structures of 2KGA, 3F2KGA and 4F2KGA

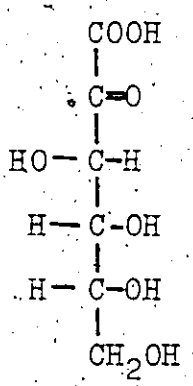

2KGA

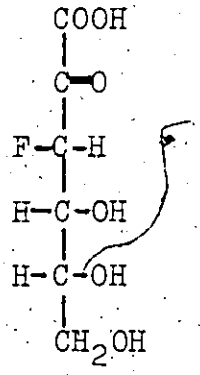

3F2KGA

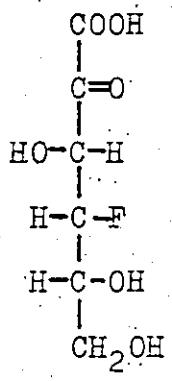

4F2KGA

REFERENCES

1. Palleroni. N.J. (1975) In "Genetics and Biochemistry of Pseudomonads, " p. 1-36, Clark, P.H. and Richmond, M.H. ed., A Wiley-Interscience Publication, N.Y.

2. Richmond, M.H. (1975) In "Resistance of Pseudomonas Aeruginosa," p. 1-33, Brown, M.R.W. ed., A Wiley-Interscience Publication, N.Y.

3. Clark, P.H. and Ornston, L.N. (1975) In "Genetics and Biochemistry of Pseudomonads," p. 191-261, Clark, P.H. and Richmond, M.H. ed., A Wiley-Interscience Publication, N.J.

4. Stanier, R.Y., Palleroni, N.J. and Doudoroff, M. (1966) J. Gen. Microbiol. 43, 159-271

5. Lo, T.C.Y. (1979) Can. J. Biochem. 57, 289-301

6. Nikaido, H. (1973) In "Bacterial Membranes and Walls" p. 131-208. Leive, L. ed., Marcel Dekker Inc., N.Y.

7. Meadow, P.M. (1975) In "Genetics and Biochemistry of Pseudomonads," p. 67-98, Clark, P.H. and Richmond, M.H., ed., A Wiley-Interscience Publication, N.Y.

8. van Heijenoort, J., Elbaz, L., Dezelee, P., Petit, J. -F., Bricas, E., and Ghuysen, J.-M. (1969) Biochemistry 8, 207-213

9. Ghuysen. J.-M. and Shockman, G.D. (1973) In "Bacterial Membranes and Walls," p. 37-130. Leive. L. ed., Marcel Dekker Inc., N.Y.

10. Rosen, B.P. and Heppel, L.A. (1973) In "Bacterial Membranes and Walls," p. 209-239. Leive, L. ed., Marcel Dekker Inc., N.Y.

11. Osborn, M.J. and Wu, H.C.P. (1980) Ann. Rev. Microbiol. 34, 369-422

12. Lo, T.C.Y. and Bewick, M.A. (1981) J. Biol. Chem. 256, 5511-5517

13. D'Amore, T. and Taylor, N.F. (1982) FEBS Lett. 143, 247-251

14. Guymon, L.F. and Eagon, R.G. (1974) J. Bacteriol. 117, 1261-1269

15. Stephenson, M.C., Midgley, M. and Dawes, E.A. (1978) Biochim. Biophys. Acta 509, 519-536

16. Weiner, J.H. and Heppel, L.A. (1971) J. Biol. Chem. 246, 6933-6941

17. Kadner, R.J. and Winkler, H.H. (1975) J. Bacteriol. 123, 985-991

18. Kaback, H.R. (1974) Science 186, 882-892

19. Weiner, J.H. (1974) J. Membr. Biol. 15, 1-14

20. Hayashi, S. and Lin, E.C.C. (1965) Biochim. Biophys. Acta 94, 479-487

21. Sanno, Y., Wilson, T.H. and Lin, E.C.C. (1968) Biochem. Biophys. Res. Commun. 32, 344-349

22. Dills, S.S., Apperson, A., Schmidt, M.R. and Saier, M. H. Jr. (1980) Microbiol. Rev. 44, 385-418

23. Romano, A.H., Eberhard, S.J., Dingle, S.L. and McDowell, T.D. (1970) J. Bacteriol. 104, 808-813

24. Kundig, W., Ghosh, S. and Roseman, S. (1964) Proc. Natl. Acad. Sci. U.S.A. 52, 1067-1074

25. Postma, P. and Roseman S. (1976) Biochim. Biophys. Acta 457, 213-257

26. Saier, M.H. Jr. (1977) Bacteriol. Rev. 41, 856-871

27. Hays, J.B. (1978) In "Bacterial Transport," p 43-102. Rosen, B.P. ed., Marcel Dekker Inc., N.Y.

28. Stryer, L. (1981) In "Biochemistry," 2nd Edition, p. 861-882. Stryer, L. ed., Freeman, W.H. and Co., San Francisco.

29. Weigel, N., Waygood, E.B., Kukuruzinska, M.A., Nakazawa, A. and Roseman, S. (1982) J. Biol. Chem. 257. 14461-14469

30. Gee, D.L., Baumann, P. and Baumann, L. (1975) Arch. Microbiol. 103, 205-207

31. Reeves, R.E., Warren, L.G. and Hsu, D.S. (1966) J. Biol. Chem. 241, 1257-1261

32. Sawyer, M.H., Baumann, P., Baumann, L., Berman, S.M., Canovas, J.L. and Berman, R.H. (1977) Arch. Microbiol. 112, 49-55

33. Durham, D.R. and Phibbs, P.V.Jr. (1982) J. Bacteriol. 149, 534-541

34. Bernsman, P., Alpert, C.A., Muss, P., Deutscher, J. and Hengstenberg, W. (1982) FEBS Lett. 138, 101-103

35. Jin, R.Z. and Lin, E.C.C. (1984) J.Gen. Microbiol. 130, 83-88

36. Misset, O. and Robillard, G.T. (1982) Biochemistry 21, 3136-3142

37. Misset, O., Blaauw, M., Postman, P.W. and Robillard, G.T. (1983) Biochemistry 22, 6163-6170

38. Fox, D., Kukuruzinska, M., Liu, K.D.F., Meadow, N.D., Saffen, D. and Roseman, S. (1984) Biochem. Soc. Trans. 12, 155-157

39. Anraku, Y. (1968) J. Biol. Chem. 243, 3116-3122

40. Shamanna, D.K. and Sanderson, K.E. (1979) J. Bacteriol. 139, 64-70

41. Stinson, M.W., Cohen, M.A. and Merrick, J.M. (1976) J. Bacteriol. 128, 573-579

42. Kellerman, O. and Szmelcman, S. (1974) Eur. J. Biochem. 47, 139-149

43. Ferenci, T., Boos, W., Schwartz, M. and Szmelcman, S. (1977) Eur. J. Biochem. 75, 187-193

44. Boos, W. (1984) Biochem. Soc. Trans. 12, 141-146

45. Romano, A.H., Voytek, A. and Bruskin, A.M. (1980) J. Bacteriol. 142, 755-762

46. Stinson, M.W., Cohen, M.A. and Merrick, J.M. (1977) J. Bacteriol. 131, 672-681

47. Berger, E.A. (1973) Proc. Natl. Acad. Sci. U.S.A. 70, 1514-1518

48. Curtis, S.J. (1974) J. Bacteriol. 120, 295-303

49. Wilson, D.B. (1974) J. Bacteriol. 120, 866-871

50. Plate, C.A., Suit, J.L., Jetten, A.M. and Luria, S.E. (1974) J. Biol. Chem. 249, 6138-6143

51. Liebermann, M.A. and Hong, J.S. (1976) Arch. Biochem. Biophys. 172, 312-315

52. Hong, J.S., Hunt, A.G., Masters, P.S. and Lieberman, M.A. (1979) Proc. Natl. Acad. Sci. U.S.A. 76, 1213-1217

53. Ames, G.F. and Spudich, E.N. (1976) Proc. Natl. Acad. Sci. U.S.A. 73, 1877-1881

54. Kustu, S.G. and Ames, G.F. (1974) J. Biol. Chem. 249, 6976-6983

55. Mitchell, P. (1961) Nature (London) 191, 144-148

56. Mitchell, P. (1966) Biol. Rev. (Cambridge) 41, 445-502

57. Mitchell, P. (1973) J Bioenerg. 4, 63-91

58. Rosen, B.P. and Kashket, E.R. (1978) In "Bacterial Transport," p. 559-620. Rosen, B.P. ed., Marcel Dekker Inc., N.Y.

59. Harold, F.M. (1972) Bacteriol. Rev. 36, 172-230

60. Harold, F.M. (1977) Curr. Top. Bioenerg. 6, 83-149

61. Simoni, R.D. and Postma, P.W. (1975) Ann. Rev. Biochem. 44, 523-554

62. Boos, W. (1974) Ann. Rev. Biochem. 43, 123-146

63. Schuldiner, S. and Kaback, H.R. (1975) Biochemistry 14, 5451-5461

64. Matin, A. and Konings, W.N. (1973) Eur. J. Biochem. 34. 58-67

65. Ramos, S., Schuldiner, S., and Kaback, H.R. (1976) Proc. Natl. Acad. Sci. U.S.A. 73, 1892-1896

66. Griniuviene, B., Dzheija, P. and Grinius, L. (1975) Biochem. Biophys. Res. Commun. 64, 790-796

67. West, I.C. (1970) Biochem. Biophys. Res. Commun. 41, 655-661

68. West, I.C. and Mitchell, P. (1972) J. Bioenerg. 3, 445-462

69. Flagg, J.L., and Wilson, T.H. (1977) J. Membr. Biol. 31, 233-255

70. Dubler, R.E., Toscano, W.A. Jr., and Hartline, R.A. (1974) Arch. Biochem. Biophys. 160, 422-429

71. Edwards, W.V., Sando, J.J. and Hartline, R.A. (1979) J. Bacteriol. 139, 748-754

72. Al-Jobore, A., Moses, G. and Taylor, N.F. (1980) Can. J. Biochem. 58, 1397-1404

73. Stephenson, M.C., Midgley, M. and Dawes, E.A. (1978) Biochim.. Biophys. Acta 509, 519-536

74. Stinnet, J.D. Guyman, L.F. and Eagon, R.C. (1973) Biochem. Biophys. Res. Commun. 52, 284-290

75. Lagarde, A.E. and Haddock, B.A. (1977) Biochem. J. 162, 183-187

76. Lagarde, A.E. (1977) Biochem. J. 168, 211-221

77. Lagarde, A.E. and Stoeber, F.R. (1975) Eur. J. Biochem. 55, 343-354

78. Lagarde, A.E. and Stoeber, F.R. (1977) J. Bacteriol. 129, 606-615

79. West, I.C. and Mitchell, P. (1973) Biochem. J. 132, 587-592

80. Collins, S.H., Jarvis, A.W., Lindsay, R.J. and Hamilton, H.A. (1976) J. Bacteriol. 126, 1232-1244

81. Daruwalla, K.R., Paxton, A.T. and Henderson, J.F. (1981) Biochem. J. 200, 611-627

82. Henderson, P.J.F. (1974) In "Comparative Biochemistry and Physiology of Transport," p. 409-424. Bolis, L., Bloch, K., Luria, S.E. and Lynen, F. eds., Elsevier Publishing Co.

83. Ramos, S. and Kaback, H.R. (1977) Biochemistry 16, 854-859

84. Harold, F.M. and Spitz, E. (1975) J. Bacteriol. 122, 266-277

85. Gutowski, S.J. and Rosenberg, H. (1976) Biochem. J. 154, 731-734

86. Gutowski, S.J. and Rosenberg, H. (1975) Biochem. J. 152, 647-654

87. Robin, A. and Kepes, A. (1973) FEBS Lett. 36, 133-136

88. Drapeau, G.R. and MacLeod, R.A. (1963) Biochem. Biophys. Res. Commun. 12, 111-115

89. Lanyi, J.K. (1979) Biochim. Biophys. Acta 559, 377-397

90. Tokuda, H. and Kaback, H.R. (1977) Biochemistry 16, 2130-2136

91. Harold, F.M. and Papineau, D. (1972) J. Membr. Biol. 8, 45-62

92. West, I.C. and Mitchell, P. (1974) Biochem. J. 144, 87-90

93. Zilberstein, D., Schuldiner, S. and Padan, E. (1979) Biochemistry 18, 669-673

94. Tokuda, H. and Kaback, H.R. (1977) Biochemistry 16, 2130-2136

95. Reenstra, W.W., Patel, L., Rottenberg, H. and Kaback, H.R. (1980) Biochemistry 19, 1-9

96. Borbolla, M.G. and Rosen, B.P. (1984) Arch. Biochem. Biophys. 229, 98-103

97. Bassilana, M., Dimiano, E. and Leblanc, G. (1984) Biochemistry 23, 1015-1022

98. Krulwich, T.A. (1983) Biochim. Biophys. Acta 726, 245-264

99. Waggoner, A. (1976) J. Membr. Biol. 27, 317-334

100. Rosen. B.P. and Alder, L.W. (1975) Biochim. Biophys. Acta 387, 23-36

101. Rottenberg, H. and Lee, C.P. (1975) Biochemistry 14, 2675-2680

102. Lee, C.P. (1971) Biochemistry 10, 4375-4381

103. Mitchell, P. and Moyle, J. (1969) Eur. J. Biochem. 7, 471-484

104. Harold, F.M. and Papineau, D.J. (1972) J. Membr. Biol. 8, 27-44

105. Kay, W.W. and Kornberg, H.L. (1971) Eur. J. Biochem. 18, 274-281

106. Ramos, S., Schuldiner, S. and Kabaek, H.R. (1979) Methods Enzymol. 55, 680-688

107. Colowick, S.P. and Womack, F.C. (1969) J. Biol. Chem. 244, 774-777

108. Henderson, P.J.F. (1971) Ann. Rev. Microbiol. 25, 393-428

109. Nicholls, D.G. (1982) In "Bioenergetics," p. 25-39 Nicholls, D.G. e.d., Academic Press, N.Y.

110. Hirata, H., Altendorf, K. and Harold, F.M. (1973) Proc. Natl. Acad. Sci. U.S.A. 70, 1804-1808

111. Henderson, P.J.F., Bradley, S., Mac Pherson, A.J.S., Horne, P., Davis, E.O., Daruwalla, K.R. and Jones-Mortimer, M.C. (1984) Biochem. Soc. Trans. 12, 146-148

112. Konings, W.N., Otto, R., Brink, B.T., Robillard, G.T., Elferink, M.G.L. and Hellingwerf, K.J. (1984) Biochem. Soc. Trans. 12, 152-154

113. Robillard, G.T. and Konings, W.N. (1982) Eur. J. Biochem. 127, 597-604

114. Wood, W.A. (1955) Bacteriol. Rev. 19, 222-233

115. Eisenberg, R.C., Rutters, S.J., Quay, S.C. and Friedman, S.B. (1974) J. Bacteriol. 120, 146-153

116. Roberts, B.K., Midgley, M. and Dawes, E.A. (1973) J. Gen. Microbiol. 78, 319-329

117. Jermyn, M.A. (1960) Biochim. Biophys. Acta 37, 78-92

118. Al-Jobore, A. and Taylor, N.F. (1979) Proc. Can. Fed. Biol. Soc. 22, 78

119. Lynch, W.H. and Franklyn, M. (1978) Can. J. Microbiol. 24, 56-62

120. Lynch, W.H., MacLeod, J. and Franklin, M. (1975). Can. J. Microbiol. 21, 1553-1559

121. Lynch, W.H., MacLeod, J. and Franklin, M. (1975). Can. J. Microbiol. 21, 1560-1572

122. Midgley, M. and Dawes, E.A. (1973). Biochem. J. 132, 141-154

123. Quay, S.C., Friedman, S.B. and Eisenberg, R.C. (1972) J. Bacteriol. 112, 291-298

124. Matsushita, K., Shinagawa, E., Adachi, O. and Ameyama, M. (1979) J. Biochem. 85, 1173-1181

125. Matsushita, K., Shinagawa, E., Adachi, O. and Ameyama, M. (1979) J. Biochem. 86, 249-256

126. Agbanyo, F. and Taylor, N.F. (1983) Proc. Can. Fed. Biol. Soc. Abstr. 26, 72

127. Stanier, R.Y. (1947) J. Bacteriol. 53, 297-315

128. Davis, B.D. and Mingioli, E.S. (1950) J. Bacteriol. 60, 17-28

129. Barnett, J.A. and Ingram, M. (1955) J. Appl. Bacteriol. 18, 131-148

130. Hill, L. (1973) Ph.D. Dissertation, University of Bath, Bath, U.K.

131. Moses, G.C. (1980) Ph.D. Dissertatiion, University of Windsor, Windsor, Ontario, Canada

132. Rottenberg, H. (1979) Methods Enzymol. 55, 547-569

133. Taylor, N.F., Hill, L. and Eisenthal, R. (1975) Can. J. Biochem. 53, 57-64

134. Bartlett, G.R. (1958) J. Biol. Chem. 234, 459-468

135. Kay, W.W. and Gronlund, A.F. (1969) Can. J. Microbiol. 15, 739-741

136. Lynch, W.H., Mac Leod, J. and Franklin, M. (1975) Can. J. Microbiol. 21, 1553-1559

137. Lanning, M.C. and Cohen, S.S. (1951) J. Biol. Chem. 189, 109-114

138. Gornall, C.J., Bardawill, C.J. and David, M.M. (1949) J. Biol. Chem. 177, 751-766

139. Lowry, O.H., Rosenbrough, N.J., Farr, A.L. and Randall, R.J. (1951) J. Biol. Chem. 193, 265-275

140. Lineweaver, H. and Burk, D. (1934) J. Amer. Chem. Soc. 56, 658-668

141. Dixon, M. (1953) Biochem. J. 55, 170-171

142. Matsushita, K., Shinagawa, E., Adachi, O and Ameyama, M. (1979) J. Biochem. 86, 249-256

143. Henderson, P.J.F., Giddens, R.A. and Jones-Mortimer, M.C. (1977) Biochem. J. 162, 309-320

144. Guerrant, G.O., Lambert, M.A. and Moss, C.W. (1982) J. Clin. Microbiol. 16, 355-360

145. D'Amore, T. (1983) Ph.D. Dissertation, University of Windsor, Windsor, Ontario, Canada.

146. Kaback, H.R. (1971) In "Methods in Enzymology", Vol. 22, p. 99-120, Jakoby, W.B. ed., Academic Press,

Inc. N.Y.

147. Konings, W.N., Barnes, E.M. Jr. and Kaback, H.R. (1971) J. Biol. Chem. 246, 5857-5861.

148. Al-Jobore, A. (1978) Ph.D. Dissertation, University of Windsor, Windsor, Ontario, Canada

149. Yamato, I., Futai, M., Anraku, Y. and Nonomura, Y. (1978) J. Biochem. 83, 117-128

150. Barnes, E.M. Jr. (1972) Arch. Biochem. Biophys. 152, 795-799

151. Schuldiner, S., Kerwar, G.K., Kaback, H.R. and Weil, R. (1975) J. Biol. Chem. 250, 1361-1370

152. Matsushita, K., Yamand, M., Shinagawa, E., Adachi, O. and Ameyama, M. (1980) J. Bacteriol. 141, 389-392

153. Liu, Chung Y. and Webster, D.A. (1974) J. Biol. Chem. 249, 4261-4266

154. Ciba Foundation Symposium (1972) Carbon-Fluorine Compounds: Chemistry, Biochemistry and Biological Activities. Associated Scientific Publishers, London

155. Barnett, J.E.G., Holman, G.D. and Munday, K.A. (1973) Biochem. J. 131, 211-221

156. Lopes, D.P. and Taylor, N.F. (1979) Carbohydr. Res. 73, 125-134

157. Barnett, J.E.G. (1972) In "Ciba Foundation Symposium. Carbon-Flourine Compounds: Chemistry, Biochemistry and Biological Activities," p. 94-115. Associated Scientific Publishers, London

158. Taylor. N.F. and Louie, Li-Yu (1977) Can. J. Biochem. 55, 911-915

159. Taylor, N.F., White, F.H. and Eisenthal, R. (1972) Biochem. Pharmacol. 21, 347-353

160. Michaelis, L. and Menton, M.L. (1913) Biochem. Z. 49, 333-369

161. Briggs, G.E. and Haldane, J.B.S. (1925) Biochem. J. 19, 338-339

VITA AUCTORIS

NAME: Francisca Roseline Akuvi Agbanyo

BORN: October 10, 1956. Kadjebi-Akan, Ghana.

EDUCATION:

1968-1975 Holy Child Secondary School, Cape Coast, Ghana

1975-1978 B.Sc. (Hons.) Biochemistry (Major). University of Ghana.

1979-1984 University of Windsor, Windsor Ontario, Canada. Fulfilled all requirements, with the exception of my Dissertation, for the Degree of Doctor of Philosophy in Biochemistry.

WORKING EXPERIENCE:

1978-1979 Instructor (Organic Chemistry), Holy Child Secondary School, Cape Coast, Ghana.

1979-1984 Teaching Assistant (Chemistry), University of Windsor, Windsor, Ontario, Canada

AWARD:

1981-1984 University of Windsor Scholarship.

SOCIETY: Student member of Canadian Biochemical Society.

PUBLICATION: Agbanyo, F.R. and Taylor, N.F. (1983). The transport of 2-keto-D-gluconate in vesicles prepared from *Pseudomonas putida*. *Proc. Can. Fed. Biol. Soc.* 26, 72